Scientific Basis for a Safety Case of Deep Geological Repositories

GRS - 771

Gesellschaft für Anlagen-
und Reaktorsicherheit
(GRS) gGmbH

Scientific Basis for a Safety Case of Deep Geological Repositories

Ulrich Noseck
Dirk Becker
Judith Flügge
Anne Gehrke
Klaus-Peter Kröhn
Michael Kröhn
Sabine Spießl
Jens Wolf

January 2025

Remark:

This report refers to the in-house research project 02E11941 which has been funded by the German Federal Ministry for Environment, Nature Conservation, Nuclear Safety and Consumer Protection (BMUV).

The work was conducted by the Gesellschaft für Anlagen- und Reaktorsicherheit (GRS) gGmbH.

The authors are responsible for the content of the report.

GRS - 771
ISBN 978-3-910548-63-3

Keywords
Clay, Crystalline rock, Knowledge management, Modelling, Permafrost, Radioactive waste, Rock salt, Safety Assessment, Safety Case, Scenarios, Sensitivity analysis, Uncertainty

Abstract

The assessment of the long-term safety of a repository for radioactive or hazardous waste and therewith the development of a safety case requires a comprehensive system understanding, a continuous development of the methods of a safety case and capable and qualified numerical tools. The objective of the project “Scientific basis for the assessment of the long-term safety of repositories”, identification number 02E11647, was to follow national and international developments in this area, to evaluate research projects, which contribute to knowledge, model approaches and data, and to perform specific investigations to improve the methodologies of the safety case and the long-term safety assessment.

This project was founded by the Federal Ministry for Environment, Nature Conservation, Nuclear Safety and Consumer Protection (BMUV) and carried out in the period from the 1st September 2021 to 30st September 2024. The results of the key topics investigated within the project are published in the following report:

- GRS-771: Scientific Basis of a Safety Case for Deep Geological Repositories

Moreover, substantial contributions were developed for the following international reports and flyers:

- OECD/NEA: The concept of the Set of Essential Records to Preserve Information about a Repository for Future Generations – Experiences from application to real programmes and update of the concept. NEA report Nr. X, Paris 2025. To be published.
- SANDIA: “Sensitivity Analysis Comparisons on Geologic Case Studies: An International Collaboration, Volume 2. Sandia Report, SAND2025-00230
- Decovalex, 1: Value of abstraction in performance assessment – When is a higher level of detail necessary? In: GeoMech. Engin. Env. 39 (2024)
- Decovalex, 2: Comparing modelling approaches for a generic nuclear waste repository in salt. In: GeoMech. Energy Env. 40 (2024)

Zusammenfassung

Das Projekt hat dazu beigetragen, das Verständnis für einen Safety Case zu vertiefen, neue Erkenntnisse aus internationalen Forschungsarbeiten für den nationalen Sicherheitsnachweis auszuwerten und das Verfahren und die Methodik für Langzeitsicherheitsbewertungen entsprechend dem Stand der Technik weiterzuentwickeln. Aktivitäten wie beispielsweise Vergleichsrechnungen mit Programmen anderer Organisationen trugen zur Verifizierung und Qualifizierung der verwendeten Berechnungscodes bei. Außerdem wurde das Thema der Bewahrung von Informationen und Wissen über ein Endlager und deren Weitergabe an zukünftige Generationen im Rahmen eines internationalen Vorhabens vertieft. Damit leistete das Projekt einen relevanten Beitrag zu verschiedenen Aspekten des Sicherheitsnachweises für Endlager.

Eine wichtige Aufgabe des Projekts ist die Mitarbeit in internationalen Gremien und Arbeitsgruppen, um neue Entwicklungen in anderen Ländern und auf internationaler Ebene zu verfolgen und zur Entwicklung von Strategien, Methoden und Werkzeugen für einen Sicherheitsnachweis geologischer Tiefenlager beizutragen. In diesem Zusammenhang spielte die Mitarbeit in der NEA-Integration Group for the Safety Case (IGSC), und ihren Untergruppen, speziell dem Salt Club und Crystalline Club sowie der NEA-Arbeitsgruppe für Information, Data- and Knowledge Management (WP-IDKM) eine wichtige Rolle. In den letzten drei Jahren (Laufzeit dieses Projekts) hat die IGSC mit neuen Aufgaben begonnen, unter anderem mit einer Aktualisierung des Projekts zu Methoden zur Sicherheitsbewertung (MeSA), die sich mit dem Zusammenhang zwischen Anforderungsmanagement und dem Safety Case befasst. Es werden neue Flussdiagramme entwickelt, die Schnittstellen zur Implementierung, zum Sicherheitskonzept und zum Endlagerlayout enthalten und die Entwicklung des Sicherheitsnachweises im Laufe der Zeit beschreiben. Die zeitliche Entwicklung des Sicherheitsnachweises wird auch im IGSC-GeneSiS-Projekt betrachtet, wo Erfahrungen aus der Erstellung von Sicherheitsnachweisen von den generischen Phasen bis hin zu standortspezifischen Phasen zusammengestellt werden und Ländern, die sich in frühen Phasen des Endlagerprogramms befinden, als Anleitung dienen können. Höhepunkt der aktuellen IGSC-Arbeiten war die Planung und Vorbereitung des vierten Safety Case Symposiums, das im Oktober 2024 erfolgreich in Budapest durchgeführt wurde.

Eine zentrale Aufgabe des NEA Salt Clubs war die Analyse des aktuellen Stands der Szenarienentwicklung für die Sicherheitsanalyse geologischer Tiefenlager für

radioaktive Abfälle in Salzformationen. Die Arbeit spiegelt die Unterschiede in den Vorschriften der Mitgliedsstaaten des NEA Salt Clubs wider, und beschreibt die Gemeinsamkeiten und Unterschiede zwischen den verwendeten Ansätzen. Da Salz in der Geschichte der Menschheit immer eine wichtige Ressource war, erfordert das menschliche Eindringen in das Endlager im Salz im Vergleich zu anderen Wirtsgesteinen besondere Aufmerksamkeit bei der Szenarienentwicklung und wurde in Online-Meetings separat behandelt. Ein Schwerpunkt der Arbeit des Crystalline Clubs war unter anderem die Entwicklung einer Datenbank mit Veröffentlichungen, die sich mit den chemischen Bedingungen im Endlagersystem im Kristallingestein befassen. Insbesondere solche Publikationen wurden ausgewählt, die beschreiben, welche Prozesse die chemischen Bedingungen kontrollieren, wie sie entstehen und wie sie sich aufgrund von Einflüssen aus dem Endlager entwickeln können. Es umfasst verfügbare Literatur zu Modellen, die zur Simulation und Vorhersage chemischer Bedingungen entwickelt wurden, sowie Literatur zu Behältermaterialien und Behälterkorrosion. Die Datenbank wird online gehostet und enthält bisher 629 Referenzen. Ziel ist es, die Datenbank im Jahr 2025 zu veröffentlichen.

Nationale Programme zur Entsorgung radioaktiver Abfälle erfordern sehr große Mengen an Daten und Informationen aus zahlreichen und unterschiedlichen Disziplinen, z.B. Nukleartechnik, Abfallwirtschaft, Geowissenschaften, Physik, Chemie oder Ingenieurwesen. Während der aktiven Lebensdauer eines Endlagers für radioaktive Abfälle, der Vorbetriebs- und der Betriebsphase, die sehr wahrscheinlich einen Zeitraum von mehr als 100 Jahren umfassen wird, werden zahlreiche Berichte und Daten erstellt. Die Verwaltung dieser sehr großen Datenmengen erfordert beträchtliche Ressourcen. Durch die Reduzierung der extrem großen Anzahl von Daten- und Informationsmengen auf einen essentiellen Satz von Unterlagen (den sogenannten Set of Essential Records (SER)) können Ressourcen reduziert und die Zugänglichkeit sowie das Verständnis der darin enthaltenen Information für zukünftige Generationen verbessert werden. Die von der NEA im Jahr 2019 gegründete Arbeitsgruppe für Informations-, Daten- und Wissensmanagement (WP-IDKM) untersucht dieses Thema auf dem Gebiet der nuklearen Entsorgung. Dabei stellt die Weiterentwicklung des Set of Essential Records (SER)-Konzepts ein besonderes Thema dar, das in der Expertengruppe EGAR des WP-IDKM behandelt wurde. Das SER-Konzept und die Erfahrungen aus ersten Anwendungen auf nationale Unterlagen einzelner Länder wurden in einem NEA-Bericht zusammengestellt und die wesentlichen Ergebnisse in diesem Bericht hier zusammengefasst.

Die Joint Sensitivity Analysis Group (JOSA) wurde vor sieben Jahren ins Leben gerufen. Der Schwerpunkt der Arbeiten in JOSA liegt auf der Verwendung von Sensitivitätsanalysen (SA) von Fallstudien zur geologischen Endlagerung abgebrannter Kernbrennstoffe mit dem übergeordneten Ziel, Leitlinien für die Durchführung solcher Analysen im Rahmen von Sicherheitsbewertungen für geologische Endlager zu entwickeln und bereitzustellen. Das Ziel der Arbeiten besteht darin, ein besseres Verständnis der Stärken und Schwächen verschiedener SA-Methoden zu erlangen, die Leistungsfähigkeit der Methoden zu bestimmen und Best Practices und andere aus dem Benchmark gewonnene Erkenntnisse herauszuarbeiten. Mehrere Länder beteiligten sich und untersuchten verschiedene SA-Methoden anhand einer Reihe von Fallstudien. Die hier beschriebene zweite Phase von JOSA befasste sich mit ausgefeilteren Methoden und komplexeren Modellfällen. Der Schwerpunkt lag auf der Untersuchung von Metamodellmethoden, höheren Sensitivitätsordnungen (Parameterinteraktionen) und neueren Ansätzen. Von Interesse war die Frage, ob die verschiedenen Methoden hinsichtlich der Sensitivität von Parametern und Parameterkombinationen übereinstimmen oder nicht. Die untersuchten Systeme weisen Besonderheiten wie starke Nichtlinearität, Bimodalität, Bifurkation und stochastische Einflüsse auf. Am Ende von Phase 2 formulierte das JOSA-Team detaillierte Empfehlungen für die Durchführung von Sensitivitätsstudien. Die Arbeit der GRS konzentrierte sich auf die Untersuchung des LILW-Modells und eines Referenzfalls für ein Endlager im Kristallin mit Metamodellierungsmethoden, um Parameterinteraktionen zu analysieren, was mit Standardmethoden nicht (oder nicht zufriedenstellend) möglich ist. Es wurde festgestellt, dass Metamodellierungsmethoden für diesen Zweck geeignet sind, die Ergebnisse jedoch in hohem Maße von Metamodelleinstellungen wie Polynomordnungen abhängen. Ein generelles Fazit von Phase 2 ist, dass bei Sensitivitätsanalysen noch einige Probleme existieren, die gelöst werden müssen. Für die nächste Phase von JOSA vorgeschlagene Themen sind verschachtelte Stichproben, nichtparametrisierte (z. B. räumliche) Unsicherheit, Einfluss von Stichprobentypen, Screening-Methoden, Bifurkationseffekte, aktive Unterräume und die Verwendung von Eingabe- oder Ausgabetransformationen.

Auch in DECOVALEX 2023 wurde mit dem Task F2 eine Benchmark-Übung gestartet, bei der Modellierungsteams verschiedener Organisationen zusammengebracht wurden, um unterschiedliche Methoden und Tools zur Simulation des Fluid- und Schadstofftransports in einem Endlager in Steinsalz anwenden, und ihre Ergebnisse zu vergleichen. Hierzu wurden zwei einfache Benchmark-Tests identifiziert, für die analytische Lösungen verfügbar sind. Darüber hinaus wurde ein Referenzfall definiert, der eine einfache

Endlagerstruktur mit Einlagerungsstollen für abgebrannte Brennelemente und Bohrlöchern für verglaste HLW-Behälter darstellt. Von den teilnehmenden Teams wurde ein breites Spektrum an Modellannahmen abgedeckt, von segmentierten Netzwerken bis hin zu vollständigen 3D-Modellen des Endlagers. Kein einzelnes Modell umfasst eine originalgetreue Darstellung aller in der Aufgabenspezifikation aufgeführten Merkmale, Ereignisse und Prozesse (FEPs), aber fast alle Merkmale und Prozesse werden in mindestens einem Modell dargestellt. Es wurden deterministische Berechnungen durchgeführt und dabei mehrere Varianten des Referenzfalls berücksichtigt. Beträchtliche Unterschiede zwischen den Modellen wurden hinsichtlich der Flüssigkeitssättigung und der Volumenströme festgestellt und sind zu frühen Zeitpunkten vor 1000 Jahren am deutlichsten. Diese Unterschiede sind größtenteils auf die unterschiedliche Modellierung der Kriechverschlussvorgänge zwischen den Teams und die daraus resultierende Rate der Porositätsreduktion zurückzuführen, die wiederum von den Annahmen in den Kompaktionsmodellen abhängt. Sie spiegeln die Bedeutung der Implementierung eines präzisen Mechanismus für die Salzkompaktion in das konzeptionelle Salzmodell wider, um das Verhalten des Endlagers zu untersuchen. Die Ergebnisse zeigen, dass der Tracer-Transport aus den Abfallstrecken und durch die Abdichtungen in allen Modellen weitgehend diffusiv erfolgt. Die Unterschiede beim diffusiven Transport sind im Allgemeinen geringer sind als die Unterschiede beim Flüssigkeitsfluss. Die Ergebnisse deuten darauf hin, dass die Diffusion ein wichtiger physikalischer Mechanismus ist, der den langfristigen Transport von Radionukliden im Endlager bestimmt. Die Diffusion ist über die Verringerung der Porosität und die Kopplung zwischen Porosität und effektiver Diffusion eng mit dem Kriech- und Verschlussmechanismus des Salzes verknüpft. Darüber hinaus wird die Diffusion in den Modellen durch numerische Dispersion beeinflusst. Obwohl es keine auffälligen Widersprüche oder Inkompatibilitäten gibt und die Unterschiede weitgehend nachvollziehbar sind, zeigte der Benchmark, dass unterschiedliche Modellierungskonzepte für Endlager im Salz zu recht unterschiedlichen Ergebnissen führen können. Weitere Forschungsarbeiten sind erforderlich, um die Bedeutung der Modelleigenschaften zu untersuchen und ihr Verständnis für die Langzeitsicherheitsanalyse zu verbessern. Die Arbeiten werden in DECOVALEX-2027 fortgesetzt.

Die Wiederaufsättigung von Bentonit als spezifisches Thema des Sicherheitsnachweises wurde in den letzten zwei Jahrzehnten durch aktive Mitarbeit in der Task Force on Engineered Barrier Systems (TF EBS) behandelt. Im Frühjahr 2023 wurde ein von GRS im Rahmen des Projekts WiGru-7 durchgeführtes Aufsättigungsexperiment mit begrenztem Wasserzufluss als neue Aufgabe für die TF EBS vorgeschlagen und angenommen und die GRS zum Principal Investigator dieser Aufgabe ernannt. Der Auftrag als Principal Investigator umfasst das Verfassen einer Aufgabenbeschreibung, das Klären offener Fragen, die bei der Bearbeitung der Aufgabe bei den Teilnehmern auftreten können, das Sammeln und Vergleichen der Ergebnisse sowie abschließend das Verfassen eines zusammenfassenden Berichts. Die Aufgabenbeschreibung wurde einige Monate vor dem Ende dieses Vorhabens fertiggestellt und einige vorläufige Simulationsergebnisse wurden auf dem letzten TF-Workshop präsentiert. In diesem Bericht wird die detaillierte Aufgabenbeschreibung vorgestellt. Dazu gehört die Beschreibung aller technischen Aspekte und Details des an der GRS durchgeführten Experiments zur Untersuchung der Wasseraufnahme durch verdichteten MX-80-Bentonit unter Bedingungen eines begrenzten Wasserzuflusses, wie sie bei Gesteinsbedingungen mit geringem Fließverhalten zu erwarten sind, und der daraus resultierenden räumlichen Verteilungen der Trockendichte, des Grades der Wassersättigung und der Porositäten. Abschließend werden die von den Benchmark-Teilnehmern zu erledigenden Aufgaben skizziert. Ergebnisse des Benchmarks werden im Bericht des Nachfolgeprojekts FLANKE vorgestellt.

An der Danmarks Tekniske Universitet (DTU) wurde eine innovative Methode entwickelt, um die Entwicklung natürlicher Kluftnetzwerke auf der Grundlage der geologischen Geschichte und fundamentaler geomechanischer Prinzipien zu simulieren. Für die Anwendung der Methode sind lediglich allgemeine Informationen über die geologischen Eigenschaften einer Formation hinsichtlich der Geometrie und mechanischer Aspekte erforderlich, und das Ergebnis ist ein geologisch realistisches Kluftnetzwerk. Ziel dieser Arbeit war die Entwicklung eines Modells mit dem Strömungs- und Transportcode d^{3}f++, um das Potenzial dieses Ansatzes für die Grundwassermodellierung auf dem Gebiet der Endlagersicherheitsanalyse abzuschätzen. Als geeignete Region zur Demonstration des Potenzials der neu entwickelten Klufterzeugungsmethode wurde das Drenthe-Aa-Tal im Nordosten der Niederlande ausgewählt. Die Ergebnisse legen nahe, dass die Methode ein hohes Potenzial hat, da die vom DFM-Generator erhaltenen Permeabilitätsverteilungen zu einem plausiblen Strömungsfeld führen. Darüber hinaus weist der Ansatz auf mögliche Kluftschichten hin, die bei herkömmlichen Bohrkernanalysen übersehen werden könnten. Da Kluftschichten höhere Permeabilitäten aufweisen als ungeklüftete Schichten, impliziert die Annahme von Kluftsystemen einen höheren Grad an Konservativität in Bezug auf Strömungs- und Transportsimulationen. Die neue Methode kann offensichtlich nicht so genau sein wie die direkte Erkundung. Aber sie liefert allgemeine Informationen über Kluftsysteme in viel größerem Maßstab und nutzt dabei ausschließlich verfügbares geologisches Wissen, und das alles auf mehr oder weniger theoretischer Basis. Die Methode ermöglicht somit eine erste schnelle und kostengünstige Prüfung der Eignung potenzieller Standorte für ein geologisches Endlager. Ein Vergleich verschiedener Standorte könnte dadurch erheblich erleichtert werden.

In den letzten Millionen Jahren kam es zu mehreren Eiszeiten, die im gesamten heutigen Deutschland für Permafrostverhältnisse sorgten. Permafrost wird einen erheblichen Einfluss auf den Grundwasserfluss haben, da das Gefrieren des Untergrunds dazu führt, tiefere Grundwasserleiter hydraulisch von der Oberfläche zu trennen. Es ist jedoch bekannt, dass Taliks, die Oberflächengewässer mit tieferen Grundwasserleitern verbinden, in Permafrostregionen existieren und möglicherweise zu einem konzentrierten Fluss von kontaminiertem Grundwasser an die Oberfläche führen können. Durch numerische Modellierung können Einblicke in die weitgehend unbekannten Umstände ihrer Entstehung und ihrer Stabilität gewonnen werden. Daher wurde ein numerisches Tool für den Grundwasserfluss unter Permafrostbedingungen angewendet. Das Hauptziel, die Bildung von Taliks numerisch zu verfolgen, wurde jedoch verfehlt, und die möglichen Gründe dafür werden diskutiert. Die ansonsten sinnvollen Modellierungsergebnisse regen jedoch zu weiteren systematischen Untersuchungen an. Diese sollten sich auf physikalische Prozesse beziehen, die in das Modell einbezogen werden müssen. Weitere Arbeiten sollten sich auf Mechanismen konzentrieren, die den Boden eines Sees erwärmen könnten, was wahrscheinlich eine Untersuchung der Gefrierdynamik von Seen im Allgemeinen erfordert. Darüber hinaus sollten Parametervariationen durchgeführt werden, z. B. Variationen des Wärmeflusses aus dem Erdinneren oder der Permeabilität und der Porosität des Gesteins. Außerdem wird die Einführung neuer Features in das Modell vorgeschlagen, wie z. B. einem (möglicherweise nicht horizontalen) Grundwasserspiegel, Heterogenitäten im Gestein oder einen tiefen Grundwasserleiter. Insgesamt gibt es noch viele offene Fragen, so dass eine systematische Weiterführung der vorliegenden Arbeit dringend empfohlen wird.

Da künftige Eiszeiten voraussichtlich das gesamte Gebiet Deutschlands betreffen werden, ist zu erwarten, dass alle potenziellen Standorte für die Endlagerung radioaktiver Abfälle dann entweder Permafrostbedingungen aufweisen oder von Eisschilden bedeckt sein werden. Grundwasser in Klüften von kristallinem Gestein, einem möglichen Wirtsgestein für ein Endlager, gefriert unter diesen Bedingungen. Um einen ersten Einblick in die Gefriereigenschaften von Wasser in den Klüften zu erhalten, wurde ein Strömungsexperiment mit einer realistischen transparenten 3D-gedruckten Kluftnachbildung basierend auf hochdetaillierten 3D-Scans aufgebaut. Sowohl das Experiment als auch das

Testverfahren wurden sorgfältig ausgearbeitet, um genaue und konsistente Ergebnisse zu gewährleisten. Es stellte sich heraus, dass einige Beobachtungen tatsächlich reproduzierbar waren, andere jedoch nicht. Außerdem wurden einige unerwartete Phänomene wie das Auftreten von Eisspitzen oder ein teilweises Einfrieren, also die Bildung von Eis nur auf einer der beiden Kluftflächen, beobachtet. Für Versuche zum Einfrieren in Klüften erwies sich der Versuchsaufbau jedenfalls als geeignet. Selbst Probleme, die durch eine Verfärbung der gedruckten Kluftflächen durch den Methylenblau-Tracer entstehen, könnten dadurch umgangen werden, dass man neue Replikate druckt und so den Vorteil nutzt, identische 3D-gedruckte Kluftrepliken für die Tests zu verwenden. Weitere Arbeiten zum Thema Einfrieren in Klüften erscheinen daher sinnvoll. Es sollten dabei Fragen geklärt werden, die im Verlauf der Experimente aufgeworfen wurden, wie z. B. die Art, Ausdehnung und Entwicklung der teilweise gefrorenen Gebiete oder die genauen Bedingungen für die Einleitung des Gefrierens. Parallel dazu sollte der Versuchsaufbau weiterentwickelt werden, um Messungen der hydraulischen Durchlässigkeit von gefrorenen Klüften zu ermöglichen. Das ultimative Ziel wäre dann die Bestimmung der effektiven Permeabilität als Funktion der Temperatur.

Table of contents

1 Introduction

Within this project strategies and methods to build a safety case for deep geological repositories are further developed. The safety case methodology established internationally, has been used for twenty years and is continuously further developed, particularly in committees of the Nuclear Energy Agency (NEA) and the International Atomic Energy Agency (IAEA). According to a common definition by the IAEA and NEA, the safety case is a compilation of arguments and facts that describe, quantify and support the safety and the degree of trustworthiness of the safety of the geological repository. The safety case includes the results of the safety assessments in conjunction with additional information, such as supporting evidence and reasoning, as well as a discussion of the robustness and quality of the repository, its design and the quality of the safety evidence, including the assumptions underlying it. As part of the work in the project described here, the strategies and methods for carrying out a safety case or for assessing the safety of a repository as well as the scientific fundamentals that form the basis of a safety case are to be further developed.

An essential element in assessing the safety of a repository is the long-term safety analysis, namely the process of systematic analysis of the hazards associated with the facility and the ability of the location and design to ensure the required safety functions and meet the technical requirements /NEA 12/. The basis of the long-term safety analysis is a powerful and proven set of instruments with which the relevant processes and components of a repository system, in particular the characteristics of the various host formations considered in Germany - rock salt, clay rock and crystalline - can be described. The computer programs to be used must be further developed through a constantly developing, in-depth understanding of the relevant processes, in line with the state of research. The methods for dealing with uncertainties, which represent a very important aspect of safety analysis, must also be further developed and implemented in the calculation programs.

The general procedure for assessment and demonstration of safety for geological repositories must comply with national regulations, but it should also be internationally accepted and must therefore be continuously adapted to international developments as well as new findings from research, science and technology. In order to ensure this, following and evaluating developments at the international level, especially in the working groups and projects of the NEA, IAEA and EC, is important and necessary. The

Integration Group for the Safety Case (IGSC) and its working groups Salt Club, Clay Club and Crystalline Club play an important role. I

Another topic for assessing the long-term safety of a repository that has come to the fore in recent years concerns the preservation of documents and knowledge about a repository. On the one hand, the implementation process of a repository can take place over many decades, and it must be ensured that no elementary knowledge about the repository is lost over this period. On the other hand, the preservation of knowledge for future generations over longer periods of several hundred years in the post-closure phase is also relevant in order to reduce the probability of unintentional penetration into the repository or to enable future generations to make their own decisions about an existing repository. Questions of this kind are addressed in the NEA's Information, Data and Knowledge Management (IDKM) working group.

Moreover, a goal of the project is to check the completeness, relevance and appropriate description of the processes and effects to be taken into account with regard to their use in safety analysis and to underpin data sets and their bandwidths. For this purpose, results from safety analysis or work relevant to safety analysis is followed and evaluated. This includes the topic of bentonite re-saturation in a repository addressed by the Taskforce on EBS, the creation of fracture networks for crystalline rock as well as the further development of model approaches to describe the influence of permafrost on flow and transport in geological formations.

2 International developments and co-operation

An important task of the project is the participation and concrete work in international committees and working groups to follow new developments in other countries and on the international level and to contributing the development of strategies, methods and tools related to the safety case of deep geological repositories. In this context the participation in the NEA Integration group for the safety case (IGSC), its subgroups, namely the salt club and crystalline club and the NEA Working Party on Information, Data and Knowledge Management (WP-IDKM) played a key role. Major activities in these groups, where GRS was involved are described in the following.

2.1 IGSC

Ulrich Noseck (GRS, Germany) and Manuel Capouet (ONDRAF-NIRAS, Belgium) were elected in 2022 as co-chairs of the IGSC and are still acting in this role. This included the presentation of IGSC in international fora and conferences (e.g. /CAP 22/), guiding the work together with the core group, particularly further developing the programme of work and actively supporting the tasks addressed by the IGSC.

A historical outline of the IGSC and the variety of aspects addressed in different initiatives, projects or events was presented at the International High Level Waste Conference of the American Nuclear Society /CAP 22/. The modern concept of the "safety case" was introduced in the field of high- and intermediate-level radioactive waste disposal in the 1990s by the Nuclear Energy Agency (NEA) Expert Group on Integrated Performance Assessment (IPAG). It is defined generically by the NEA as "the synthesis of evidence, analyses and arguments to affirm that a repository will be radiologically safe without human intervention after repository closure". The safety case addresses the challenge of evaluating and demonstrating the safety of a geological disposal facility over the prolonged period during which the waste remains hazardous, accounting for the substantial and increasing levels of uncertainty that arise during that period.

Since its inception, the concept of the safety case has been further developed by the NEA through the work of the Integration Group for the Safety Case (IGSC), the main technical advisory body to the Radioactive Waste Management Committee (RWMC), on geological disposal of radioactive waste as well as by national programs in many different countries. Furthermore, since 2006, the safety case has formed a central pillar of the

International Atomic Energy Agency (IAEA) Safety Standards for the geological disposal of radioactive waste /IAEA 06/.

The IGSC has contributed to and documented the evolution of the structure and content of safety cases, and the methodologies used to assess safety as repository programs have progressed. The safety case concept is used as a tool for program integration, for regulatory decision-making at major project stages, for knowledge transmission and wider communication, and for prioritization of research, site evaluation and repository design.

Subsequent work of the IGSC has further clarified the link between safety assessment and safety case through the MeSA project, as well as the regulatory requirements and expectations in relation to the safety case. The IGSC has investigated the aspects of communicating the safety case, and especially the handling of uncertainty, to stakeholders through a long-term collaboration with the NEA Forum on Stakeholder confidence (FSC). In recent years, the IGSC has broadened its interests to include aspects related to technical feasibility, operational safety and their integration with post-closure safety considerations and the difficult challenge of carrying out safety case updates.

Driven by the holistic vision of the RWMC, the IGSC recently extended its mandate to include the transfer of knowledge from and to other types of disposal facilities other than Deep Geological Repositories (DGR). With this new mission, the IGSC commits to investigate areas of work beyond deep geological disposal, whilst continuing to pursue its work of safety case development to the benefit of geological disposal programmes. This original mission remains indeed relevant at a time when some countries are now embarking on the implementation phase of their respective programmes, which is expected to lead to new and pioneering developments. In order to implement the new mandate, the ad hoc group TARGES (the IGSC ad-hoc group on transfer and return of gained experiences on safety cases for disposal facilities) has been created. TARGES has as its objective to identify general topics that will provide the basis to design the future IGSC programme of work (PoW) with a holistic perspective on waste management and that balances DGR safety case developments with focus on aspects such as evolving safety case and the challenges bound to construction, with the transfer of safety case knowledge from/to disposals in operation. TARGES has identified five potentials topics for investigation within the future IGSC PoW:

Topic 1 considers the application of the graded approach in the safety case. The motivation of this topic is the varying nature of national waste inventories that may need development of other disposal options complementary to near surface disposal (NSD) and DGR. The application of this high-level concept and its impact on the disposal options, the safety case methodology and the regulatory framework will be considered for examples such as low level – long lived waste (LL-LLW) or the waste available in a limited volume and suited for deep bore hole disposal /WAS 25/.

Topic 2 aims at developing how the flow of requirements related to long term and operational safety and feasibility aspects is managed and developed from the early generic stage of the disposal programme to the implementation stage. This activity will be embedded in the existing methodological MeSA framework /RÖH 25//.

Topic 3 addresses the return of experiences from operating facilities to DGR regarding in particular operational and safety procedures, Including development and implementation of waste acceptance criteria (WAC).

Topic 4 proposes to identify best practices when moving from a generic to a site-specific safety case. Issues include conceptual and numerical model developments, regulations, and moving from generic to site-specific characterisation and is described in some more detail in Section 2.1.1, since GRS was strongly involved in this working group.

Topic 5 proposes to learn from the update of safety assessment and safety case of facilities in operation. This REX could serve the DGR community to learn on how to, and to what level, upgrade safety assessment models and safety cases to introduce higher complexity or more detailed knowledge and how to account for evolving regulatory requirements and/or operational experience as well as to get prepared before construction and operation to the future safety case/safety assessment updates.

2.1.1 GeneSiS project

The Integration Group for the Safety Case (IGSC) so far launched activities on topic 1, topic 2 and topic 4. Topic 4, where GRS is deeply involved, is addressed by an ad-hoc group dealing with the “Generic to Site-Specific Safety Cases” (GeneSiS). The aim of this project is to support the development of generic safety cases and the transition to site-specific safety cases, particularly for member countries in less advanced stages /NEA 25/. One objective of the GeneSiS project is to produce guidance on the different approaches available across key safety case topics, and key considerations and best practice when selecting an approach, which will often depend on the stage of the repository programme.

Over the last two decades, the safety case has become an important decision-making tool in all phases of geological disposal programs. More and more national programs are aiming to license and implement deep geological repositories (DGR) for highly radioactive waste. Licensing is a critical advancement that involves an iterative development of the safety case that includes research, site characterization, design development, safety assessment and integration over several decades. This process is accompanied by regulatory reviews and communication with stakeholders, taking into account the entire life cycle of the waste. A key element is optimization to achieve the best results in terms of safety, technical feasibility, sustainability and costs and to meet stakeholder expectations. The safety case provides a framework for integrating all relevant information to support decisions at each stage of the process. The NEA Safety Case Integration Group (IGSC) has developed a structure and basic elements of the Safety Case that allow for stepwise elaboration from the design phase to implementation. The preservation and transfer of knowledge through generations of experts are considered crucial to the successful development of the safety case. In addition, the maturity of the safety proof concept is used as a basis for leveraging experiences from existing repositories for other types of radioactive waste /GRA 25/, /NOS 25a/.

The safety case is the main tool used to support decision-making at every stage of a geological disposal programme (e.g. NEA 2013). Fig. 2.1 depicts well-established programme stages (cf. /IAEA 20/) and safety case stages (GeneSiS) over a DGR programme's lifecycle /GRA 25/.

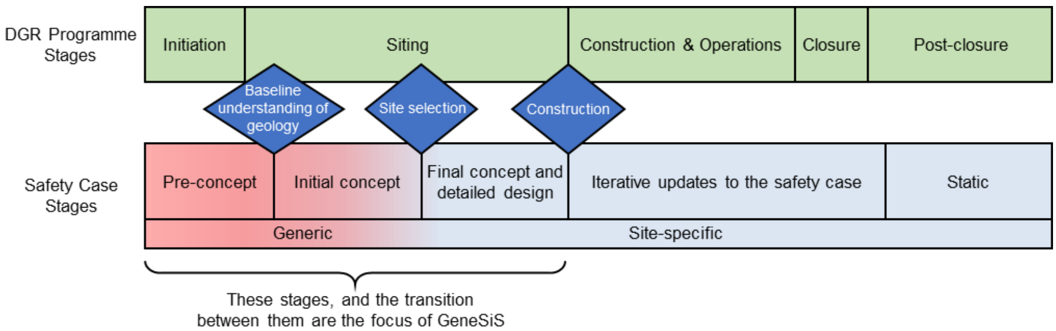

Fig. 2.1 DGR programme stages and safety case stages, with the transition from generic to site-specific safety case stages /GRA 25/, /NOS 25a/

Generic safety case stages (pre-concept and initial concept) involve identifying and collecting the information needed to develop a safety case. For the purpose of this project, generic safety cases may include instances where data from actual sites is used to develop safety assessment tools in the lead up to developing progressively more detailed, and site-specific, safety case documents, whereas site-specific safety cases consider site- and design-specific information for the purpose of demonstrating safety (i.e. meeting or exceeding requirements) at a specific site.

So far experiences from initial interviews with countries at advanced stages of their DGR programme have been gathered and to some extent evaluated. Interviews with programmes from less advanced countries are currently developed and will be performed soon. All outcomes will continue to be developed into guidance; however, some initial key messages can be summarised here:

International experience has informed safety case work: guidance from other countries and international developments in safety case methodology have helped countries determine what to include in their safety cases, and some fundamental aspects of today's safety cases date back to early studies (e.g. crystalline rock studies in Switzerland were refined and adapted by Nagra for the Opalinus Clay host rock). Some aspects of safety case methodology (e.g. safety functions, safety concepts, and requirements management) were developed or gained prominence in geological disposal relatively recently so were historically absent or underrepresented in early repository programmes but can be useful tools for early-stage programmes today.

Early studies enable regulatory authorities to build knowledge and capacity for future interactions and regulatory assessments, and help stakeholders develop a familiarity with geological disposal and arguments for its safety, and early safety assessments can guide site selection even if no formal safety case is produced.

During the transition from generic to site specific safety case development, the variability of a country's geology, and particularly how many different rock types are candidates for site selection, can impact workload, the number of different assessments needed, and the timescales associated with the repository programme, and this should be understood from the outset (recommended by Posiva).

For national programmes that require prioritisation of one site over another based on technical aspects (e.g. Switzerland), demonstrating sites are safe within an ample safety margin relative to regulatory targets is essential, but challenging.

Although a 'final' concept may be developed well in advance of construction licence applications (e.g. Nagra could be said to have submitted a final concept for their general licence application), a detailed design would be needed for construction licence applications, and the design and safety case itself may continue to evolve after this (e.g., due to new information during construction and monitoring).

2.1.2 Safety Case Symposium 2024

For the fourth time since 2007 the IGSC Safety Case Symposium: “Moving towards the construction of a safe DGR – Getting real”, organised by NEA-IGSC took place in Budapest, from 8 to 11 October 2024. It offers a platform for discussing safety case developments, with presentations of programs in different phases and an exchange on current challenges. The outcomes of the symposium will be documented in /NEA 25/.

During the phase of this project – until 30th September 2024 – the programme committee (PC) for the symposium intensively planned and prepared the symposium. Over the past two decades, the safety case has become a powerful and essential tool to support decision making for every stage of a geological disposal programme. The motto of the symposium has been chosen, since now an increasing number of national programmes are advancing towards licensing and the realisation of their deep geological repository (DGR) for high-level radioactive waste.

Licensing is a milestone achievement in the evolution and periodic updating of the safety case following an iterative process of research, site characterization, design development and demonstration, safety assessment and integration, generally spanning over multiple decades. This is accompanied by regulatory reviews and ongoing communication with involved stakeholders. Throughout this process the entire lifecycle of the waste, from its generation to its ultimate disposal is duly considered. Of particular importance is the embedding of optimisation within the process, so as to achieve the best outcomes for safety, technical feasibility, sustainability, costs and to fulfil stakeholder expectations and requirements.

This stepwise process follows the holistic approach to waste management and entails, amongst others, the transfer of information between the different stages of waste generation and management, in the form of data, criteria, liabilities, decisions and requirements. The safety case provides the framework for integrating all information relevant to the DGR to support the decisions taken at each stage of this process. The IGSC has developed the structure and essential elements of the safety case, such that a conceptual safety case, first developed at the early stages of a programme, can be progressively developed and deployed at later stages of the programme. Safety case digitalisation as well as knowledge preservation and transfer through expert generations are now being recognised as key for the successful iteration and development of the safety case towards DGR implementation.

In view of this, the objectives of the IGSC symposium 2024 are to:

- Identify the key success factors from safety cases that have supported successful licensing steps, examining the lessons learned and the challenges faced in this regard by advanced DGR programmes
- Understand how a safety case evolves through the different initial stages of a disposal programme, from the generic through to the site-specific stage, and then through the construction stages
- Explore the role of specific features, such as requirements management systems and information, data and knowledge management (IDKM) in building a safety case and in supporting its evolution throughout successive key milestones in a disposal programme
- Practically apply knowledge sharing by involving early career scientists in the symposium, enabling them to exchange knowledge and discuss their views, ideas and expectations, with the aim of building an enduring network to support the next generation
- Exchange experience with other non-DGR disposal facilities, especially concerning the application of holistic approaches to waste management

The symposium programme includes keynote lectures on radioactive waste management and the safety case in Hungary, requirement management systems, learning from nuclear facilities & mining industry as well as information, data and knowledge management.

Plenary sessions comprised the regulator, implementer and stakeholder dialogue, safety assessment and research, development & demonstration, the role & evolution of the safety case when moving to implementation, information, data and knowledge management (IDKM), derivation and management of criteria and requirements and learning from nuclear facilities, disposal of unconventional & legacy waste and waste from next generation reactors. For the two latter ones additionally two expert panels were organized.

Finally, nearly 200 participants have registered to the event showcasing 94 scientific papers on a broad range of topics related to disposal systems. Ondraf/Niras (Manuel Capouet) and GRS (Ulrich Noseck) chaired the event. Organizing the event received the excellent support of the NEA secretariat and the local waste management organisation PURAM.

2.2 Salt Club

The “Expert Group on Repositories in Rock Salt Formations (Salt Club)” was established in 2012 by OECD/NEA. Current member states are the United States, Germany, the Netherlands, United Kingdom, Poland, Australia and Romania. The key objective of the Salt Club is to promote the exchange of information and share approaches and methods to develop and document an understanding of salt formations as a host rock for a high-level radioactive waste repository. The Salt Club holds regular annual meetings at which its Programme of Work (PoW) are established, updated and reported about. In the current PoW of the Salt Club the following work activities are listed:

- Common Features, Events and Processes (FEP) catalogue for a HLW repository in rock salt and Salt Knowledge Archive (scope, definition, collection of ideas, available information on state-of-the-art of knowledge management)
- Scenario development for repositories in salt
- State-of-the-art report on important commonalities and differences of repositories in flat-bedded and domal salt
- Geomechanical integrity evaluation, including numerical and experimental work with crushed salt
- Thermodynamic aspects of brine chemistry
- Actinide and Brine Chemistry (ABC) Salt Workshops
- Joint International Pitzer Database (JIPD) and
- Microbial gas generation in saline systems.

The first item, the importance of the FEP approach as a basis of scenario development, was discussed intensively in the last decade in the NEA Salt Club resulting in a common FEP data base (www.saltfep.org, /FRE 20/) and a paper analyzing this topic on a detailed level /KUH 24/.

A specific site and the repository system will undergo exactly one evolution, which will be governed both by climatic and geological processes at the site and processes induced by the repository construction and the emplacement of heat-generating waste. Despite a detailed understanding of the various influencing factors, this real evolution cannot be predicted unequivocally in all details. The resulting uncertainty with regard to the future evolution of the repository system can be reduced only marginally by addition-al research and site investigations. Therefore, a limited number of reasonable possible evolutions are derived in a safety case based on a systematic assessment of relevant influencing factors with the objective to identify and describe in detail relevant scenarios, which allow to assess post-closure repository safety. The primary goal of a repository system scenario development is to derive a set of scenarios covering key aspects of uncertainties regarding the future evolution of the repository system – specifically the portion of the uncertainty not explicitly treated in numerical models. The safety assessment requires this set of scenarios cover all significant evolutions regarding the safety of the repository.

Scenarios sit at a key point in safety case development for the disposal of radioactive waste involving cataloging and exploration of all possible system components and behaviors, through the compilation of FEPs. The FEP approach was developed for radioactive waste disposal in the late 1970s as an abstraction of the fault-tree analysis method /KUH 24/. The major advantage of the FEP approach lies in the demonstration of comprehensiveness of the safety assessment to regulators and the public. The compiled FEPs are screened in or out based on several criteria such as probability or consequence. Scenario development then takes the collection of as many as several hundred screened-in FEPs, forms scenarios, and then groups them to create a much smaller set of scenarios classes.

The member states of the NEA Salt Club analysed the current state of scenario development for safety case development of deep geological repositories for radioactive waste in salt formations. The analysis was summarized in a report that will be published as NEA report. The following sections summarized some important aspects of this report.

The report reflects the implementation differences in the regulations that govern the process in the member states of the NEA Salt Club and describes the commonalities and differences between the approaches. In addition to the FEP report /FRE 20/ the report on scenario development includes a description of FEP that are unique for salt and important for the implementation of safety-relevant scenarios for repositories in salt rock. These are:

- Salt diapirism,
- Subrosion,
- Fluid inclusion and thermomigration,
- Dissolution of salt minerals,
- Dehydration of salt minerals,
- Regional ground water flow,
- High ionic strength solutions,
- Salt creeping convergence,
- Heat flow and thermal conductivity,
- Pressure induced permeation, and
- Vertical movement of heat-generating waste packages.

The FEP descriptions were structured in the following subsections:

- definition;
- general description;
- difference between bedded and domal salt;
- significance for long-term safety;
- open questions; and
- references.

All the screened-in FEPs must make it into one or more scenarios (comprehensiveness), and all the scenarios must be evaluated in a consistent way, but how exactly depends on the approach taken. Purely probabilistic approaches use probabilities (constrained to sum to one) to weight the consequences estimated from numerical safety analysis models. Probabilistic models are more complex to implement, but in the end, they result in a straightforward mechanical summation of results. A purely deterministic approach can either develop weights or likelihoods to recombine results, or it may directly compare each scenario's consequence to a standard individually (bounding approach). As discussed in more detail in /KUH 24/ the purely probabilistic approach places all the complexity and uncertainty into the numerical models and relies on sample size or importance sampling to ensure rare (but possibly consequential) events are adequately captured in the results. A purely bounding approach instead focuses the effort on the rare events as individual variant scenarios, using expert judgment to ensure any consequences are adequately captured and represented in the results.

Since salt has been an important resource during the history of mankind, human intrusion into the repository (HI) in salt requires special attention in scenario development in comparison to other host rocks. In general, the probability of HI cannot be reduced to zero. As in other host rocks the main counter measure against HI is the depth of the repository: the deeper the repository, the better. The footprint of the repository also plays a significant role. Both aspects are important aspects for reducing the probability of HI for repositories in salt, too. But in contrast to other host rocks, the value of the host rock as a resource is so high, that these general strategies to reduce the probability of HI is limited. In salt, technical options, such as dissolution mining, allow the profitable exploitation even at great depth and structures with a small footprint.

Since the regulations address HI in general (not specific for one specific host rock), the particular role of HI in salt is not addressed in national regulations. The only exception is the regulation for the WIPP (bedded salt), where HI is prominently addressed in long-term performance assessment modeling and drilling of boreholes at different times during their assessment period of 10.000 years define the base scenario. The example of the WIPP show the importance of HI (drilling) for the safety case for a repository in salt. Except of the FEP approach of WIPP the FEP on FHA listed in the IFEP of NEA are not used as (bottom-up) basis for the consideration of HI scenarios. The common (top-down) approach is to define directly stylized scenarios for HI. These scenarios are analyzed separately and the consequences of HI scenarios are excluded from comparison with safety indicators. The most common stylized scenario is the drilling of a borehole into a displacement area. This scenario is seen to cover all relevant aspects of other relevant HI scenarios. The experience from the WIPP supports this assumption.

The exclusion from the “classic” comparison with safety indicators does not mean that the consideration of HI is of low priority. On the contrary, experience in the different programs shows, that a thorough consideration of HI plays a key role for the communication of a safety case with different stakeholders and is seen as an important element for confidence building in the safety case.

2.3 Crystalline Club

Deep geological repositories use a combination of engineered and natural barriers to safely contain and isolate radioactive waste from people and the environment. Repository development for long-lived radioactive waste is a strategic area in the work programme of the NEA Radioactive Waste Management Committee (RWMC). Among the different geological formations considered suitable for hosting geological repositories, crystalline rocks are characterised by their high strength, thereby providing high rock-stability and a low thermal expansion coefficient. Unfractured crystalline rock shows a low permeability. Crystalline rocks, e. g. granite or gneiss are highly resistant to chemical alteration compared to other host rocks.

Many countries are developing or considering developing deep geological disposal facilities for radioactive waste or performing research in underground research facilities in crystalline host rocks. Although scientific and geotechnical understanding of crystalline rocks continues to advance from the dedicated research carried out by these countries, there are research areas in which member countries may benefit from the scientific exchange and joint R&D efforts.

Similar to other NEA expert groups, the Expert Group on Geological Repositories in Crystalline Rock Formations (Crystalline Club, CRC) is composed of technical experts with experience in evaluating or reviewing the understanding of crystalline rock as host rocks for deep geologic disposal projects. Members represent waste management organisations, regulatory authorities, academic institutions, and research and development institutions. The CRC was founded in 2017 with founding members from Czech Republic, Germany, Japan, Russian Federation, Spain and USA. By 2024, CRC has 38 members from ten member countries (Australia, Canada, Czechia, Germany, Japan, Republic of

Korea, Romania, Spain, Switzerland and USA). Since 2020 Judith Flügge (GRS, Germany) is acting as the chair of the CRC.

The CRC promotes the exchange of scientific evidence and information related to the safety of developing geological disposal facilities in crystalline rock formations. To further its goal, the CRC will:

- promote the exchange of information on approaches, methods, methodologies and technologies in order to understand the characteristics of crystalline rocks and the advantages to host a repository;
- develop and exchange specific information to the geological media of interest among countries currently pursuing or considering crystalline rock as a candidate deep geological repository medium;
- identify areas of interest for fundamental research, i.e. where understanding is incomplete or improvements are required;
- develop reports and technical proceedings based on shared expertise and experience;
- promote task groups within the CRC; and
- communicate identified topics of common interest and/or exchange with other working groups or international projects.

Annual plenary meetings are held on a regular basis in order to further the information exchange between the CRC members. During the reporting time, the following plenary meetings were held: CRC-3, 01 – 03 June 2021, online; CRC-4, 28 – 29 June 2022, Dresden/Germany; CRC-5, 13 – 15 June 2023, Daejeon/Republic of Korea; CRC-7, 18 – 20 June 2024, Baden/Switzerland.

The topical sessions of CRC meetings 2021 and 2022 were associated with the main goal of the CRC Program of Work (PoW) 2019 – 2022: to identify the crucial parameters of the crystalline host rock environment and to formulate the requirements for the development of siting and design criteria for radioactive waste repositories. The way to this goal lies in the comparison of the different approaches to safety assessment (SA) and to transfer the results into the safety case used by CRC member countries. The differences in safety assessment are due to using different kinds of data and different concepts of how to transfer data to models, how to develop and verify models, and how to deal with uncertainties, which are inevitable.

The work of the OECD/NEA Crystalline Club (CRC) in 2021 was strongly impacted by the restrictions caused by the Covid-19 pandemic. The CRC-4 plenary meeting, which was scheduled for June 2020 in Dresden/Germany, had to be postponed 2021. Due to prevailing travel restrictions in 2021, the meeting eventually had to be held online on 01 – 03 June 2021. The topical session on modelling with the title "The comparison and evaluation of the transfer of data for the compilation of both descriptive and safety assessment models" addressed the second step of the PoW 2019 – 2022. After a summary of the topical session on "Data acquisition, processing and management for model development" held during CRC-3 in Krasnoyarsk, Russian Federation, four presentations focused on (1) "Key aspects of safety concepts in crystalline host rock", (2) "Data integration & development of SDM for plutonic rocks in Japan", (3) "Fracture statistics and integration into computational models", and (4) "Safety assessment models used in South Korea". During the following discussion, two main topics were identified as crucial. The first one related to uncertainties and how to select, what uncertainties are important to reduce and at what stage this reduction would be sufficient. The proposed answers were: (i) To use sensitivity analysis as a tool allowing to reveal the features providing the most impact into the total uncertainty, (ii) To stop the investigation-modelling loop if the safety is ensured within given level of uncertainty, and (iii) To refer to regulator, who is expected to check if the safety assessment is reasonable enough. The second topic focused on who the "ringleader" is: Do models formulate requirements on the data or does data availability limit model abilities? It was stated that combined solution by model users and other specialists within the common knowledge base system would be required. Two problems were considered during the second part of the general discussion. (i) How to deal with different scales in models for crystalline rock, since rock properties differ at different scales? The transformation from discrete fracture networks (DFN) to equivalent porous medium models (ECPM) seems like an adequate approach, although the topic still is an open question. (ii) When and for what purpose can FEP be used? It was stated that FEP analysis is an important and even unique tool to specify scenarios and to justify their completeness and that a FEP data base should be developed after decision on disposal concept.

The 5th meeting of the Crystalline Club (CRC-5) took place on 28 – 29 June 2022 in Dresden/Germany and was hosted by Helmholtz-Zentrum Dresden-Rossendorf (HZDR).

During the CRC-5 meeting the topical session addressed the problem of the identification of the key data to be obtained from crystalline rock environments (the geosphere) that are relevant to the safety assessment process. The focus of the topical session was therefore the identification of requirements for the development of safety documentation concerning crystalline host rock environments. The session was chaired by Florian Kober (Switzerland), the session rapporteur was Andrew Parmenter (Canada). After the introduction by Florian Kober, Judith Flügge (Germany) and Lukáš Vondrovic (Czech Republic) summarized the outputs of the CRC-4 topical session held online in 2021 (second step of the PoW 2019-2022). The intended outcome was to compare different approaches of geosphere data integration into site descriptive models. The first presentation of the topical session at CRC-5 was given by Lukáš Vondrovic (SÚRAO, Czech Republic) on “Geological parameters”. He presented important geological parameters used in the SÚRAO decision making process during the site selection process. The presentation included an overview of key future dates for site selection and licensing, and disposal concept, and legislative requirements including geological requirements. Sung-Hun Ji (KAERI, Korea) presented on “Hydraulic parameters: Their uncertainty in fractured rock”. Uncertainties of hydraulic parameters, starting with overview of regulation on technical standards for radiation safety control and general guidelines for deep geological repositories for HLW were presented. Key parameters for SA modelling are the length of the flow path and the flow velocity in each hydrogeological unit. There is serious uncertainty in the field investigation, conceptualization and numerical modelling for hydrogeological study at fractured rock. The third presentation by Takafumi Hamamoto (NUMO, Japan) focused on “Application of geological environmental data for safety assessment in NUMO Safety Case”. He presented about their recently completed safety case and how geological data is used therein to demonstrate importance of geological parameters for assessing repository safety. Their site descriptive model (SDM) was used to perform repository design and undertake safety assessment analyses. It was noted that crucial parameters for undertaking representative safety assessment (SA) processes are those that correlate well with exposure dose, including hydraulic gradient and matrix diffusion depth, as well as matrix diffusion area, channel length, and sorption coefficient (K_d) of the rock. “Requirements on host rock environment related to the system” were presented by Piet Zuidema (ZUIDEMA CONSULT GMBH, Switzerland). Requirements on host rock environment to engineered barrier systems (EBS) were reviewed, starting with review of EBS components. Conceptual crystalline rock characteristics, including geological domains, small scale fractures and their heterogeneity and hydrochemistry were then presented. It was noted that fluid flow in fractures can lead to bentonite erosion, i.e., loss of bentonite from mechanical and chemical erosion. Mechanical loading can breach canisters, including induced shear by earthquakes. Important geosphere conditions include: hydraulic properties, porewater composition, and mechanical stability. Finally, Dusty Brooks (SANDIA, USA) presented on “Sensitivity analyses for deep geologic repository simulations in crystalline rock”. The presentation started with the purpose of sensitivity analyses, general approaches, demonstration of sensitivity analysis, and finally discussed which parameters are most important. It was noted that the purpose is to identify Features, Events, and Processes (FEPs) and related parameters, to quantify importance of FEPs, and use results to improve understanding. It was further noted that global sensitivity analyses are more useful for performance assess-ment (PA). A crystalline rock base (reference) case was presented. Model inputs were described, e.g., epistemic and fracture network parameters. Then results were presented, which overall indicated that the most sensitive parameters are spatial heterogeneity in fracture networks and fractional dissolution rate. It was concluded by stating that fracture networks have a dominant impact on performance, since it is expected that all canisters will fail.

Several key messages of the topical session were:

The parameters which are determined to be most crucial are defined by several factors, including:

- Country specific definitions of requirements, including officially legislated requirements,
- Site-specific geological conditions,
- Scale at which questions are being asked,
- Heterogeneity of the investigation area(s), at all scales, and
- Phase of investigation at which questions are being asked.

Acknowledging the impact of these factors, the key parameters identified to have general important to all programs include:

1. Fracture (network) characterization (parameterization). There are many parameters to consider (e.g., length, orientation, stress, degree of openness, etc.) and the approach taken during parameterization will have an impact on all other analyses. A

proper understanding of the fracture network under investigation allows for the development of robust discrete fracture network models (DFNs).

2. Geochemistry, including porewater/groundwater composition in relation to understanding geosphere stability and potential impacts of climate effects, as well as the interaction between the geosphere and the EBS; also rock chemistry, including thermal and sorption characteristics.

It was noted that there are many uncertainties associated with these parameters, and furthermore there was a general understanding that an overarching goal of crystalline rock characterization programs is to reduce these uncertainties through sensitivity analyses, and increasingly detailed and focused site investigation programs.

Other activities in 2022 referred to the discussion and definition of the Program of Work (PoW) 2023 – 2024 and the completion of the PoW 2019 – 2022 by formulating a questionnaire for CRC member countries on (i) software tools and different safety assessment approaches for different purposes of deep geological repository development and (ii) Which are the most important parameters that influence the various stages of the siting process including methods of their measurements and their level of prioritisation?

The main goal of the CRC Program of Work (PoW) 2023 – 2024 was to identify crystalline host rock chemical conditions relevant to crystalline repository performance and to identify processes that may control those chemical conditions. It was intended to include their impact on canister corrosion whenever results are available.

The properties and location of a crystalline host rock have direct effects on chemical conditions at the depths of a potential repository. In turn, chemical conditions at repository depth have direct effects on waste package degradation rates, waste form degradation rates, buffer performance, and radionuclide solubility and transport. Therefore, a good understanding of chemical conditions in crystalline host rock and how they could evolve over time is needed for effective crystalline repository performance assessment.

The selection of suitable canister materials for repositories in crystalline rock is dependent on the geochemical conditions in the host rock formation. The corrosion behaviour under the conditions of the near field is one of the main parameters influencing the selection of suitable canister materials, and canister design/canister concepts have to be developed in order to avoid corrosion processes.

The CRC-6 plenary meeting took place on 13 – 15 June 2023 in Daejeon, Republic of Korea, and was hosted by the Korean Atomic Energy Research Institute (KAERI). The topical session of CRC-6 was associated with the main goal of the CRC Program of Work (PoW) 2013 – 2024 and was entitled “Crystalline host rock chemical conditions relevant to crystalline repository performance”. The session was chaired by Patrick Dobson (Lawrence Berkeley National Laboratory, USA), the session rapporteur was Florian Kober (Nagra, Switzerland). After the introduction of the session chair, Thorsten Schäfer (University of Jena, Germany) presented on “Geochemistry, transport and retardation processes in crystalline rock: from the nanoscale to URL experiments”. The presentation introduced the field of fractures and their associated key properties, as well as advective flow versus matrix diffusion in crystalline rock and how to analyse it. Fracture flow and groundwater composition has a strong impact on radionuclide transport, retention, colloid interaction, microbial activity. Methods for sampling and analysis were introduced and the power of modelling that can support and/or simplify complex processes and phenomena was highlighted. Ju Wang (BRIUG, China) presented on “Geochemical conditions of Beishan - The potential granite site for China's deep geological repository of high level radioactive waste”. He introduced the Beishan granitic site, the ongoing site investigation program and the current construction progress in light of the Chinese high-level waste program with its stepwise approach towards a deep geological repository. Focus was on the investigation program and the 3D geological model derivied from the findings. Paolo Trichero (Amphos 21, Spain) presented on “The challenge of modelling microbial sulfide production in fractured granitic environments”. After introducing the multibarrier concept exemplified by the SKB, KBS3 concept and the link to safety function indicators to ensure favourable hydrogeological/hydrogeochemical conditions that are possible to assess with reactive transport modelling, he provided a detailed discussion of sulfide production by copper corrosion, also considering microbial and abiotic processes, and reactive transport modelling, which is employed to evaluate sulfide levels. His presentation was followed by a presentation by Min Soo Lee (KAERI, Korea) on “Corrosion experiment of disposal cansiter materials in KURT granitic environment”. The presentation introduced the multibarrier, KBS-3 type concept in which corrosion must be verified, keeping in mind varying aerobic to anaerobic conditions over time. Corresponding aerobic tests have been conducted at Kaeri’s KURT URL site. Anoxic long-term corrosion tests were in progress in a deep borehole at near KURT site. Andrew Parmenter (NWMO, Canada) presented on “Hydrogeochemical conditions at the Revell Site, NW Ontario, Canada and their contribution to understanding long-term crystalline repository performance”. It gave an overview of NWMO-Canadas Revell site (Ignace Area), a site of crystalline bedrock of 2.7 Ma years in age. A field (drilling, 6 x 1.000m) and laboratory test program has been run to understand and characterize the site-specific hydrogeochemical conditions. The investigations provided the necessary input for a verified geological model, which was revised only to a limited extent after adding drilling information. In summary, a homogeneous rock body is present. A discrete fracture network (DFN) model was also created. The topical session was completed by a presentation by Junichi Goto (NUMO, Japan) on “Results of geochemical research on crystalline rocks at Mizunami URL and their reflection in the NUMO safety case”. It was divided into two parts: (i) General R&D and phased approach with experience of the Mizunami Underground Laboratory Project, and (ii) Study on overpack thickness based on the groundwater chemical model in the generic NUMO Safety Case.

The topical session was the basis for the future work of CRC in the frame of the PoW 2023 – 2024. The next step is the curation of a list of publications that improve understanding of those chemical conditions, how they are controlled, how they originate, and how they may evolve due to repository perturbations and global temperature cycles. The list of publications will include available literature on models that have been developed to simulate and predict chemical conditions as well as literature on canister materials and canister corrosion. Several preparatory meetings were held in 2023, and a working group was initiated to focus on this task. The database is hosted online using the Mendeley Reference Manager. To date, it contains 629 references. The review process is almost completed. It is aimed at publishing the database in 2025.

The CRC-7 plenary meeting took place on 18 – 20 June 2024 in Baden, Switzerland, and was hosted by NAGRA. The topical session of CRC-7 was associated with the main goal of the CRC Program of Work (PoW) 2023 – 2024 and was set up as a workshop on the CRC Geochemistry Database. The session was chaired by Paul Mariner (SANDIA, USA), the session rapporteur was Andrew Parmenter (NWMO, Canada).

The introduction by the CRC-7 session chair provided an overview of chemical components and chemical processes considered in performance assessment. Importantly, in crystalline rock, the rock and engineered barriers (canister, fuel, buffer) must work together, and the performance of the latter depends on chemistry. After the introduction Patrick Dobson (LBNL, USA), chair of the topical session during CRC-6, gave a summary of the CRC-6 topical session. He provided a review of the presentations from CRC-6, and discussed the motivation for that session, namely, rock and fluid conditions and effects on the behaviour and performance of the waste package and engineered barrier, with specific focus on the impact of brine chemistry.

Paul Mariner and Patrick Dobson started the workshop with a presentation on “The CRC Geochemistry Database: Introduction, goals and first results”. They provided an overview of the first results of the Crystalline Club Geochemistry Literature database (CCGLD) compilation. Literature review topics included: groundwater compositions and chemical conditions in deep crystalline rock, chemical processes important to repository performance, and chemical models used in performance assessment. Goals of project are to build a database and to publish a report with the aim of having a reference database for topics related to deep crystalline rock and associated repositories.

Andrew Parmenter presented an example of a geochemistry database in his presentation on “University of Waterloo Precambrian Canadian Shield Groundwater and Gas Geochemistry Database”. He focused on the results of work completed by a research team at the University of Waterloo, who built a geochemical database of the Precambrian Canadian Shield, including a summary of data locations, primarily mine sites and Atomic Energy of Canada (AECL) study sites. The presentation highlighted challenges in the compilation of data (e.g. incomplete metadata, bias to shallow samples, need to normalize data, little isotope data, anthropogenic influences). Urs Mäder (Rock-Water-Consulting, Switzerland) presented on “Porewaters in crystalline rocks: Deciphering interactions with fracture waters”. He provided summary of fracture water in crystalline rocks and the role of porewater in understanding geochemical evolution, with specific examples from Grimsel, Alps, Scandinavian Shield, including past history of groundwater flow. This presentation was followed by Tiziana Missana (CIEMAT, Spain) with a presentation on “Hydrogeochemical Parameters Influencing Bentonite Barrier Erosion and Clay Colloid Stability/Mobility in Deep Geological Repositories for Radioactive Waste”. She discussed bentonite erosion and clay colloid formation in crystalline rock environment. Colloids are small particles suspended in fluid, they are mobile, small, and they move faster than water. They have a large surface area and are therefore very reactive, and sorptive. Solveig Pospiech (HZDR, Germany) concluded the topical session with an innovative presentation on “A workflow for combining geostatistics with geochemistry: A process to select features for designing spatial models for crystalline host rocks”. She discussed about upscaling and reducing complexity in modelling by developing suitable workflow that incorporates geostatistics.

In a following workshop, the current status of the database and ways forward to completing it were discussed. The accompanying report will organize, describe, and provide a summary of the database, highlighting research from CRC and non-CRC countries.

The next CRC plenary meeting (CRC-8) is scheduled to take place in 2025 and preparations are currently underway. During the meeting, the Program of Work (PoW) 2025 – 2026 will be discussed and adopted.

2.4 Information, knowledge and data management (IDKM)

National programmes for radioactive waste management require very large amounts of data and information across multiple and disparate disciplines of science and technology such as nuclear science, waste management, physics, chemistry, geoscience and engineering. Activities related to radioactive waste management are knowledge intensive, this knowledge is usually stored in institutional records and data. Most national legislations have regulations in place in line with international conventions, directives and recommendations governing the preservation of records on disposal of radioactive waste for use by future generations.

Numerous records and data are being created during the active lifetime of a radioactive waste repository, the pre-operational and operational periods, considered to embrace a period of upward 100 years /NEA 25b/ (see the different stages of a repository programme in Fig. 2.2). Additionally, RWMOs often find to have inherited legacy records that also require attention. Managing very large amounts of data and records requires considerable resources and reducing the large number of records to an essential set of records can increase the future accessibility and survivability of vital repository records. Thus, reducing the number of repository records to a manageable set makes perfect sense both from business and knowledge management perspectives.

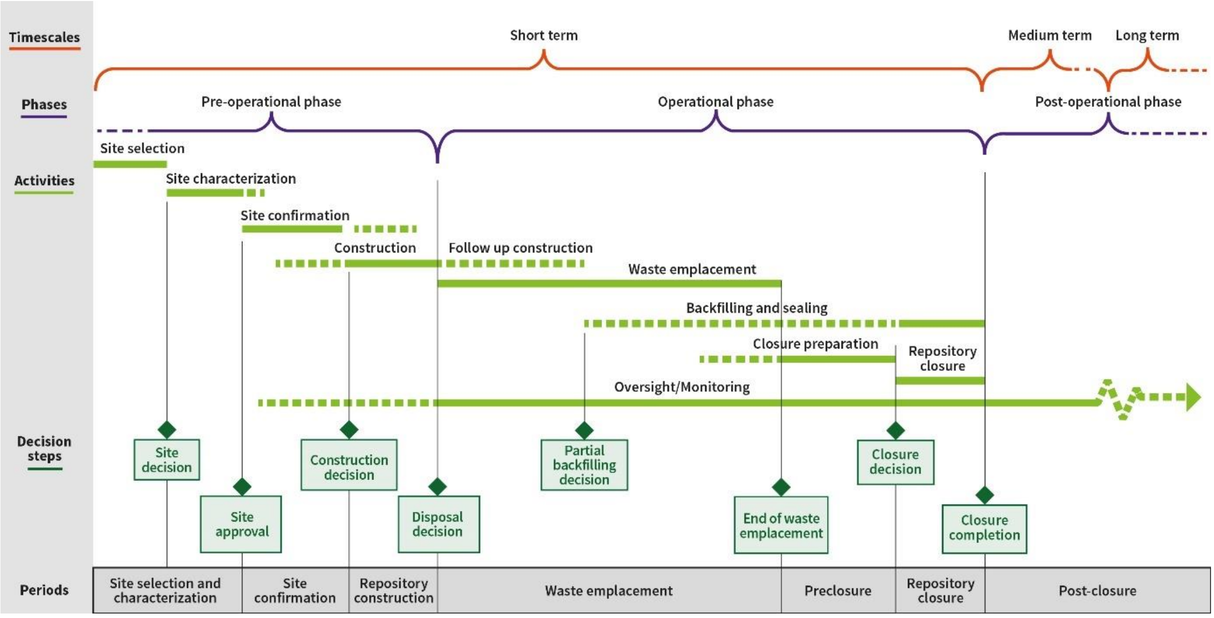

Fig. 2.2 Reference time frames and examples for important activities, periods and decisions during the implementation process of deep geological radioactive waste repositories /NEA 19/

Management of knowledge, information and data can be a critical issue in radioactive waste disposal and decommissioning. Planning, construction and operation of a repository involves large volumes of information over an extended duration. Information, data and knowledge about repositories must be accessible and understandable by multiple generations. Archiving and preserving information, data and knowledge for a timescale across many generations is a common challenge for all countries. Since 2019, international experts of NEA member countries have collaborated to address these problems /NEA 19b/.

The NEA's Radioactive Waste Management Committee (RWMC) established the Working Party on Information, Data and Knowledge Management (WP-IDKM) to examine the management of information, data and knowledge for radioactive waste disposal programmes. Various working streams with different tasks were created under the WP-IDKM, one of these tasks is to further develop the Set of Essential Records (SER) concept. Through these activities, the WP-IDKM strives to propose standardised approaches for managing information and data of radioactive waste and repositories. The working party also tries to identify solutions to minimise the risk of losing implicit knwledge.

The concept of a set of essential records (SER) was developed to assist radioactive waste management professionals in the selection of records deemed essential to aid future generations to make informed decisions. The SER should be understood as a wider collection of records that can aid post-closure generations evaluate repository safety. The SER includes records related to repository characteristics, design and performance and has been applied to national programmes and experiences. In the following key results from the NEA Expert Group on Archiving (EGAR) produced during the project phase under the working Party WP-IDKM, which have been published in /NEA 25b/ are presented.

Various guidance is made available in /NEA 25b/ relating the SER, a roadmap has been developed to assist with the SER selection process demonstrating how the generic SER method can be implemented with respect to national regulations and specific needs. It is advantageous to early in the program develop a roadmap to have from the beginning a clear vision about the roles and responsibilities of the different stakeholders, about which steps should be taken at which stage of the programme and start the first compilation of the SER not later than, when a site is selected. The SER implementation is also an evolutionary process during the construction and operational phase until closure of a repository. Due to its long duration and potential changes in perception and needs of the society SER categories and also the needs of future generations, which build a basis for the selection procedure, will require revisiting und, if necessary, updating at regular intervals.

2.4.1 Target audience of the SER

The size of the SER will depend on its purpose and particularly on its target audience, which are dependent on national boundary conditions and regulations /NEA 25b/. One key target group are generations living in the time after closure of the repository. For these generations the SER should serve as a tool to ensure an adequate understanding of the repository system and its performance. They should be enabled to review and verify the repository performance – for example by doing their own safety analysis – as well as to trace back decisions from the implementation process and to make informed decisions. If the SER is only focussed on this target group, its size will be low and the number of records might be in the range of few hundreds as for example indicated by a test application to records for the currently constructed ILW/LLW repository Konrad, Germany. Records from the Safety case will form a significant part of the SER. However, to keep the SER as understandable and compact as possible, not all records produced for a safety case need to be part of the SER. But also additional records are necessary particularly to trace back key decisions during the implementation process. By this the SER enhances the information and adds additional context to the safety case.

On the other hand, the SER may serve as a tool, where workers, scientists and other stakeholders can find answers for questions on their daily work during repository construction and operation. The advantage here is that the SER has an important meaning from the beginning on and organisations and experts involved directly see the advantages of the tool, particularly since significant effort and resources are needed to implement and apply the SER concept. It is obvious that in this case the number of records is significantly higher than in the former approach and will likely contain many more records than compiled in safety case, since more detailed information than in a safety case is needed for daily work related to the repository.

The Hungarian PURAM example considers both types of future generations by a system of marking records and data to be retained up until repository closure (for future generations of workers) and indefinitely (for future societies). Records that are no longer required after repository closure and which can be disposed of are marked as “retention until site closure”. Records data and information to be preserved for future generations of societies are marked as “preserve for indefinite period”. This way the repository records and data are preserved for reference during the consequent institutional oversight period and future generations of societies /NEA 25b/.

There is some agreement in international communities that quite detailed, technical information should be provided for future generations. Such information is usually written in scientific, technical reports or papers and therefore targeted to specialists like technicians or scientists. In addition, information should be preserved, which will serve social scientists and historians as a basis to retrace key decisions related to the repository and its implementation process. In general, all this information is a prerequisite for policy makers in coming to any well-founded decision related to the repository.

The situation as well as the perception of society living after repository closure is difficult to anticipate /NEA 25b/. It might happen that part of the information will just be recognized as a historical record from an ancient past and regarded as outdated. Every civilization tends to overestimate the objective nature of its own thought and this tendency is never absent (Claude Lévi-Strauss, 1962). However, this might be the case for some of the records, but one key idea of the SER is to provide technical information, which is not accessible for future generations or only with extremely high effort, like waste characteristics, materials used for the engineered barriers, exact locations of the waste and other facilities. Future generations might have further developed technologies, but it is unlikely (at least not guaranteed) that they will be able to identify without health risk or partly disturbance of the repository for example the radionuclide inventory of the waste containers. Therefore, the medium term is still seen as a very important target time frame of the SER. Fig. 2.3 summarizes and illustrates the availability and the target audience as a function of the time throughout the repository programme.

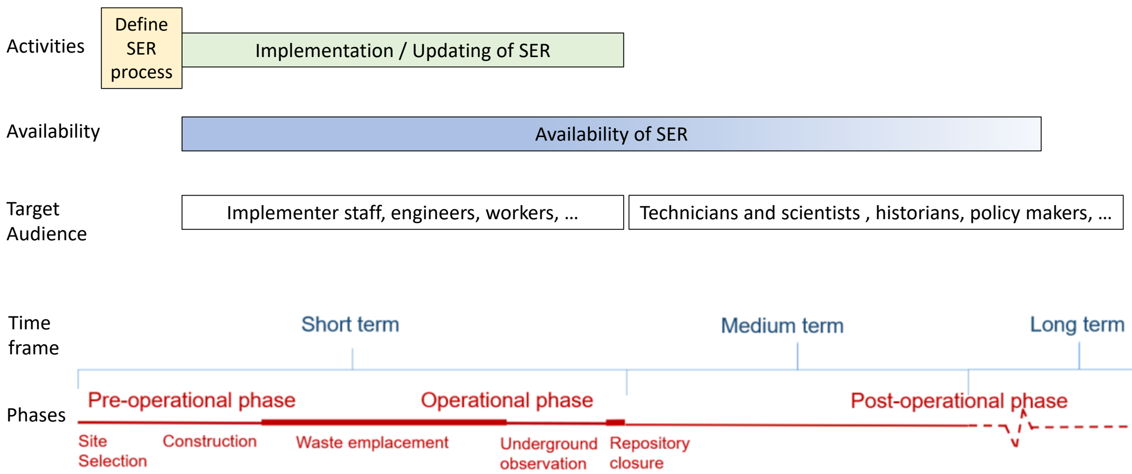

Fig. 2.3 Activities related to the SER, availability, target audience related to the time frames and repository phases /NEA 25b/

2.4.2 Roadmap for the SER

The main recommendation from the RK&M was that information and knowledge preservation initiatives should apply a diversified preservation strategy that integrates different methods with varying characteristics, with no single preservation strategy viewed as best. Further, it was emphasized that it is not just a question of handing down a message, but of keeping that message interpretable, meaningful, credible, and usable over long time periods /NEA 19/.

One of the key elements of the diversified preservation strategy is the Set of Essential Records. The constitution of the SER is a long-term process that may span several decades up to more than 100 years, depending on the active lifetime of the repository. The content of the SER will change during that period according to the continuing process of ongoing record selection, updating and review. It is advantageous to have from the beginning a clear vision about the roadmap, namely, which steps should be taken at which stage of the programme. A more general illustration of such a roadmap is given in /NEA 25b/; the key aspects are described in the following.

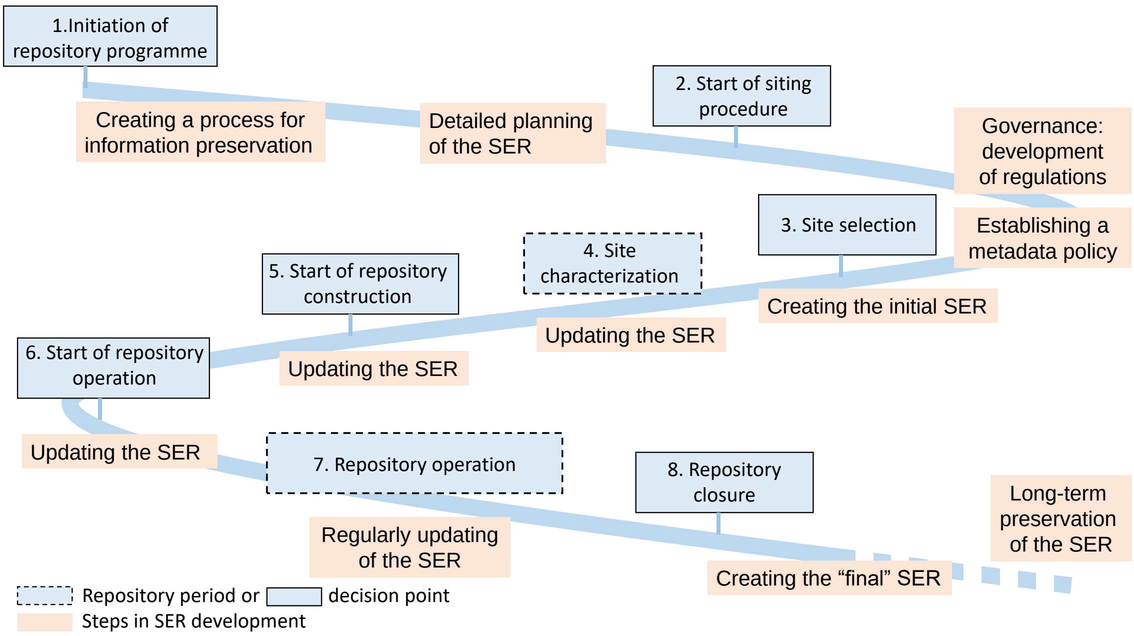

Fig. 2.4 Roadmap for implementation and maintaining the SER /NEA 25b/

The roadmap in Fig. 2.4 illustrates how the implementation of the SER is related to the different stages of the repository programme /NEA 25b/. With the initiation of a repository programme (1) it is recommended that a process and an organisational framework for information, data and knowledge management (IDKM) and preservation should be established including compliance to existing statutory framework and a strategy, policies, processes, knowledge management systems and tools. IDKM can contribute more to the success of the DGR programme if these systems and frameworks are established early.

The planning of creation and management of the SER should be done as early as possible in the repository programme to have methods and tools available when the siting procedure and therewith the production of essential records starts (2). During detailed planning of the SER a key aspect concerns establishing, tailoring the SER selection criteria and creation of relevant selection responsibilities. As proposed in /NEA 19/ to establish such criteria the intended audience for the SER and the potential needs of this audience have to be discussed and perceived. Based on such needs a categorisation scheme can be developed and applied for the selection of essential records. It must become clear, which organisation / organisational unit is responsible for the record selection and structures, rules as well as resources must be implemented to enable a successful SER selection process. Even authors of records produced for the repository programme should be sensibilized and urged to provide information, metadata, necessary for the SER identification. Legal requirements of the respective country may of course influence the selection process. After the planning phase respective governance and regulations should be developed to guide the processes and to set the responsibilities /NEA 25b/.

At the time of site identification and selection (3), it is recommended to have selection criteria for data and records available and to assign ownership of data and records, including metadata policies for data and records. It is important to establish process and system requirements for storing SER metadata. Metadata adds context to the records and supports records finding in record management systems, understanding and use of records and data and therewith ensures the continued usability and value of records and datasets over time. Indicating in the record’s metadata that it is considered SER should support the preservation of the record.

The creation of the SER should be started early in the repository programme, to avoid loss of records produced in the early stage, which are seen as important for the SER. A start before the selection of a site may create a high effort for selecting and subsequently rejecting an extremely large number of records. Thus, a suitable point in time might be when the decision about a site is made (3). However, it should be kept in mind that some essential records will likely already be created before site selection.

A large amount of geological and hydrogeological information will be created during the site characterisation (4), when also existing information might become outdated or need to be adjusted due to new insights from underground characterization, making a first update of the SER meaningful. The next update is then expected to be connected with the next decision step, namely the license application for construction (5).

The SER will develop then during the repository lifetime. More and more records become available and older ones may become outdated at the different stages of the programme. Thus, multiple updates of the SER are required. This implies that versioning, adoption and following relevant standards and/or internal policies on document and record versioning is key to ensure that up-to-date information is used and therewith to guarantee transparency and traceability of the SER.

During construction until the next license step for operation (6) and particularly during operational phase (7), which will last for several decades of the repository a large amount of data and records is generated and used to populate the SER, describing the as-built state of the repository. Thus, during repository operation a regularly update of the SER is recommended.

Repository closure (8) likely encompasses transfer of responsibility implying significant changes that affect the SER such as changes in the ownership of the associated records and data. Thus, there is a need for substantial knowledge transfer, preservation, and archiving activities. Besides the creation and maintenance of the SER, important questions are related to its storage and preservation: e.g. on what type of media and where the SER should be kept. With respect the preservation of the SER during the repository's lifetime, electronic media have the advantages of providing high data storage, simple and efficient search functions and multiple copies and can be used by more than one person at a time, even in different geographic locations (NEA, 2019a). However, the situation becomes different after repository closure. At the time of repository closure, it is likely that organisations such as the implementer and with that the storage option of the SER at the implementing organisation will no longer exist. At this time a nearly final version of the SER should be available and prepared for long-term preservation. Some information sampled and compiled after repository closure, e.g. from monitoring, might be added in the final version.

At that stage dedicated archives/information centre would facilitate the findability, accessibility, interoperability and reusability of its records, data, objects, and artefacts according to current and anticipated future user needs. As a measure of post-closure/indirect oversight, the ongoing preservation strategy should be examined and adapted if needed at determined regular time intervals. This examination includes an inspection of the review process itself, so that it is perpetuated in an efficient and resource-sensitive manner.

However, for long-term preservation over several 100 years or more after closure a successive information transfer from generation to generation (mediated transfer) cannot be guaranteed. Therefore, additionally, a direct, non-mediated transfer of the SER to future generations should be foreseen. Beside memory institutions, which comprise archives, museums, and libraries, in particular (national) archives are seen as important due to their long-term mission to permanently preserve collections of records for future generations. There are also other long-term storage mechanisms as time capsules which might be located at the abandoned repository site or another prominent places (NEA,

2019) to transfer the information to future generations. For such a long-term preservation digital media are not recommended due to their relatively low durability and the need for permanent maintenance, updates or upgrades of hardware and software tools /NEA 19/.

Moreover, it is recommended to create an SER explanation document, supplementing the SER /NEA 25b/. This document should be capable in assisting future professionals to understand the context, the underlying assumptions and reasoning against which the SER was compiled and to assist these future professionals to assess and understand the information that can be accessed from the SER. Such a document should also be created early in the repository programme and updated with each update of the SER itself. In the long-term after repository closure, it might be distributed much wider than the SER and can point to the location of the SER.

2.4.3 Application of SER concept to records from Konrad repository

The application of the SER selection procedure to the records related to the repository programme of Konrad mine in Salzgitter, Lower Saxony, Germany, was done to identify any shortcomings of the proposed procedure, to check whether specific tools can contribute and to evaluate how far the process can be automatised /NEA 25b/. The intention was not to create a complete SER for Konrad. The repository is in the state of construction; in this respect, the application procedure considers the construction phase with all its specific characteristics resulting from the fact that a large number of records were created more than 30 years ago but no waste has yet been disposed of.

At the time of the first working group meeting on application of the SER selection procedure to the records for the Konrad mine (Status: 7 July 2021), 77 016 records were available in the RMS for Konrad. The records belong to 228 different record types, including, among others, correspondence with different organisations, minutes of meetings, reports of different types and various other records like administrative, maps, profiles, descriptions and court records.

It was decided to start the SER selection procedure with the following three record types: reports, interim reports and final reports. At the start of investigation, there were 4 866 such records. For the SER selection procedure, for each record, the following information was extracted into an Excel table: date, title, author, information, whether the report is a record for license application (y/n) or an explanatory record for license application (y/n).

Most documents in the existing database are pdf files. However, at the time of application there was a considerable number of records available only on paper (non-digitised) or as TIFF or jpeg files, i.e. non-searchable. Furthermore, the existing RMS did not contain metadata to be used for filtering records of specific content. This specific characteristic for the Konrad site is due to the fact that many of the key documents are more than 30 years old. However, BGE is now transferring the existing records into a new RMS to improve this situation. An additional consequence/challenge of the significant number of key records that are more than 30 years old is that most authors are no longer available.

A key question addressed in /NEA 19/) was how to identify a reduced set of records, keeping the information preserved for future generations clear, transparent and traceable. The RK&M initiative developed an example procedure based on representative needs of future generations related to the repository. It is driven by balancing the requirements to keep the SER as small as possible for clarity and traceability and to provide as much information as possibly necessary for future generations to fulfil their needs. The three needs proposed in /NEA 19/ are that future generations may want to:

1. Perform their own long-term safety assessment.
2. Trace back decisions from the implementation process.
3. Retrieve material from the repository.

The procedure is based on the assumption that the anticipated needs are representative for future generations. It is worth mentioning that in regulations in some countries like France or Germany, the possibility to retrieve the waste from the repository is required. In France, the disposal must be reversible for at least 100 years.[1] In Germany, it must be possible to recover heat-generating high-level waste (HLW) for 500 years after repository closure.[2] Therefore, the implementer must ensure that all records necessary for retrieving the waste 500 years from now be available for generations living at that time. It should also be noted that, although the three needs including retrieval from material from the repository were considered, there is no regulatory requirement for the Konrad repository to enable retrievability or recovery of waste.

[1] Article 12 of the Programme Act No. 2006-739 of 28 June 2006

[2] Section 26 of the Repository Site Selection Act of 23 July 2013

The example selection procedure proposed here is based on a classification and rating scheme. The procedure then comprises the application of this scheme to an extensive list of records produced during the repository programme. The proposed classification and rating scheme comprises the relevance of the respective record for the formulated need of the future generation and an estimation of the effort it would take for a future generation to recreate the information contained in the record (i.e. if record transfer from the past fails).

With respect to relevance, the four record categories are: not relevant (0), nice to have (1), should have (2) and must have (3) (see /NEA 19/ for details). Concerning effort, two categories have been distinguished: (a) “Without this record, the information can be obtained by future generations with some effort” and (b) “Without this record, the information can only be obtained by future generations with extreme difficulty or cannot be directly obtained at all”. The selection of essential records is proposed to include all records classified in the two “must have” categories and the “should have” category (2b).

Tab. 2.1 Classification and rating scheme for the selection of records for the SER /NEA 19/

Relevance/effort		a) Some effort	b) Extremely high effort
Not relevant	0		
Nice to have	1		
Should have	2		SER
Must have	3	SER	SER

Note. For final selection, the highest rating of each of the three needs is used.
Source: NEA (2019a).

Applying this approach to the Konrad records, relevant information available for each record – the publication date, the report title, the author(s), the identification number and the information, and whether the report had been part of the records submitted for the license application – were compiled in an Excel table. This table contained 4788 reports. In a group of mainly technical specialists from BGE and GRS a large number of these records have been evaluated using different approaches and categorized in the scheme illustrated in Tab. 2.1. All details are described in /NEA 25b/. In the following the lessons learned are summarized.

The application of the generic SER selection procedure /NEA 19/ to the records from the Konrad repository and the related discussions highlighted a number of interesting aspects /NEA 25b/. The objective was to apply and test the applicability of available procedures and tools for identifying essential records from the vast amount of existing Konrad records. The Konrad case clearly shows how important it is to:

- develop a strategy for the creation of a SER and start the SER selection process at an early stage in the repository programme;
- clearly define the objectives of the SER in advance, since it has an impact on the selection process;
- have a suitable and advanced RMS available;
- involve experts from different fields in the SER planning and selection;
- improve report writing by keeping the SER in mind;
- keep some flexibility in the SER selection and management process due to its long duration and potential changes in perception and needs of the society, but have clear rules for updating the SER;
- allocate resources and staff for the tasks related to the creation and management of the SER.

Early planning of the SER creation and management process avoids the loss of records and inefficiency since records might be rather old and authors no longer available for support if questions on the content or objectives of the respective record arise. This was one key experience from the evaluation of the Konrad example, since the majority of essential records were created more than 30 years ago.

Clearly defining the objectives of the SER, including the audience and target time frame, is highly important for framing the selection procedure. If – as decided by the group here – the main focus is to deliver knowledge to future generations living far in the future when the repository is already closed, nearly all the records related to repository operation can be disregarded and a related flow scheme can be applied to identify these records. This means that in this case, the SER is not seen as a tool for workers, scientists and other stakeholders to find answers for questions on their daily work. The organisation's RMS (expected to be available until repository closure) should be used. But the SER can be used to train new members of the involved organisations and provide a compact overview on the key features and decisions related to the repository and the safety case.

The SER selection procedure is based on the needs of future generations, which are assumed to be representative based on today's knowledge and skills. It is an ongoing discussion that these needs and perceptions of generations can and will change. Based on this perspective, the start of SER creation should be done as late as possible during the repository programme, which is contradictory to the recommendation to start the SER selection process as early as possible to not loose important records and spend too many resources sorting records, as mentioned above. One solution might be to start the SER selection process early but keep some flexibility. The needs of future generations (being the basis of this process) should be questioned regularly, e.g. in connection with the regular review of the SER and extended if evidence for additional needs are given. It is not expected that the proposed needs are no longer valid in the future. They have been robust for more than 30 years.

The selection procedure for the SER could be a continuous process, namely classifying new records once they are finalised, when they are received by the responsible organisation and transferred into the RMS. The experience from the Konrad records showed that it cannot be done by one person alone but requires a discussion between experts from different fields, particularly from safety assessment, geology and engineering fields. So far, an automatised process could not be established, but supporting tools like a general flowchart, RepMet and FEP tables have been tested. Therefore, it is proposed that a dedicated, well-trained core team at the responsible organisation (aware of these tools), with support from the main author, take the decision about whether the record is included in the SER or not. In addition to such a continuous process there should be a regular review procedure by a multidisciplinary team, where the whole SER is checked and updated.

For several records, the content or objectives were not clear and together with the fact that a fraction of the records was not available in a digitally readable format, the selection process was very inefficient. To improve the efficiency of the record selection procedure, it is recommended to improve reports created during the repository programme: The report title should contain precise information about its specific content, whether it is a final or interim report (include versioning), and whether it contains results or simply describes the planning of an activity. Moreover, it is suggested that the summary or abstract of the report include the purpose of the record, its relation to older records on the same topic and the relevance of the record for the needs of future generations.

Further, a good basis for an efficient selection and management of the SER is an adequate RMS. Using a machine learning system could even help in the SER selection process. This will be tested for the Konrad records, since these are currently transferred to a system based on the code iFinder.

The exercise also showed the dynamics of the SER selection process and that it will change during the different stages of the repository programme. One example is the database for describing the waste to be disposed of in Konrad. At the stage of repository construction, the exact extent and structure does not yet exist in their final state. This will, of course, be the case when repository operation starts.

Finally, the creation and management process of the SER requires staff and resources at an early stage of the programme. The organisation responsible for the SER should foresee this in the planning of budget and human resources.

3 Specific Safety Case topics

3.1 Uncertainty and sensitivity analysis – The JOSA exercise

Numerical model calculations are the only method to investigate the contaminant release from a repository over very long time periods, and therefore play an important role in the Safety Case. Apart from uncertainties about the models themselves and their correctness in describing the relevant processes, such calculations are subject to significant uncertainties originating from random-influenced effects and conditions (aleatory uncertainties) as well as from lack of knowledge about the input parameters (epistemic uncertainties). Probabilistic uncertainty and sensitivity analysis is a widely accepted means for handling uncertainty in model calculations. For some decades, triggered by the increase of computational power, sensitivity analysis (SA) is a focus in mathematical research, and a variety of methods have been developed. The international working group JOSA (Joint Sensitivity Analysis Exercise), which was established in 2017, has been dealing since then with investigating approved and modern mathematical methods of probabilistic sensitivity analysis in the context of repository performance assessment.

The active JOSA group consisted of teams from 7 organisations:

- Sandia National Laboratories (SNL), USA,
- TU Clausthal (TUC), Germany
- GRS, Germany,
- SCK*CEN, Belgium,
- POSIVA/Fortum (Finland),
- Universidade da Coruña (Spain),
- IBRAE (Russia, until Feb. 2022).

The JOSA participants identified a number of model cases for which complete sets of probabilistic evaluations already existed, it was unwanted to perform model calculation runs explicitly for the JOSA exercise. Due to this precondition, all SA methods that require some specifically tailored sampling were excluded from the investigations.

In the first phase of JOSA, four relatively simple model cases were investigated that show a rather smooth and predictable behaviour. The results are documented in /SWI21a/. In the second phase three more complex models with specific properties like nonlinearity, non-continuousness or bimodality were considered in order to investigate the performance of different SA methods when applied to such systems. One of these systems was the salt LILW model already investigated in /SPI 17/ and /NOS 21/, another one was the Crystalline Reference Case of SNL as described in /SWI 21b/. The third one, which was not investigated by GRS, was a Reactive Transport Model elaborated by University of La Coruña (UDC).

The second phase of JOSA concentrated on more sophisticated SA methods, some of them based on metamodeling, in order to investigate higher-order sensitivities, or, generally spoken, influences of parameter interactions. Moreover, some newer techniques like Feature Importance Measures or Shapley Effects were investigated with these systems.

The work of GRS in this context was concentrated on the investigation of

- Second- and total-order sensitivity analysis of the salt LILW case (GRS) and the crystalline reference case (SNL) using different metamodeling techniques,
- Investigation of the PAWN method /PIA 15, PIA 18/ for calculating sensitivities based on CDF distances.

The work is documented in detail in the JOSA report, Volume 2 /SWI25/. Since this is a comprehensive presentation of the complete exercise, covering most of the relevant investigations performed by GRS, we abstain from repeating details here and give just a short summary. Moreover, we show some results of numerical experiments that are not documented in the JOSA report.

3.1.1 Particularities of the investigated model systems

The investigations were made with the two model systems mentioned above. These were selected as particular challenges to the different methods of sensitivity analysis, since they exhibit some properties that might have disturbing effects on proper sensitivity analysis, specifically when using metamodels.

3.1.1.1 The LILW case

The model is described in /SPI 17/. It calculates the time-dependent annual dose resulting from the release of radionuclides from a repository for low- and intermediate-level waste (LILW) installed in an abandoned salt production mine. It was motivated by a model developed for investigation of the Morsleben repository /BEC 09/, but is not identical to that model and describes a hypothetical repository.

A schematic of the model structure is presented in Fig. 3.1. The near field part consists of sub-models for two emplacement chambers (AEB and NAB), one of which is sealed from the rest of the mine (AEB), a mixing region (MB), and a large area of mine openings without waste (RG). The model exit, located in the mixing region, is coupled to a far field model, which calculates the contaminant transport through a pathway in the cap rock and the aquifer, and finally to a biosphere code determining the radiation exposure in the form of the annual effective dose to an adult human individual.

In reality, there would be a slow intrusion of brine to the mine building, causing a gradually increasing rise of the fluid level and a time-dependent dissolution of contaminants. However, for simplicity it is assumed that the non-sealed part of the mine is filled up with brine instantaneously at some specific point in time. From then on, the brine seeps slowly into the sealed emplacement area AEB.

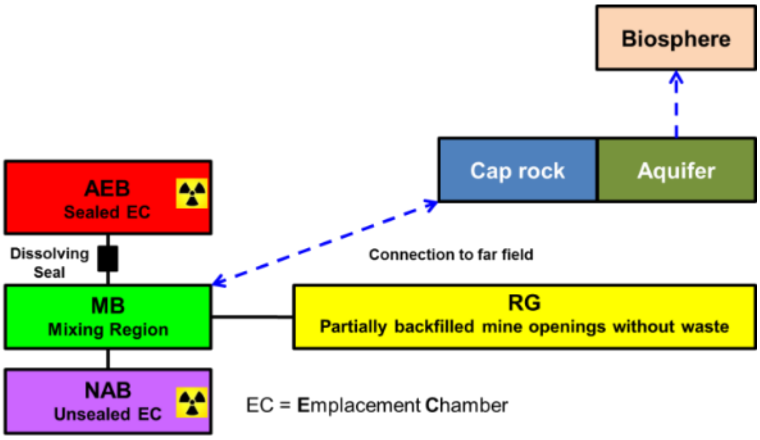

Fig. 3.1 Schematic view of the components of the LILW system

The most peculiar feature of the model is the seal between AEB and the mixing region, MB. It represents a sealing construction made of salt concrete, which is subject to chemical dissolution (corrosion) by magnesium-containing brine. As the corrosion front is assumed to proceed slowly through the material, the seal loses its isolation capability nearly suddenly at some point in time, resulting in an essential change of the model behaviour and usually a considerable increase of the radiation exposure. The time of seal failure depends on several parameters, so that, analyzed at a specific point in time, the model behaves nearly non-continuously with respect to some of these parameters.

The model was set up to be calculated with the RepoTREND package /REI 16/, using the modules LOPOS, GeoTREND-SP and BioTREND.

Tab. 3.1 lists the parameters of the model with their distributions and base values. The model was investigated with 6 and 11 parameters, as indicated by colours.

Tab. 3.1 Parameters of the LILW model

Parameter	Type of pdf	Range or pdf parameters	Standard value
GasEntryP: Gas entry pressure [MPa]	Uniform	0 - 2.5	2.0
IniPermSeal: Initial permeability of dissolving seal [m²]	Log-normal	μ=41.0605 σ=1.9809	$1.0 \cdot 10^{-18}$
RefConv: Reference convergence rate [1/yr]	Log-uniform	$1.0 \cdot 10^{-5}$ - $1.0 \cdot 10^{-4}$	$4.0 \cdot 10^{-5}$
AEBConv: Factor of local convergence variation in AEB [-]	Log-uniform	0.05 - 5.0	1.0
GasCorrPE: Organics corrosion rate [1/yr]	Log-normal	μ=12.6642 σ=1.1177	$1.0 \cdot 10^{-5}$
TBrine: Time of brine intrusion [yr]	Log-normal	μ=8.8857 σ=0.6933	7500
BrineMgSat: Relative magnesium saturation of brine [-]	Triangular	0 - 0.1 - 1.0	0.1
RGConv: Factor of local convergence variation in RG [-]	Log-uniform	0.25 - 2.5	1.0
GasCorrFe: Metal corrosion rate [1/yr]	Log-normal	μ=-6.6728 σ=1.1177	$4.0 \cdot 10^{-3}$
AEBGasProd: Proportion of the material involved in gas production in AEB [-]	Triangular	0.1 - 0.8 - 1.0	0.8
NABGasProd: Proportion of the material involved in gas production in NAB [-]	Triangular	0.1 - 0.8 - 1.0	0.8

3.1.1.2 The SNL generic crystalline case

This generic case study has been described in extensive detail in the following Sandia reports /SWI 21b/, /STE 17/, /SEV 18/, /MAR 16/. This specific example is taken from the version of the generic crystalline reference case described in Chapter 4 of /SWI 21b/.

A key aspect of the SNL generic crystalline case was the generation of 25 distinct Discrete Fracture Networks (DFN) to represent a range of realizations of the subsurface. Each DFN was generated using a specific process. The fractures are parameterized in terms of their radius r and orientation θ, the fracture intensity P_{32} [m^2/m^3], and the relationship between fracture transmissivity and fracture size. The dfnWorks software developed at Los Alamos National Laboratory /HYM 15/ was used to generate discrete fracture networks based on these statistical distributions and the DFNs were then mapped to an equivalent porous medium representation to populate the input mesh to PFLOTRAN. The properties of the DFNs were loosely based on the Forsmark case /JOY 14/

There are thousands of fractures in each DFN. To summarize global properties of each DFN, three graph metrics are employed. The underlying representation of a DFN is a graph where nodes represent fractures and edges represent intersections between the fractures. The graph metrics are summary statistics based on the graph representation which can be used in sensitivity analysis to account for the uncertainty represented by the DFNs. These are:

- STT: The relative shortest travel time between repository and aquifer,
- aveDegree: Average number of inter-sections per fracture. A measure of how connected the network is over the entire domain,
- Intersections: Number of fractures intersecting the repository. A measure of number of potential flow pathways out of the repository region.

The uncertainty analysis comprises a spatial loop of sample size 25 fracture network realizations, and a parameter loop of sample size 40 for a total of 1000 simulations. At a high-level, this sampling structure is shown in Fig. 3.2.

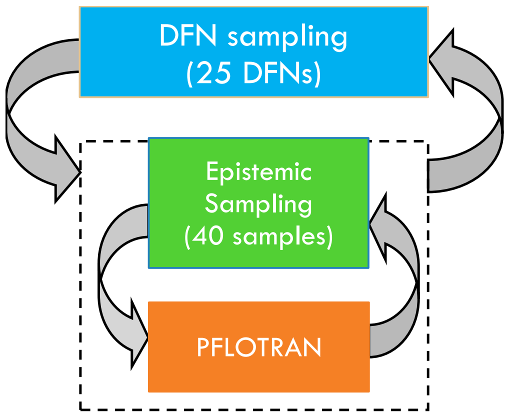

Fig. 3.2 Overall sampling structure for the SNL crystalline case

The epistemic uncertainties with their assumed distribution types and parameters are explained in Tab. 3.2. Several quantities of interest were defined but only one of them, the peak I-29 concentration in the aquifer, was considered in the investigations presented here.

Tab. 3.2 Epistemic parameter descriptions and distributions

Input	Description	Range	Units	Distribution
rateUNF	Fractional dissolution rate of spent (used) nuclear fuel	$10^{-8} – 10^{-6}$	yr^{-1}	log uniform
kGlacial	Glacial till permeability	$10^{-15} – 10^{-13}$	m^2	uniform
pBuffer	Buffer porosity	0.3 – 0.5	-	log uniform
permDRZ	DRZ permeability	$10^{-19} – 10^{-16}$	m^2	log uniform
permBuffer	Buffer permeability	$10^{-20} – 10^{-17}$	m^2	uniform
meanWPrate	Mean of the waste package corrosion rate	-5.5 – (-4.5)	$\log(yr^{-1})$	log uniform
stdWPrate	Standard deviation of the waste package corrosion rate	0.15 – 0.4	$\log(yr^{-1})$	log uniform
IRF	Instant release fraction	0.038 – 0.156		uniform

3.1.2 Selected results

This chapter presents some results that were obtained by GRS with different methods applied to the output of the two models.

3.1.2.1 Methods applied

Since there are already detailed investigations with regard to main sensitivity effects (/SPI 17/, /NOS 18/, /NOS 21/), here we concentrate on investigation of higher- and total-order effects. These are due to parameter interactions: A parameter that has little influence on the model alone can become important together with another one. This is captured by the variance-based sensitivity indices of higher order (/SWI 21a/). The indices of total order calculate by summing up the indices of all orders that contain interactions with one specific parameter. They quantify the total importance of a parameter, alone or in combination with any group of others. Robust calculation of higher- and total-order indices of complex models, however, is a challenging task.

The RS-HDMR approach is based on meta-modelling and can compute sensitivity indices of first, second and total order using any type of sample. A short description of the method with further references is provided in /NOS 18/. RS-HDMR estimates the first- and second-order variance-based sensitivity coefficients. A rough approximation for the total index of a model parameter is obtained by adding all first- and second-order indices that incorporate this parameter. Higher orders of interaction are neglected. Therefore, this method leads to underestimating the total indices.

The Bayesian Sparse Polynomial Chaos Expansion (BSPCE) method uses a Bayesian approach to build a sparse PCE, which only considers the significant polynomial terms for the data set at hand to catch the main characteristics of the model output. This may only require a small number of basis functions and polynomial chaos (PC) coefficients and thus a small number of simulations to calculate the sparse PC coefficients. BSPCE provides first and total-order indices. More details on the algorithm and the different mathematical equations of the PCE and Bayesian approaches can be found in /SHA 17/.

As a third metamodeling approach, PCE with least angle regression (LARS), implemented in the DAKOTA software by SNL, was applied. This approach can calculate first-, higher- and total-order sensitivity indices. It is described in /ADA 22/.

For the investigations, the Sobol-GSA software by S. Kucherenko and O. Zaccheus (for RS-HDMR and BSPCE) and the DAKOTA software (for PCE-LARS) were used.

The RS-HDMR approach needs to be adjusted using the parameters k and $l = l'$, which denote the maximum polynomial orders considered in the approximation, for the first and second order of interaction, respectively. These parameters must be chosen with care, and a bit of experimentation can be helpful. If too low values are taken, the representation of the original model is insufficient; if taken to high, however, overfitting artifacts can strongly disturb the sensitivity evaluation and lead to wrong results. For the tests presented here the maximum polynomial orders k = 10 and $l = l'$ = 4 proved to be reasonable in most cases. The PCE-LARS method also needs adjustment via the maximum polynomial order taken into account, which acts in a similar way.

3.1.2.2 LILW6 model

The following investigations were made using the LpTau-set of 16384 model runs of the LILW model with 6 parameters.

In Fig. 3.3 the results of three different methods for calculating total indices (SIT) are presented. For RS-HDMR the polynomial orders 10-4 were used[3], which in preceding experiments had turned out to be a reasonable setting for this case. One cannot generally recommend a specific choice of these values since the optimum depends on the behaviour of the model.

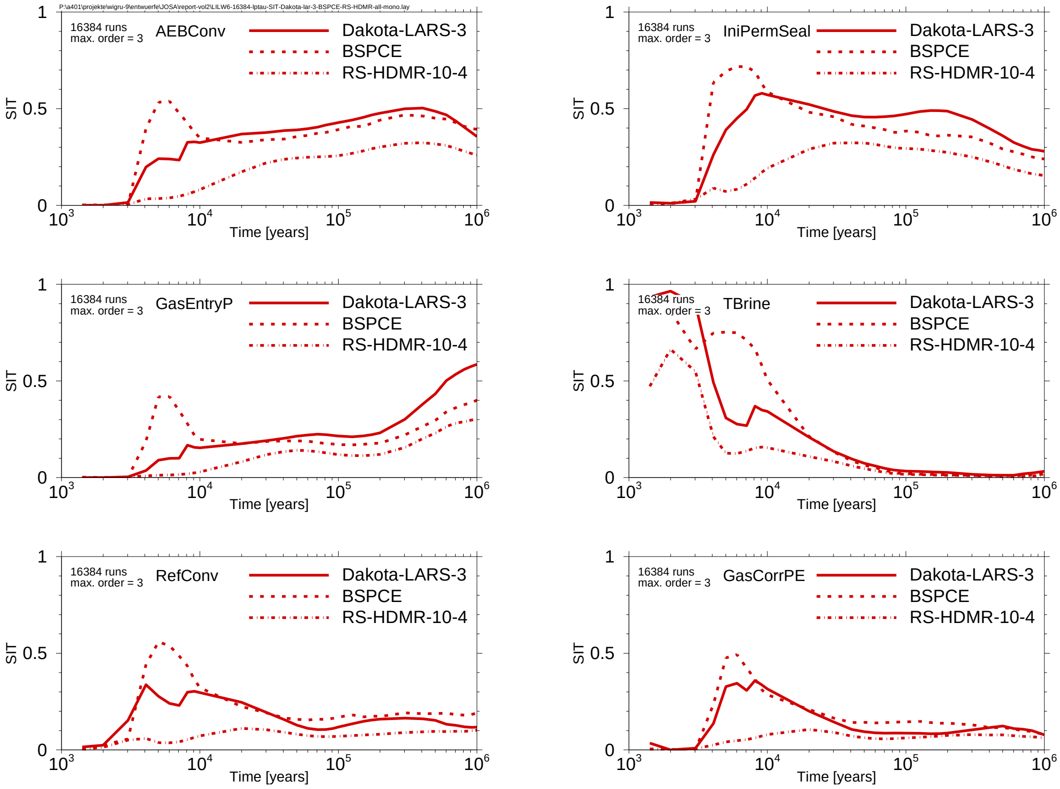

Fig. 3.3 Total-order indices of the LILW6 model, calculated with three different methods

The results of the three methods are qualitatively similar to each other but not in full agreement. In the early phase, where the majority of runs yields zero (or very low) output, BSPCE calculates high total sensitivities for all parameters, RS-HDMR, however, calculates low sensitivities. The results of PCE-LARS are somewhere in between. The parameter TBrine dominates the early phase as it determines whether there will be a non-zero dose at all. In this phase, the total variance of the model output is rather low, so that the sensitivity indices are not very significant. Obviously, the total indices are not robust under such conditions and depend to a high degree on the method of calculating the

[3] For brevity, we use the notation k-l for the polynomial orders. It is always $l = l'$.

indices, even with this high number of simulations. It is conspicuous that RS-HDMR generally calculates significantly lower SIT values than the other methods, which could be a hint that third- and higher-order interactions, which are neglected by RS-HDMR, play a relevant role.

The most relevant second-order indices, calculated with RS-HDMR and PCE-LARS, are presented in Fig. 3.4.

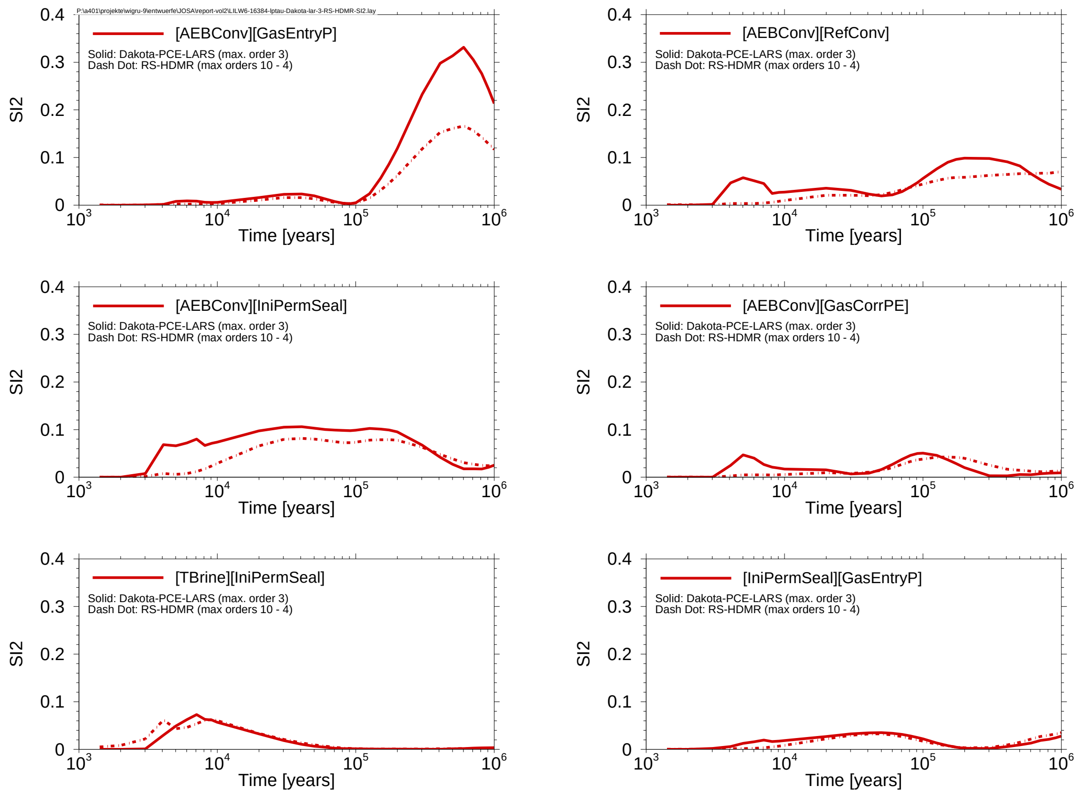

Fig. 3.4 Second-order indices of the LILW6 model, calculated with two different methods. Only the most relevant parameter interactions are presented

The results of both methods fairly agree, although there are differences mainly in the early phase. The most conspicuous difference at late times is the interaction between AEBConv and GasEntryP, which is assessed up to twice as high by PCE-LARS than by RS-HDMR. This interaction can be understood as follows: The gas entry pressure has a nearly binary influence in that its value decides whether gas can escape from AEB (GasEntryP < 1.0 MPa) or not (GasEntryP > 1.0 MPa). While in the former case, the contaminated brine remains widely in AEB, in the latter case it is pressed out from AEB through the seal by the increasing gas pressure. This can make a significant difference in dose rate. If the gas entry pressure is below 1.0 MPa, the convergence rate of AEB does not play a big role, but for a gas entry pressure above 1.0 MPa, it controls, together with the gas generation rate, the outflow of brine and contaminants.

The interaction between GasEntryP and AEBConv seems to be the most significant parameter interaction at all, but the interaction between AEBConv and IniPermSeal is more relevant in the medium time frame.

3.1.2.3 Search curve methods

This section describes an experimental investigation, which is not documented in the JOSA report and has still a preliminary character. Results have been presented on the SIAM-UQ 2024 conference /SPI 24/.

The idea is a generalization of the approach underlying, e. g., the EASI method /PLI 10/: an existing set of input-output-realizations is rearranged so that the input follows a periodic sequence plus some noise. A Fourier analysis of the rearranged output detects the input frequency and its harmonics while the noise is widely filtered out. Variance-based sensitivity indices of first order can then be calculated from the Fourier coefficients. In the generalized multi-dimensional form, instead of a sequence in one dimension a “search curve” is defined in the subspace of interest so that it covers this subspace as well as possible, and the points in the input space are rearranged to follow this curve. Spectral methods require search curves with a pronounced periodic behaviour with separable frequencies, see Fig. 3.5. This principle is the basis for the QEASI method, which is able to calculate second-order indices directly from the data and without the necessity of a metamodel. Other methods apply search curves with local neighbourhood, as resulting from the solution of a travelling salesperson problem and use localized estimators for the variance. Sensitivity indices can be estimated through the local variance of neighbouring points.

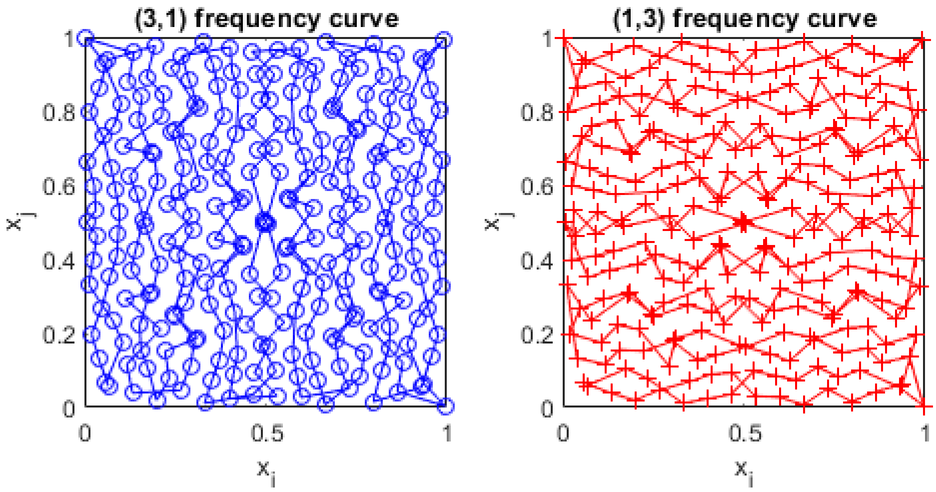

Fig. 3.5 Possible search curves in two dimensions

In the following, some results are shown and compared with those from metamodel methods. These results are based on the dataset with 16384 random-sampled runs.

In Fig. 3.6 the first-order or main effect indices, calculated with different methods, are presented. The left side of the figure shows that QEASI and the standard version of EASI calculate nearly identical values for the first order. On the right side, these results are compared with those from the RS-HDMR method with polynomial orders 10^{-4} and from PCE-LARS with maximum order 5. While RS-HDMR and EASI/QEASI are in good agreement, PCE-LARS calculates considerably higher values, but conveys the same messages regarding the relations between the parameter and the time development.

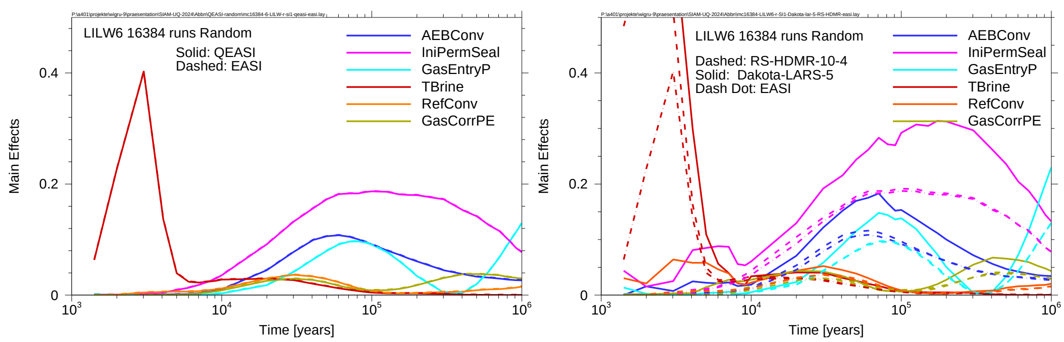

Fig. 3.6 Main effect indices of the LILW6 model, calculated with QEASI and EASI (left) and metamodel methods (right)

The second-order indices for the most relevant parameter pairs are presented in Fig. 3.7. The QEASI method calculates a matrix with the main effects in the diagonal and second-order effects in the non-diagonal elements. Theoretically, the matrix should be symmetric but in practice, its lower-left and upper-right parts differ slightly, since the algorithm depends on the order of the two considered input parameters. In the left part of the figure, both parts of the matrix are shown to visualize this difference. The right part presents the results of RS-HDMR with polynomial orders 10^{-4} and those of PCE-LARS with maximum order 5. Again, RS-HDMR is in good agreement with QEASI, while PCE-LARS calculates higher values but conveys the same general message.

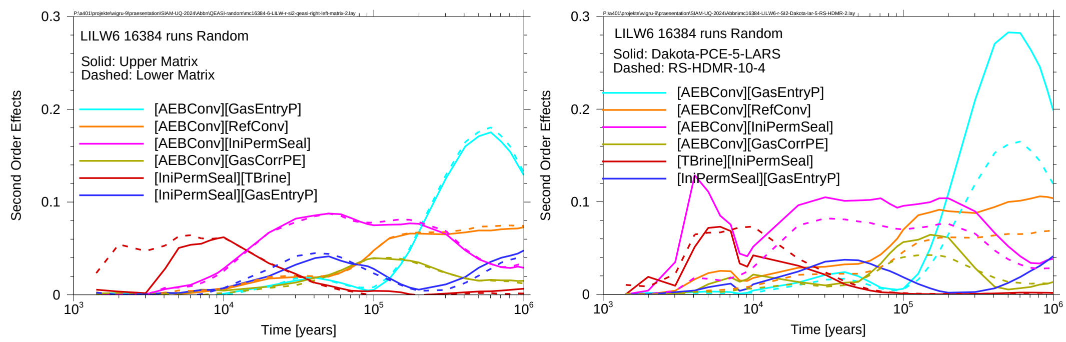

Fig. 3.7 Second-order indices of the LILW6 model, calculated with QEASI (left) and metamodel methods (right)

The investigations seem to show that QEASI is well appropriate to calculate second-order indices and provides a methodologically simpler and numerically cheaper alternative to metamodel-based approaches. Other search-curve-based methods, which make use of different local sensitivity measures, have also been considered, but this is ongoing work and not presented here.

3.1.2.4 SNL crystalline case

Investigations with metamodel methods were also carried out with the output of the time-independent crystalline case model. 1000 runs of the model were available, 40 for each of the 25 DFNs. For evaluation, one can either include the DFN graph metrics in the parameters list or consider the DFNs as a random influence as a whole without looking at the parameters used to generate them.

Fig. 3.8 depicts total effect indices estimated from a RS-HDMR metamodel with different polynomial coefficients for peak I-129 concentration excluding and including graph metrics. Without graph metrics, reasonable index values can be obtained with the lowest polynomial coefficient (1-1, 2-1, 3-1, 4-1 and 10-1). The most important parameter is rateUNF, kGlacial is less important. With graph metrics considered, there are more differences across the choice of polynomial coefficients. The rateUNF parameter is only found important with the lowest polynomial coefficients of 1-1 and 2-1.

If the graph metrics are taken into account, they dominate the sensitivity analysis. Apart from them, only rateUNF seems to have some influence. Obviously, the DFN, which is largely determined by random factors, is by far most influential to the system. If the graph metrics are left out, this influence acts like a pure random variation.

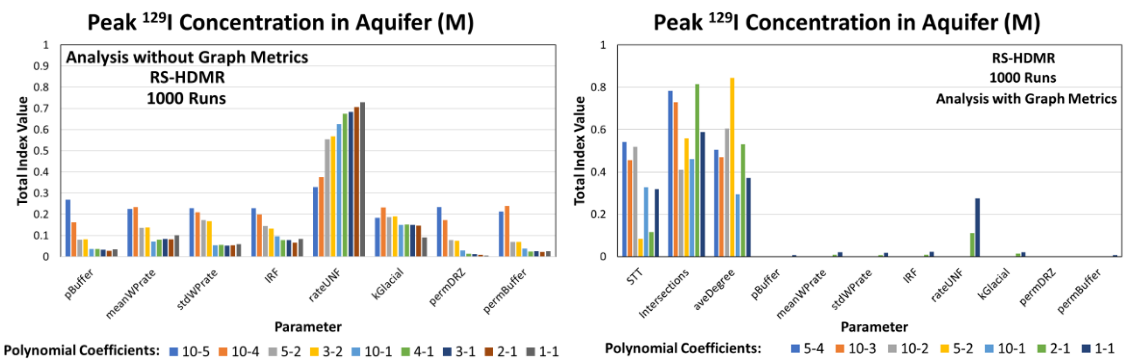

Fig. 3.8 Total effect indices estimated from a RS-HDMR metamodel with different polynomial coefficients for peak I-129 concentration, including and excluding graph metrics for the SNL crystalline reference case with all 25 DFNs

Fig. 3.9 shows the corresponding evaluation with PCE-LARS, using different PCE orders. The results look similar and convey the same message as the RS-HDMR evaluation, but the span of calculated values for the same index with different method parameters is even larger.

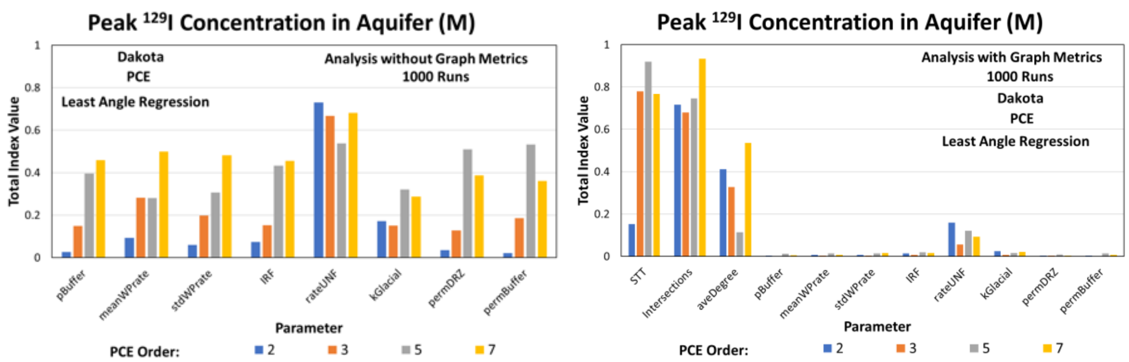

Fig. 3.9 Total effect indices estimated from the SNL PCE metamodel with different PCE orders for peak I-129 concentration excluding and including graph metrics for the SNL crystalline reference case with least angle regression and all 25 DFNs

The Dakota PCE software has the capability to use cross validation to choose the ‘best’ polynomial degree of a polynomial chaos expansion. 10-fold cross validation is used to estimate the cross-validation error of a total-order polynomial expansion. The order chosen is the one that produces the lowest cross validation error. For this case study the three graph metrics parameters were combined as a “group” causing a common influence. They were simply numbered 1 – 25, but one has to keep in mind that this number has no real meaning, as closer numbers do not mean closer DFN properties. The results are shown in Fig. 3.10. Starting with PCE order 3, the group parameter gets more important than rateUNF. Without cross validation, there is more noise in index values of lesser or unimportant parameters with PCE orders 5 and 7.

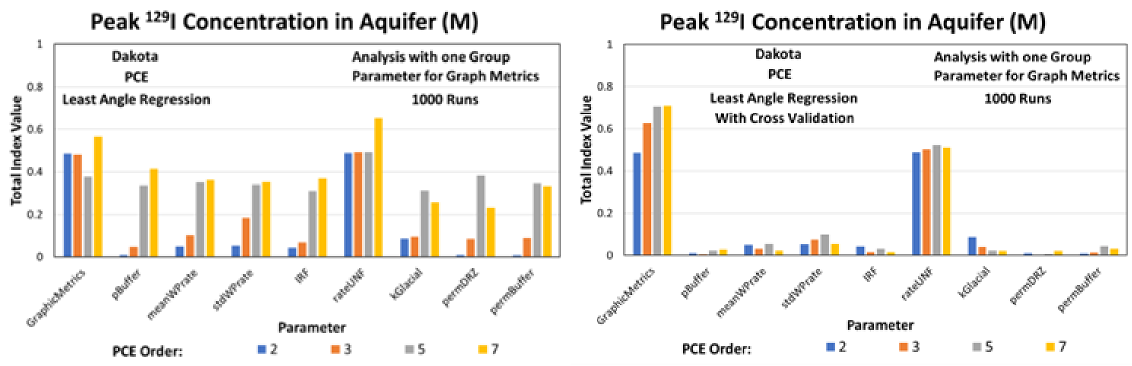

Fig. 3.10 Total effect indices estimated from the SNL PCE metamodel with different PCE orders and without and with cross validation for peak I-129 concentration for the SNL crystalline reference case with one group parameter for the graph metrics and with least angle regression and all 25 DFNs

3.1.3 Summary and outlook

The Joint Sensitivity Analysis Group (JOSA) has been working for seven years. The focus of the JOSA working group is on the use of sensitivity analysis in case studies involving geologic disposal of spent nuclear fuel with the overall aim of providing guidelines for performing such analyses in the context of safety assessments or safety cases for geological repository facilities. The goal of the sensitivity analysis exercise is to gain a better understanding of the strengths and weaknesses of various SA methods, identify cost vs. performance trade-offs of the methods, and highlight best practices and lessons learned. Multiple countries participated and demonstrated various SA methods on a series of case studies. The case studies involve computational models addressing safety assessments for geologic disposal of radioactive waste.

While the first phase of JOSA /SWI 21/ concentrated on standard methods of sensitivity analysis and model systems behaving relatively simple (or linear), the second phase addressed more sophisticated methods and more complex model cases. The focus was laid on the investigation of metamodel methods, higher sensitivity orders (parameter interactions) and newer approaches. A question of interest was where different methods agree or disagree about the sensitivity of parameters and parameter combinations.

Three case studies were considered: a salt LILW model of GRS, the crystalline reference case of SNL and a reactive transport Model elaborated by University of La Coruña (UDC). These systems exhibit particularities like strong nonlinearity, bimodality, bifurcation and stochastic influences. The JOSA group has worked collaboratively to meet the goals outlined above, each partner working on their own responsibility and with their preferred methods and tools. the end of phase 2, the JOSA team formulated a detailed recommendations for executing sensitivity studies. The outcome is documented in /SWI 25/.

The work of GRS concentrated on investigating the LILW model and the crystalline reference case with metamodeling methods in order to analyse parameter interactions, which is not (or not satisfyingly) possible with standard methods. It was found that metamodeling methods are appropriate for that purpose, but the results depend to a high degree on metamodel settings like polynomial orders to take into account. The right selection of such meta-parameters is not an easy task, as there is the danger of overfitting, which might lead to false calculated sensitivities. It requires some intuition and experience to set these values. To overcome this problem, search curve methods were investigated additionally. These methods are able to calculate second- and higher-order sensitivity indices directly from the data without the need of a metamodel. Some promising results were achieved, but this work is still on-going.

There are many issues still to be resolved in sensitivity analyses which support geologic disposal and nuclear waste repository analyses. The JOSA group may continue this effort with a proposed Volume 3. Some of the topics proposed for the next phase are: nested sampling, nonparameterized (e.g. spatial) uncertainty, influence of sample types, screening methods, bifurcation effects, active subspaces, and use of input or output transformations.

3.2 Decovalex

GRS participated in the international benchmarking project DECOVALEX-2023, Task F, which was started in 2020. The general aim was to compare models and methods used in deep geologic repository performance assessment. Reference cases were developed for

- a mined repository in a fractured crystalline host rock (subtask F1),
- a mined repository in a salt formation (subtask F2).

GRS decided to passively observe subtask F1 but participate actively and provide modelling results in subtask F2. In F2, four organisations (Covra, GRS, Quintessa, Sandia National Laboratories) worked together by executing model calculations for the salt reference case with different computational tools and comparing their results in order to mutually validate them and identify needs for refinement. GRS contributed using the RepoTREND code package /REI 16/. The integrated code LOPOS /HIS 99/, which is designed to simulate one-dimensional, single-phase transport processes in a repository mine in salt, was used for the nearfield. The transport code GeoTREND-POSA /REI 11/, which was developed to calculate a one-dimensional transport in fully saturated porous media, was used for the far field.

The investigations performed in F2 are described in detail in the following publications, which are under open access via the internet:

- DECOVALEX-2023 Task F Specification Revision 10 /LAF 23/
  https://www.osti.gov/biblio/2431152
- DECOVALEX-2023 Task F2 Final Report /LAF 24a/
  https://escholarship.org/uc/item/2874s3kv
- Comparing modelling approaches for a generic nuclear waste repository in salt /LAF 24b/
  https://www.sciencedirect.com/science/article/pii/S2352380824000881
- Value of abstraction in performance assessment – When is a higher level of detail necessary? /FRA 24/
  https://www.sciencedirect.com/science/article/pii/S2352380824000443
- Designing a repository in domal salt: what is important? /BAR 25/
  (still no link).

Together, these publications contain a comprehensive and detailed documentation of the work done in DECOVALEX Task 2, structured according to the task and in the context of the results of the entire group.

The results presented in this report are intended to give a concise insight to the work done by GRS using the RepoTREND code package, basically the LOPOS code, but not to present a comprehensive overview. The investigations are a part of the common work of the group and are described with their results in detail in the dedicated publications referenced above, which is not repeated in this report.

3.2.1 Analytical benchmark cases

Two transport benchmark cases were identified to compare modelling results with available analytical solutions. The first one is a 1D transport benchmark from /KOL 15/. The domain is a 10 m × 1 m × 1 m beam extending in the positive x direction. A steady-state flow field is applied. At the inflow face, a pulse of three tracers (conservative, decaying and adsorbing) are introduced to the system. At the inflow face (x = 0), concentrations of all three tracers are held at 1 mol/L from 0 to 15,000 s, and zero afterward. Concentrations in the model domain are compared to the analytical solution at 20,000 s.

The situation was modelled using LOPOS as a sequence of two drifts, each discretized in 101 internal elements, preceded by a small waste chamber releasing its full inventory in a very short time. The results for all three tracers are presented in Fig. 3.11 in comparison with the analytical solution. Since LOPOS is not designed to model an artificial boundary condition like the one for the benchmark case, it had to be approximated, which resulted in a moderate overestimation of the concentration in the first 3 metres of the model region. The further course of the analytical curve, however, could be reproduced well.

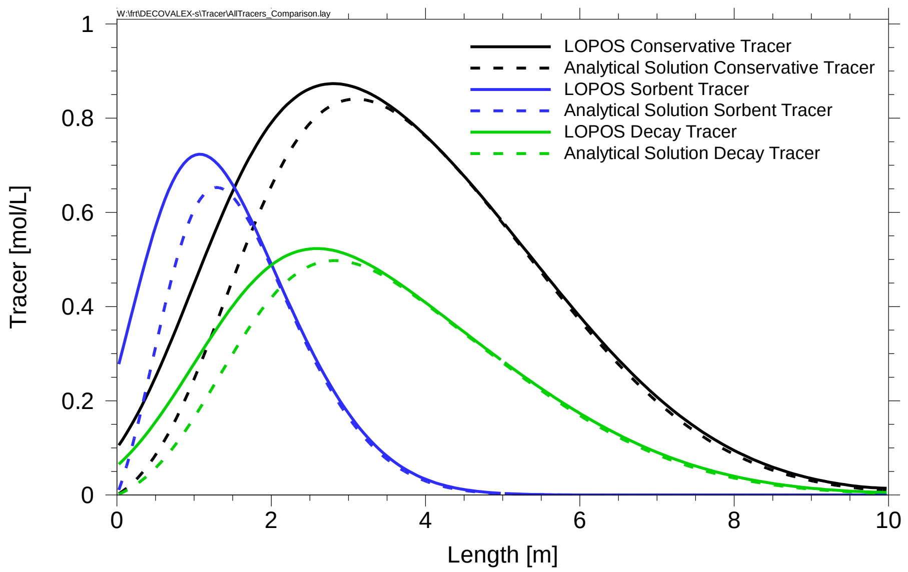

Fig. 3.11 Calculated concentration profiles after 2000 seconds

The second benchmark case was taken from /BAT 06/. It describes the 2D situation depicted in Fig. 3.12. The assumptions of the analytical model are:

- Unidirectional steady-state groundwater velocity field with flow in the x-direction,
- The medium is infinite in the x-direction and z is in the range (0,Z).
- Solute source is located at x = 0, planar and perpendicular to the velocity of the flow field.
- The source concentration may be a function of time through an exponential function for a decaying source.

The analytical solution is calculated in 2 dimensions (x,z) for a conservative tracer, tracer with retardation factor greater than one, and a decaying rate source. Since for this investigartion there was no code available in RepoTREND that was able to simulate 2D transport, the problem was simulated in 1D with GeoTREND-POSA. The results are shown in Fig. 3.13. In Fig. 3.14, the 1D results are compared with those obtained from numerical 2D calculations and the analytical solution for z = 1005 m. The 1D model essentially overestimates the concentration and meets the 2D simulation only at the end of the model region. This is a consequence of the fact that in this model radionuclides cannot leave the 1D transport path perpendicular to its direction. The results are in fair agreement, however, with those of a 1D simulation performed with the code QPAC.

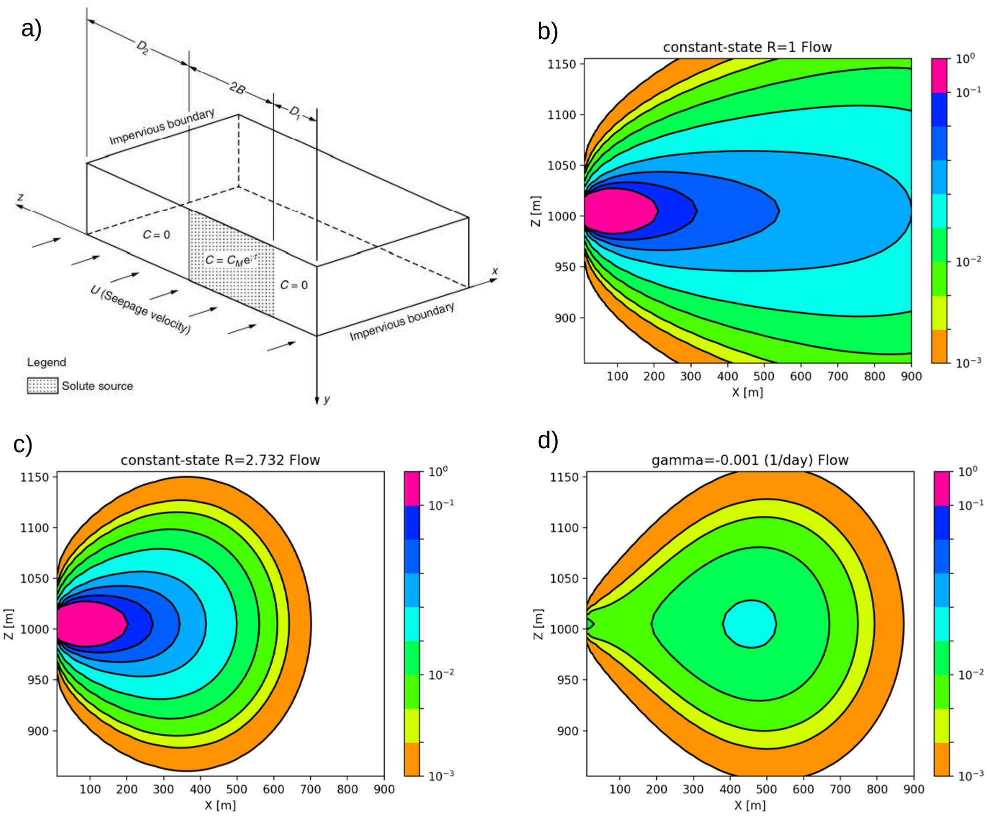

Fig. 3.12 a) Schematic of chemical diffusion and transport from a planar source in a uniform flow field (/BAT 06/). b) Tracer distribution (kg/m^3) after 20 years from conservative tracer and constant-rate source. c) Tracer distribution (kg/m^3) after 20 years with sorption and no decay in the tracer source. d) Tracer distribution (kg/m^3) after 10 years without sorption and with time-dependent tracer source g = -0.001 (1/day)

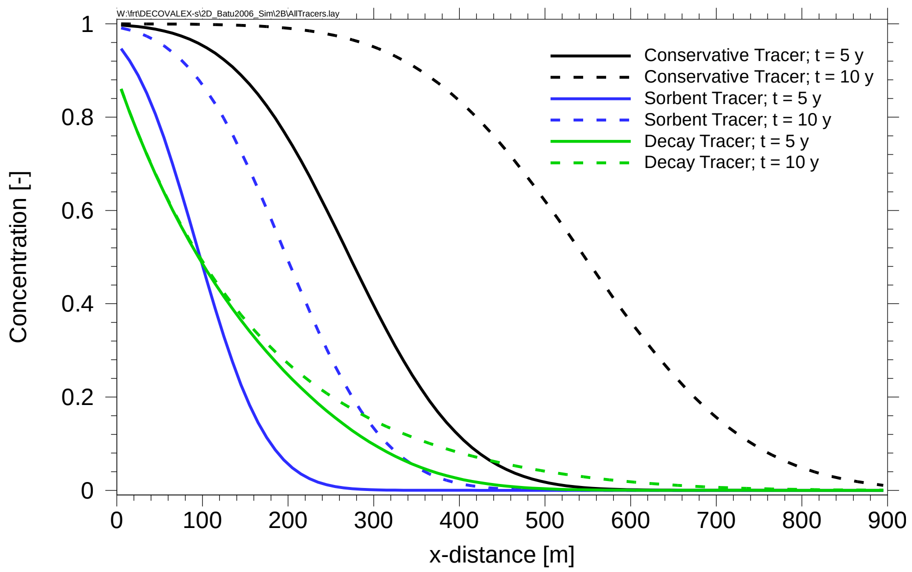

Fig. 3.13 Tracer concentration distribution for all tracers after 5 and 10 years, calculated in 1D with GeoTREND-POSA

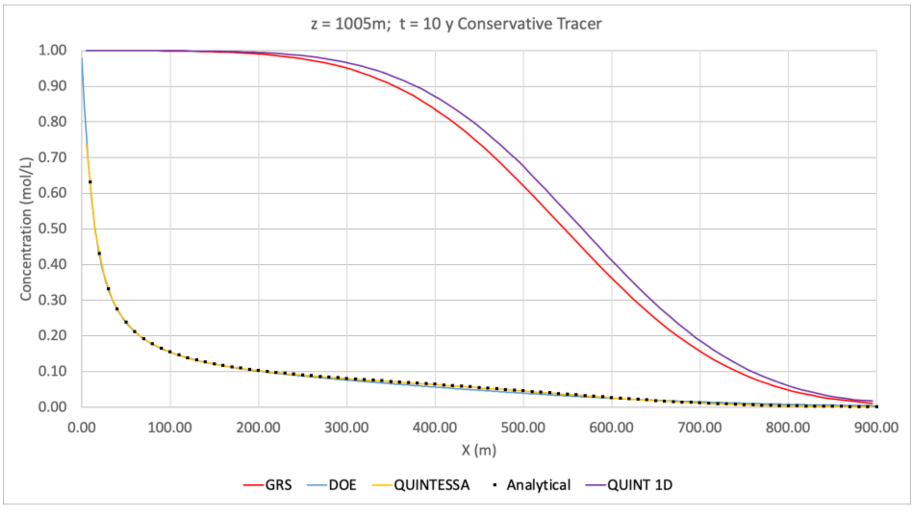

Fig. 3.14 Tracer concentration distribution for the conservative tracer after 10 years, calculated within 1 dimension with GeoTREND-POSA (red) and QPAC (purple), as well as in 2 dimensions with PFLOTRAN (green) and QPAC (yellow), compared with the analytical solution (dots)

3.2.2 The salt reference case

The salt reference case defined for code benchmarking describes the simple hypothetic repository structure presented in Fig. 3.15. The repository has a length of 730 m, a width of 910 m and a height of 4 m and is located 850 m below the ground surface. It consists of two fields of emplacement drifts for POLLUX-10 containers with spent nuclear fuel, one filed of drifts with emplacement boreholes for vitrified waste and an infrastructure area including two access shafts. The structure is symmetric in the y-direction.

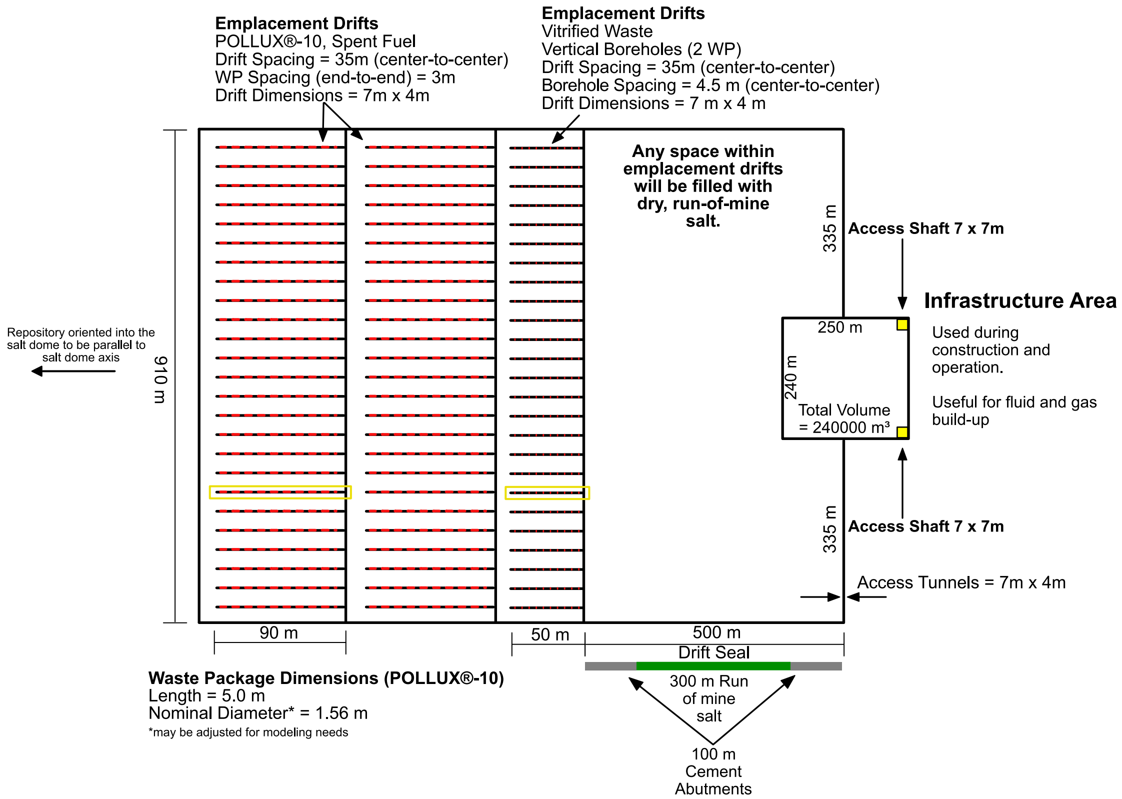

Fig. 3.15 Schematic view of the waste repository in the salt reference case. The drifts marked in yellow are used for intercomparison of results

A near field PA code for a repository in rock salt should take into account

- salt convergence and backfill compaction,
- two-phase flow,
- temperature-dependence of convergence.

None of the codes used by the participants fully complies with these requirements. LOPOS is the only tool applied in subtask F2 with the capability to calculate salt convergence and backfill compaction in coupled interaction with pressure build-up and fluid flow. Therefore, the LOPOS output was used by the other participants to introduce time- and space-dependent porosities into their models. On the other hand, LOPOS is not able to calculate two-phase flow.

Fig. 3.16 presents the model layout for LOPOS. Thanks to the symmetry, only one half of the total system had to be modelled. The emplacement drifts are combined to one model compartment (called segment in LOPOS) per field, each connected to its own access drift. The seals are composed of a converging salt segment surrounded by two non-converging segments representing the cement abutments.

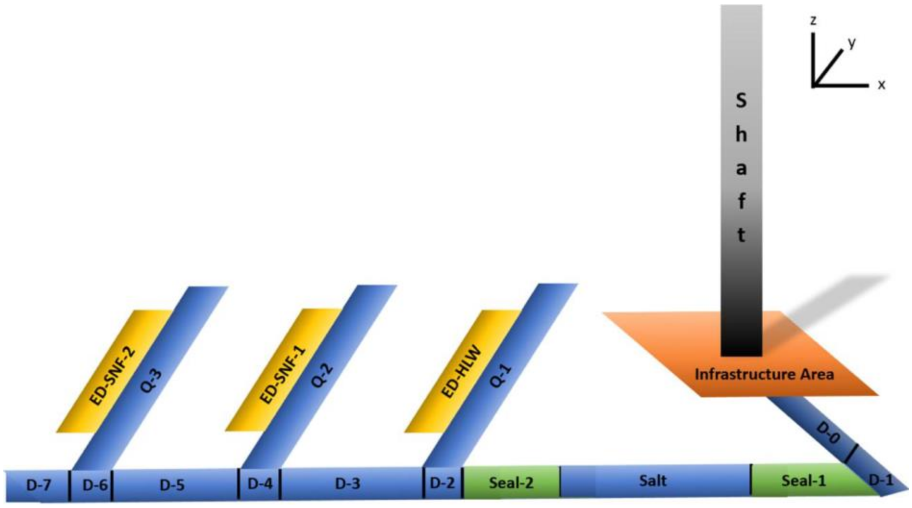

Fig. 3.16 LOPOS layout for the salt reference case

Since LOPOS simulates single-phase Darcy flow, liquid saturation is defined as the ratio between liquid volume and pore volume of the whole segment. The mined repository initially has a liquid saturation of 20 %, while the shaft has a liquid saturation of 35 %. The evolution of the liquid saturation of the main segments is depicted in Fig. 3.17. Full liquid saturation is quickly reached after a few years in case of the emplacement drifts (ED) and the salt seal. This is not caused by brine inflow, as the shaft is still intact at that time, but by salt compaction, which reduces the pore volume.

It is assumed that the shaft fails after 1000 years, which means a permeability increase by a factor of about 24. This leads to a slight desaturation of the shaft, due to the fact that the flow resistance decreases, and liquid can flow out of the shaft segment into the infrastructure area. Only when the pore volume in the drifts has reduced so far that, together with the voids in the infrastructure area, it can no longer hold all the liquid, the shaft saturation increases rapidly. The shaft compartment is fully saturated after 18,000 years. From that time on, there is a close and active transport path from the repository to the biosphere.

The convergence rate and the long-term evolution of the seal permeability are shown in Fig. 3.18. Seal-1 and Seal-2 are assumed to be made of non-compacting material, so that their permeability remains constant. One can see that less about 15 years after start of the convergence process the salt segment becomes denser than theses seals and overtakes the sealing function.

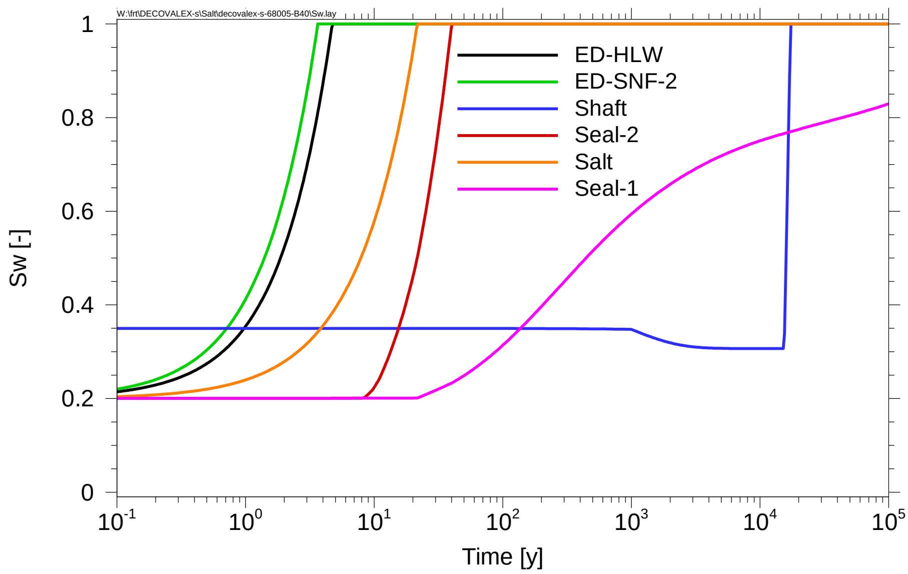

Fig. 3.17 Liquid saturation (Sw) of the shaft segment, the Seal 1/Salt/Seal 2 segment and the emplacement drift (ED) segments

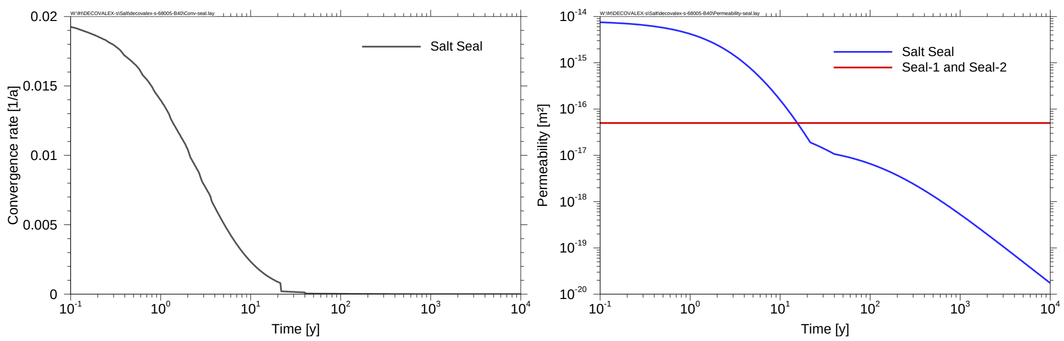

Fig. 3.18 Time development of salt seal convergence rate and permeability

Fig. 3.19 depicts the compaction rates and the related porosity evolution for selected compartments. The main porosity decrease takes place within ten years in case of ED-HLW and ED-SNF-2. The compaction process is quite fast because the initial saturation of 20 % leads to higher compaction rates (wet creep). After 10 years the pore volume has reduced so far that the initially present liquid volume fills the complete remaining pore space. After that, any further porosity decrease comes along with squeezing out liquid and has to overcome hydrodynamic pressure. This happens predominantly in the Salt compartment, since it is surrounded by the abutment drifts and squeezing is relatively easy because the surrounding compartments are not compacting, and Seal-1 does not reach full saturation during the entire 100,000 years. The drops in the compaction rate are due to the LOPOS numeric approach how to couple compaction and flow processes.

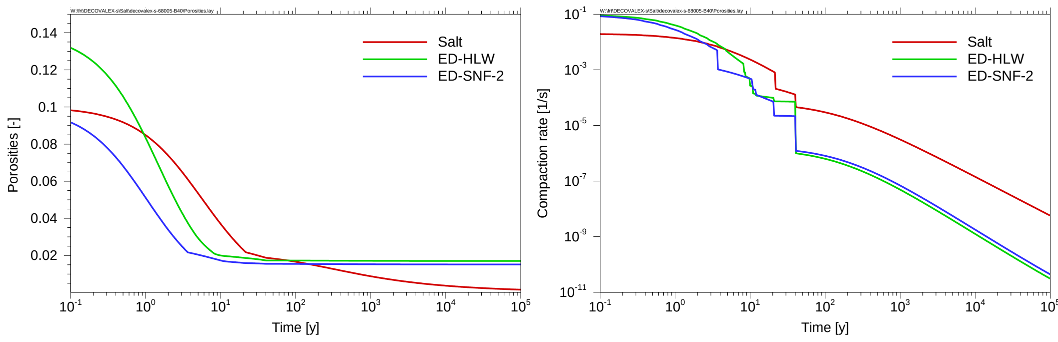

Fig. 3.19 Time development of porosity and compaction rate in specific compartments

3.2.3 Layered shaft

In the investigations presented so far, the shaft was modelled as a single homogeneous compartment. To investigate the effects of this simplification, a specific study was performed by GRS, where the shaft was composed of a number of layers with different properties, based on a realistic concept, see Fig. 3.20.

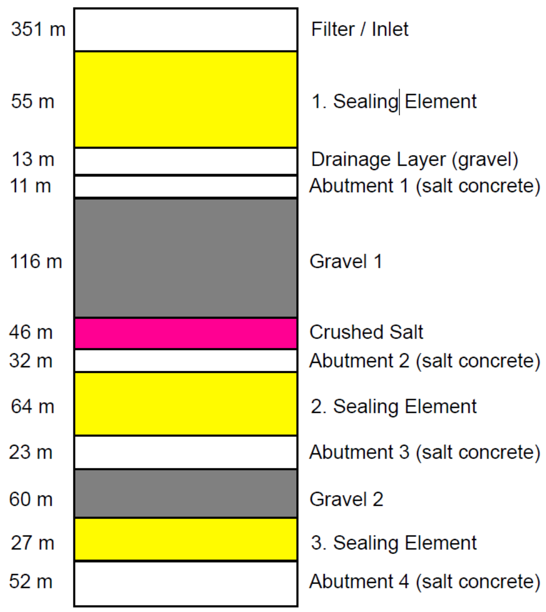

Fig. 3.20 Layered shaft design (modified from /RÜB 16/)

Fig. 3.21 presents the time development of saturation of the various layers. Although LOPOS is unable to handle two-phase effects, it was assumed that each layer segment starts with its own “saturation”, which means some initial amount of fluid. Depending on the permeability of the layer and the underlying one, fluid can vanish from or accumulate in specific parts of the shaft. The crushed salt segment is the only one with compacting backfill, so that it squeezes out its fluid in both directions. In comparison with the homogeneous shaft (Fig. 3.21, blue curve) the shaft is fully saturated only after 28500 years (compared to 18000 years). This is the point in time when the transport path is closed. So, the homogeneous model is conservative in this sense.

Fig. 3.22 illustrates the spatial distribution of the saturation in the homogeneous and layered shaft in comparison with corresponding results of the 2-phase code QPAC. Note that unlike QPAC, LOPOS does not calculate real saturation but the total fluid volume in each segment. These values are divided by the respective segment’s pore volume and located in the segment centre.

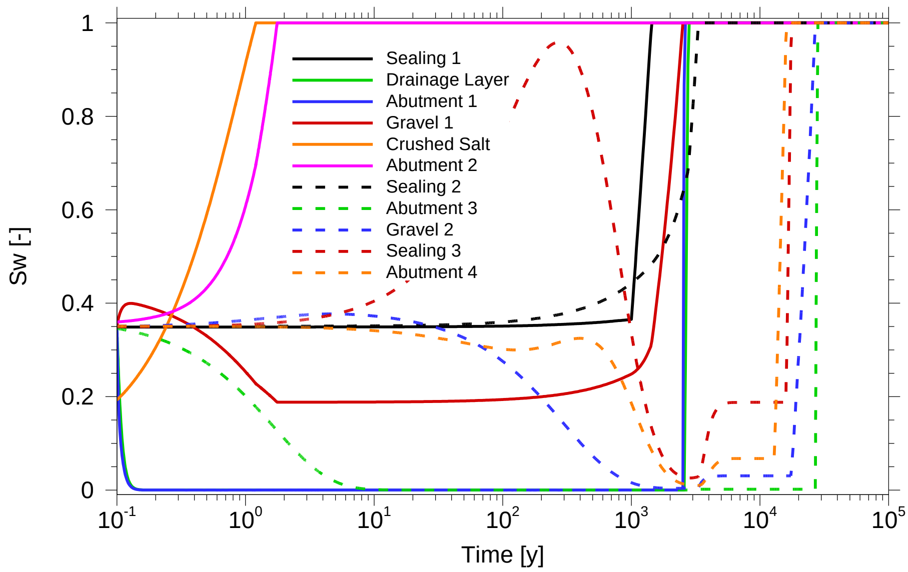

Fig. 3.21 Time development of saturation in the layered shaft

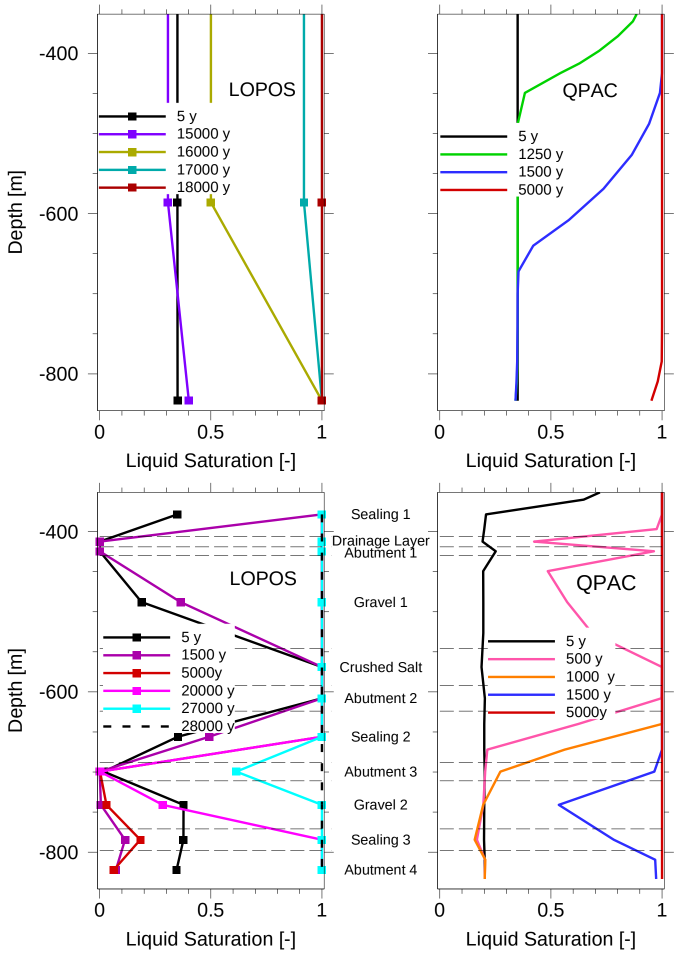

Fig. 3.22 Saturation distribution of the homogeneous shaft and the layered shaft, calculated with LOPOS and QPAC. LOPOS calculates just one value per segment, which is plotted in the segment center

3.2.4 Summary and Résumé

DECOVALEX 2023 Task F2 was initiated to bring together modelling teams from different organisations who use different frameworks and tools for simulating the contaminant transport from a mined repository in rock salt, and to compare their results in a benchmark exercise. For this purpose, two simple benchmark tests were identified for which analytical solutions are available. Moreover, a reference case representing a simple repository structure with emplacement drifts for SNF and boreholes for vitrified HLW was defined. Participating teams made a wide range of model assumptions from compartmentalized networks to full 3D models of the salt formation. No single contributed model includes full-fidelity representation of all the features, events, and processes (FEPs) detailed in the task specification, but almost all features and processes are represented in at least one model. Deterministic calculations were performed and several variants of the reference case were considered.

Detailed results that were compared between the modelling groups comprise

- For each the SNF drift, the HLW drift and the salt seal:
  - porosity evolution,
  - fluid flow,
  - tracer transport,
- fluid flow in the repository shaft.

Considered variants comprise

- lower initial saturation and compaction rate,
- earlier and later time of shaft failure,
- no concrete seal,
- swap of concrete and salt parts of seal,
- infrastructure area backfilled with salt,
- modified waste package concept.

Considerable differences between the models were found regarding liquid saturation and flow and are most pronounced at early time, before 1000 years. These differences are believed to be driven largely by the difference in creep-closure modelling between the teams and the resultant rate of reduction of porosity, which in turn depend on the assumptions in the compaction models. They reflect the importance of implementing a high-fidelity salt compaction mechanism in the salt conceptual model to study performance of the repository.

Results show that tracer transport out of the waste drifts and through the seal is largely diffusive in all models. Though the differences in diffusive transport are generally smaller than the fluid flow differences, this indicates that diffusion is a key physical mechanism that impacts long-term transport of radionuclides in the repository. Diffusivity is closely linked to the salt creep-closure mechanism via porosity reduction and the coupling between porosity and effective diffusivity. Moreover, diffusion in the models will be impacted by numerical dispersion.

Although there are no striking contradictions or incompatibilities and the differences can be widely understood, the task showed that different modelling concepts for repositories in salt can lead to quite different results. Further research is necessary to investigate the importance of model features and to improve their understanding for long-term PA. The work will be continued in DECOVALEX- 2027. The future round includes physics that are believed to be important to repository performance that were left out of the current conceptual model. These may include heating of the repository due to heat generated by the waste, gas generation, and full two-phase flow modelling. Sensitivity analysis and uncertainty quantification will be an integral part of the next four years of work, with a particular emphasis on sensitivity to initial conditions, salt compaction models, effective diffusivity, and understanding the interaction of numerical dispersion and physical diffusion.

3.3 Bentonite re-saturation

3.3.1 Abstract

Bentonite re-saturation as a specific safety case topic has been addressed by active participation in the Task Force on Engineered Barrier Systems (TF EBS). After a call for new tasks for the TF EBS in 2022, an uptake experiment with limited water supply performed in the framework of the project WiGru-7 /NOS 18/ was suggested as it demonstrates some unique features (see below). It was accepted as Task 14a in spring 2023 and GRS was appointed to be the principal investigator (PI) of this task.

The assignment as a PI includes writing a task description, clarifying open questions that may arise from the participants while working on the task, collecting and comparing the results and, finally, writing a summary report. The task description has been completed a few months before the end of the present project and some preliminary simulation results have been presented at the latest TF workshop. The intention concerning the task description is to either publish the task description when it has converged towards the end of Task 14a or after evaluating the numerical results as a comprehensive report including the results from the TF.

Note that the task description does not only contain earlier published material on the uptake experiment but had also to be had to supplemented and extended quit a lot. In the following, the task description in its present form is thus reproduced except for the extensive compilation of graphical results from the tests.

3.3.2 Introduction

The dynamics of water uptake by pre-compacted and confined bentonite have already been extensively tested in the laboratory for a long time e.g. /BÖR 84/, /KRÖ 04/, /FRA 17/. All these experiments had at least the potential to show the water uptake dynamics in great detail. However, they all allowed unimpeded access to water (UA) for the bentonite as indicated in the sketch of a typical test set-up depicted in Fig. 3.23. Water is always offered to the bentonite at (at least) a minimum of hydraulic excess pressure, for instance by a buret. The resulting water uptake rates are therefore exclusively controlled by the ability of the bentonite to take up water.

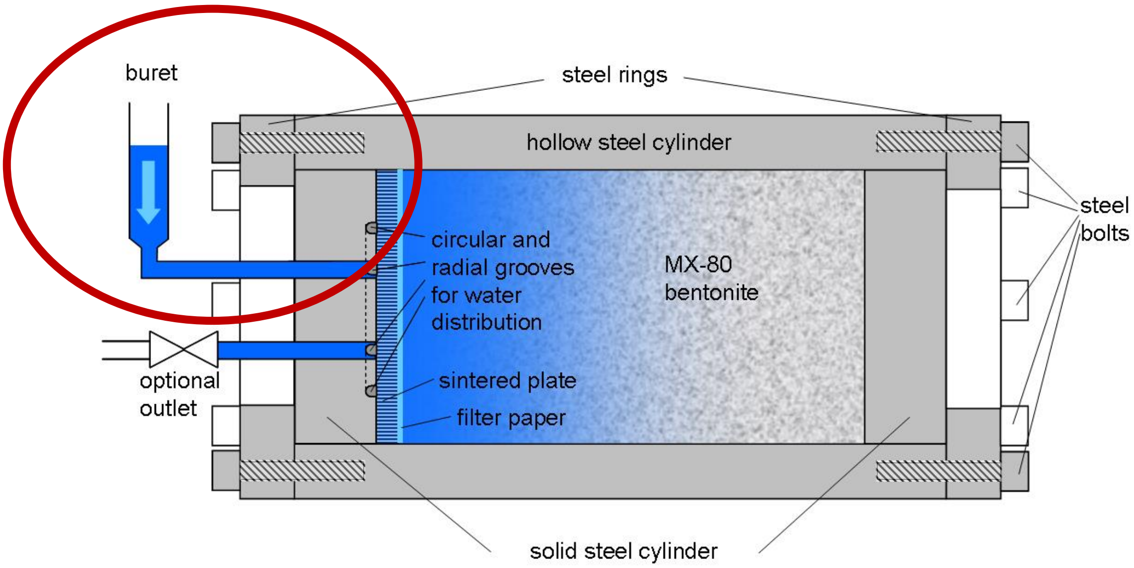

Fig. 3.23 Principle of a classic water uptake test; after /KRÖ 04/

Under in-situ conditions, by contrast, comparatively low flow from the rock can be expected. In fact, a potential host rock for a nuclear waste repository qualifies for that purpose by showing as little water conductivity as possible. The related flow rates found in different Underground Rock Laboratories (URL) indicate that such a host rock will initially not provide as much water as the bentonite would take up under UA-conditions /KRÖ 18a/. At a real repository, a limited water supply rate (LWSR) for the bentonite can thus be envisaged while larger fractures may indeed provide UA-conditions (see Fig. 3.24). Note that a similar effect is expected in a situation where the rock around a borehole or tunnel is (partially) dried when the buffer is emplaced /KRÖ 19/. Such conditions result in unsaturated flow at any possible degree of saturation.

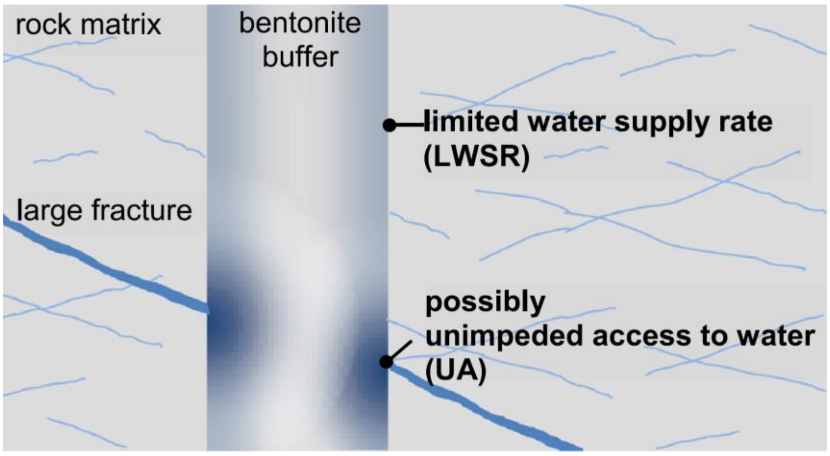

Fig. 3.24 Different inflow conditions for the buffer in crystalline rock; from /KRÖ 18a/

Unfortunately, detection of detailed transient water content profiles in the buffer under in-situ conditions is not possible due to the spatial requirements of the measuring equipment. The water uptake dynamics of a bentonite buffer under LWSR-conditions had therefore not really been known. This knowledge gap was noticed while contributing to the Buffer-Rock Interaction Experiment (BRIE) /FRA 17/ at the Hard Rock Laboratory (HRL) at Äspö in Sweden in the framework of Task 8, commonly tackled by the Task Force on Groundwater Flow and Transport of solutes (TF GWFTS) /VID 17/ and by the Task Force on Engineered Barriers (TF EBS). Relative humidity could only be measured in the BRIE at three different positions over a distance of 15 cm in the radial direction. Such a setup is also typical for comparable other in-situ experiments and provides only poor profiles thereby missing totally the initial dynamics directly at the bentonite-rock contact.

All uptake tests under UA-conditions in the laboratory showed that the water inflow rate into the bentonite is initially quite high. However, under in-situ conditions this water uptake rate may exceed the potential of a host rock to provide water at that rate. These would then be the characteristics of LWSR-conditions. The initial water uptake dynamics are illustrated in Fig. 3.25 a) and b) where the actual flow is indicated by a solid arrow while the potential flow is given by the open arrow.

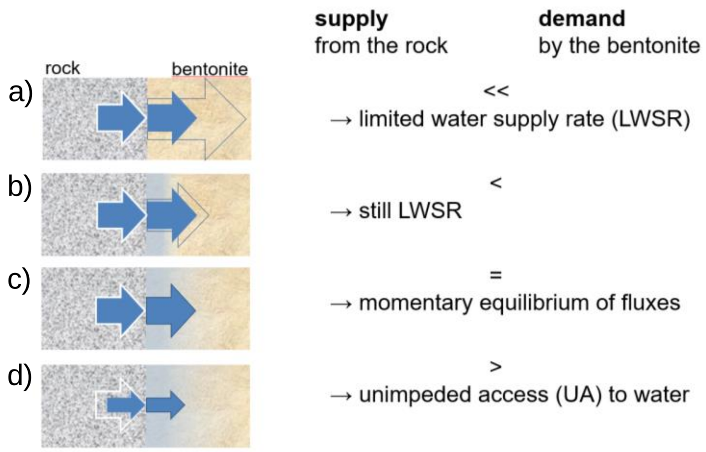

Fig. 3.25 Evolution of water fluxes across a bentonite-rock interface

As the inflow rates have been shown to decrease with time, it is thus just a matter of time until an equilibrium between water offered by the rock and water demanded by the bentonite is reached (Fig. 3.25 c). However, the state of this equilibrium is temporary. With increasing water content of the bentonite buffer, the demand for water by the bentonite decreases further. In effect, a higher water flux can potentially come from the rock than the buffer is able to take up as depicted in Fig. 3.25 d). This is characteristic for the UA-conditions that have been applied to all the uptake tests in various laboratories and prevail until full saturation of the buffer.

Note that the situation becomes even more complex where fracture flow is involved. The simplest conceptualization for fracture flow in the rock is that of single-phase flow in a parallel plate. However, this is a rather rough approximation as a varying fracture aperture should actually lead to higher and lower local transmissivities. Considering a fracture being open along the whole borehole or tunnel trace and at that in contact with the buffer or sealing material can easily be envisaged to lead to complex local flow patterns in the fracture. The situation becomes even more complex when taking drying of the rock before the emplacement of the buffer into account because this implies unsaturated fracture flow. Some speculations on the dynamics of these phenomena are given in /KRÖ 18a/ and /KRÖ 19/. All these fracture related issues are presently subject to laboratory investigations at GRS. Fracture flow is thus not considered in this task.

How water flow in the rock as well as in the buffer exactly looks like during the initial period at LWSR, is not entirely clear at the moment. Connecting water-filled rock pores to the pore space of an air-dry buffer without involving further physical processes directly means that considerable negative water pressure is exerted by the suction of the bentonite and leads to quite high negative hydraulic pressures[4] in the pore water of the rock. Such a situation is sketched for the results of a referring numerical model in /JAR 10/ where simulated data for the hydraulic pressure are given as an evolution over the simulated time of 200 years at a depth of 0.75 m in a bentonite-filled borehole and at different distances from the borehole surface. This model predicted negative hydraulic pressures highly in excess of -1 MPa in the rock close to the simulated borehole surface for a considerable period of time. The modelling results from /JAR 10/ are depicted in Fig. 3.26.

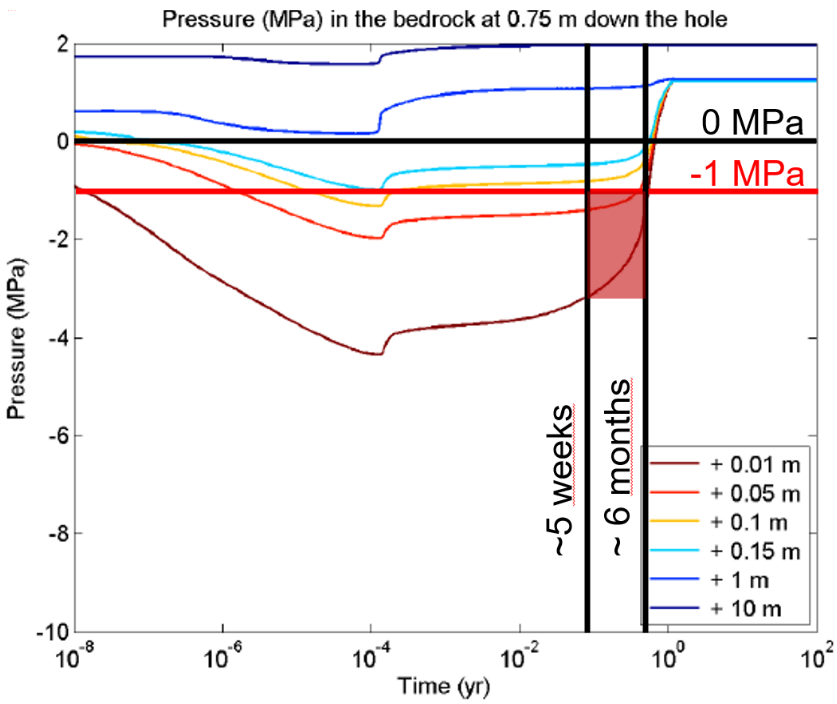

Fig. 3.26 Evolution of the hydraulic pressure at different distances from the borehole surface; after /JAR 10/

Two conclusions can be drawn from these theoretical considerations: (a) The previously performed uptake tests under UA-conditions should not uncritically applied to situations where LSWR-conditions can be encountered and (b) LSWR-conditions are bound to change to UA-conditions after some time. This raises some questions about the flow

---

[4] At the TF meeting 2024 in Prague, the terminology concerning negative hydraulic pressure has been discussed as also the expressions “suctions” and “tensile stresses” could apply. As the phenomenon refers to groundwater in a porous medium in a classic sense, “negative hydraulic pressure” will be used further on. Additionally, it was pointed out that pressure unlike suction or stress is a directly measurable quantity.

characteristics in the buffer. Of immediate concern is the time after which the switch from LSWR- to UA-conditions can be expected. But additionally, also the water distribution in the buffer after a certain period of LSWR-conditions must be known.

Note that on a purely theoretical basis, a concept for the treatment of LWSR-conditions has been developed in /KRÖ 17/ with a view to the extended vapour diffusion (EVD) concept (see /KRÖ 11/). In parallel, data from laboratory measurements at low constant inflow rates were provided /KRÖ 19/. With the help of these data, the theoretical approach for the EVD describing water uptake under LSWR-conditions could be confirmed /KRÖ 19/.

3.3.3 Working principle

3.3.3.1 Approaches

To gain insight into the water uptake dynamics of pre-compacted and confined MX-80 bentonite at LWSR-conditions, a controlled laboratory tests was envisaged. Idealising the true situation in the field they were designed for a homogeneous, compacted, and confined bentonite buffer as well as for a fully saturated host rock that supplies water at a constant rate. Also assumed were isothermal conditions.

The technical challenges for the tests involved proved to be much higher than anticipated, though. Several conceptual approaches to provide LSWR-conditions involving flow through granite and slowly rising water tables were tried but failed. They are documented in /KRÖ 19/ including the unsuccessful test designs along with the problems that came with them. The eventually successful test configuration is described in the following

3.3.3.2 Test concept

The general idea was to inject the water directly at the bottom of a test cell that contained a compacted and confined bentonite sample. A series of such tests performed with a fixed inflow rate but for different periods of time would then provide the uptake dynamics. It was decided, though, to precede this experiment by another test series with a fixed testing time but varying inflow rates in order to determine a viable combination of inflow rates and testing time. These two test series’ could in the end be supplemented by a successful pre-tests.

3.3.3.3 Flow rates

To determine meaningful ranges of flow rates for the envisioned tests, outflow rates from different URLs were compiled and compared to a typical initial inflow rate in a classic laboratory test /KRÖ 18a/. To allow for a comparison, all data were converted to the dimension of ml/(m² h). The data compiled in Tab. 3.3 indicate that, as a general rule, the initial demand of bentonite for water exceeds the flow rates in potential host rocks by far. This may not be true for major fractures in crystalline rock, though. SKB's internal regulations rule out deposition holes with concentrated inflow rates in excess of 0.1 l/min /SKB 10/ as these are considered unsuitable for canister storage. It is therefore doubtful that a buffer in any repository concept will be subject to substantially higher flow rates than that. Note: Assuming that this flow rate is distributed equally over the entire surface of a deposition hole with diameter of 1.80 m and a height of 6.00 m, this translates into a rate of 165 ml/(m² h).

Tab. 3.3 Typical flow rates for rock (outflow) and bentonite (inflow); cp. /KRÖ 18/

(fractured) porous medium	location	flow rate
Granite	HRL, Prototype Repository	13 to 1025 ml/(m² h)
	GTS, FEBEX	6 to 30 ml/(m² h)
Claystone	Mont Terri	1 ml/(m² h)
SKB's safety limit for granite (see text)	Forsmark	165 ml/(m² h)
Bentonite	GRS-laboratory	1020 ml/(m² h) (initially)

With the available syringe pump, pumping rates down to 0.01 ml/h can be provided. These rates need to be converted into ml/(m² h) yet. From previous tests, there were already suitable cylindrical test cells available that determined the sample dimensions for the present tests, in particular the sample diameter of 50 mm. Dividing the minimum obtainable pumping rate of 0.01 ml/h by the area of the sample face of 0.001963 m² yields an achievable minimum injection rate of 5.09 ml/(m² h). The graphic in Fig. 3.27 visualizes the outflow data from Tab. 3.3 and relates some possible pumping rates of the syringe pump to the outflow rates. With respect to the granite at the Grimsel Test Site as well as to that at the HRL Äspö, pumping rates between 0.01 and 0.05 ml/h thus provide an equivalent to the lower end of outflow rates from the rock for the present tests.

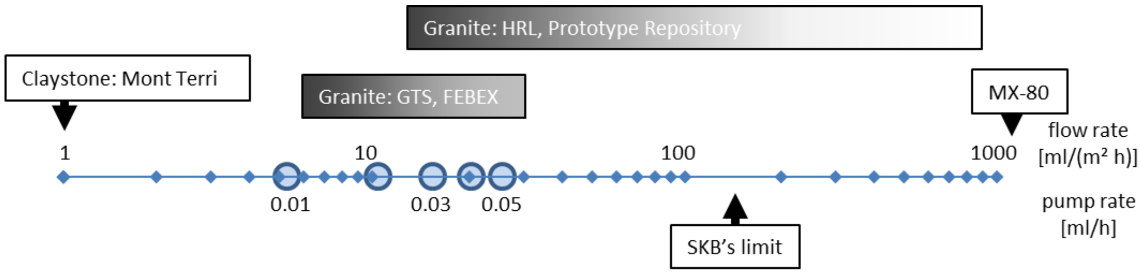

Fig. 3.27 Relation of flow rates at URLs to the present tests

3.3.4 Experimental set-up

3.3.4.1 Components of the set-up

Test cell

A modified stainless steel cell reused from previous tests was deployed. The functionality is sketched on the left hand side of Fig. 3.28 while the realised cell is shown in the photograph on the right hand side.

The bentonite sample was laterally confined by the inside of a steel ring. At the bottom and at the top, it was enclosed by sinter plates that were separated from the sample by filter papers. Normal steel sinter plates proved to draw up water by capillary forces directly to the sample. This made the set-up excessively sensitive to a virtually unavoidable slight slanting of the cell which leads to a certain misalignment between the free water table and the sinterplate surface plane. As a consequence, the sample face was not equally wetted (see see Fig. 3.29 left). To circumvent this problem, the steel sinter plates were replaced by bronze sinter plates made up by comparatively big bronze spheres (see Fig. 3.29 right).

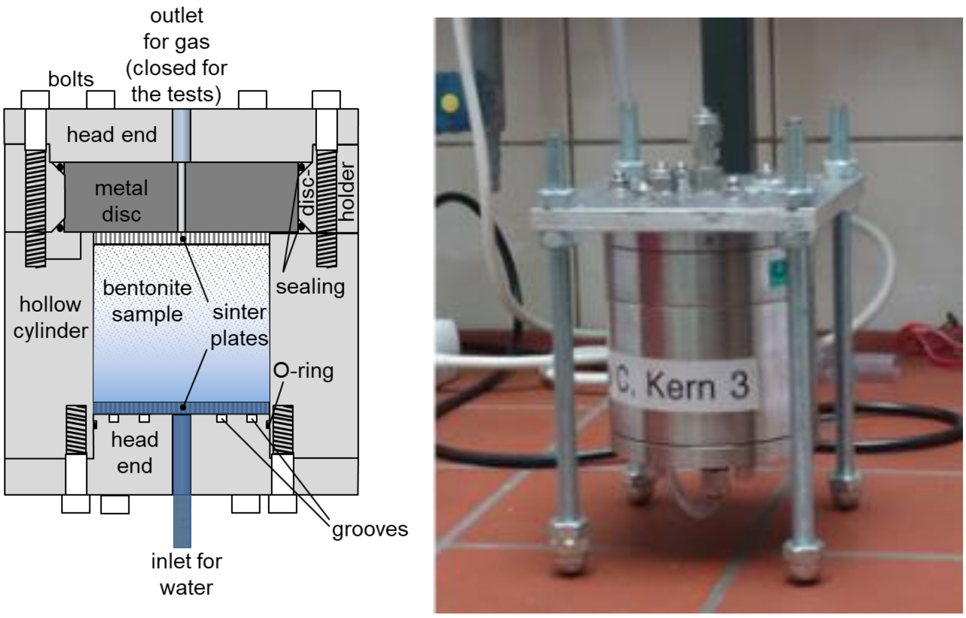

Fig. 3.28 Test cell; left: principle sketch, right: outside view with holding frame; from /NOS 18/

Fig. 3.29 Left: unregular wetting using steel sinter plates; right: bronze sinter plate (from /KRÖ 19/)

Axial confinement was taken care of by head ends that were tightly screwed to the steel ring that contained the sample. Note that reusing this cell required inclusion of an additional metal plate between upper sinter plate and top head end. Initially, it had been intended to measure the increase of the gas pressure during water uptake. For the present tests, outflow of gas from the cell was prevented by a stopper, as indicated in Fig. 3.1.

Pump

For the injection of water, a medical syringe pump (see Fig. 3.30 left) was used. Syringes between 2 and 50 ml can be accommodated by this pump. It can be set to pumping rates between 0.01 and 99 ml/h and operates at an accuracy specified as 2.5 % for intervals > 1 h and pumping rates > 2 ml. A measurement log of the manufacturer is depicted in Fig. 3.30 right. In case of flow obstructions causing pressures in excess of 0.3 bars, an alarm is triggered and the pump is stopped.

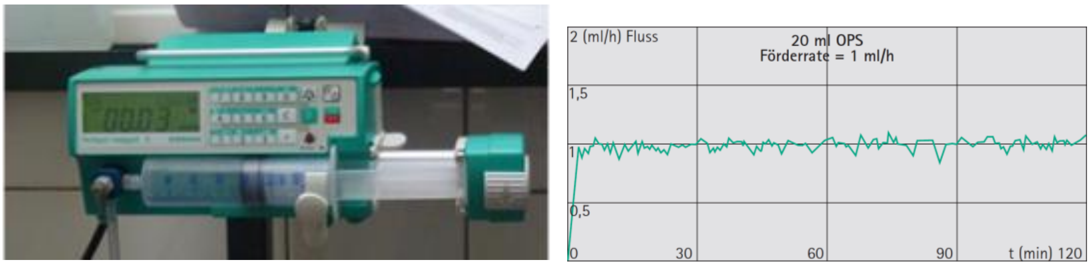

Fig. 3.30 Medical syringe pump (left, from /NOS 18/) and measurement log for pumping rate (right, from /BRA 24/)

Bentonite

For the tests, loose MX-80 granules with a maximum grain size of about 2 mm as depicted in the left picture in Fig. 3.31 were compacted in the test cell to a dry density of 1300 kg/m³ (Fig. 3.31 right).

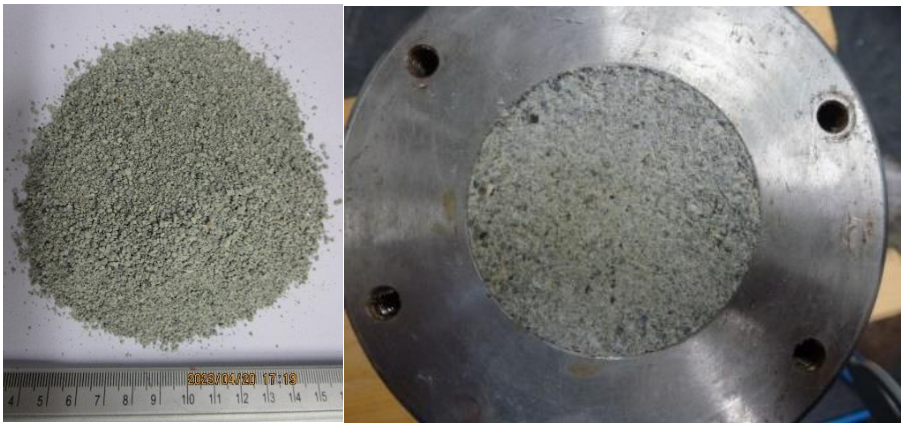

Fig. 3.31 MX-80 bentonite in the original granular form (left) and compacted in the test cell (right; from /KRÖ 19/)

To improve the degree of homogeneity, the samples were compacted in three layers of similar mass from top to bottom. For that purpose, a fitting steel cylinder was used. The top of the cell was simply closed by the planar face of a metal disc (see Fig. 3.28) so that the final compaction stage additionally involved emplacement of a filter paper and a sinterplate between steel cylinder and bentonite powder. The sample geometry is given in Fig. 3.32

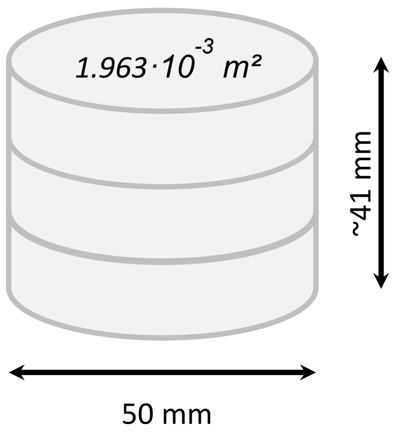

Fig. 3.32 Dimensions of the bentonite samples

The initial water content was determined twice, first on the 10th April 2017 yielding a value of 12.83 % and second on the 17th May 2017 yielding 12.64%. The arithmetic mean amounts to 12.74 %.

Solution

The solution used for the tests is slightly saline and believed to be representative for the groundwater at Äspö. The recipe is given in Tab. 3.4. The relevant properties for the solution are considered to be sufficiently approximated by those of pure water in the following, though.

Tab. 3.4 Composition of synthetic Äspö-solution in [mmol/l] (e.g. /KRÖ 04/)

Na	K	Ca	Mg	Cl	SO_4
79.67	0.25	17.06	3.33	113.92	3.4

3.3.4.2 Methodology

Single test

In principle, the classic procedure of wetting, cutting, and weighing is followed in this experiment. As this technique is destructive by nature, it implies that each individual test provides exactly one distribution for a certain period of re-saturation. The procedure for a single test providing such a distribution is described in the following.

First, the cell including the pre-compacted bentonite sample was vertically positioned to enable an as even as possible distribution of the inflowing water across the sample face. This was to be facilitated by injecting the water from below while assuring an upright position of the cell and by the grooves in the head end that distributed the water before entering the sinter plate next to the bentonite sample.

Next, the syringe of the syringe pump was connected by a tubing to the bottom of the cell. The pump was started and starting time was noted. This was obviously not the starting time of the test as the void space of the tubing and the sinter plate under the sample had to be filled first. Since the sample was completely encased in steel, the starting time of the test could not be determined by direct observation. However, the free volume in the cell below the bentonite sample could be measured quite accurately. From this volume and the actual pumping rate, that was kept constant throughout the test, the time until the void space was filled and the water reached the sample could be calculated. All runtime data in this description refer to this time as t = 0 s.

After a pre-determined period of time, pumping was terminated. With that, partial saturation of the sample was completed. The tubing was disconnected from the cell and then from the syringe. This as well as opening the bottom of the cell was done while taking care to leave the cell in an upright position to prevent free water from entering the sample. Then the top of the cell was opened.

Subsequently, the axial water content distribution was determined by cutting the sample into discs and characterizing these discs. For that purpose, the sample was carefully driven out of the hollow steel cylinder of the test cell for a certain length (see Fig. 3.33). The height of the exposed disc was measured with a caliper twice at four directions from which a mean thickness was determined. Then it was carefully cut off with a scraper.

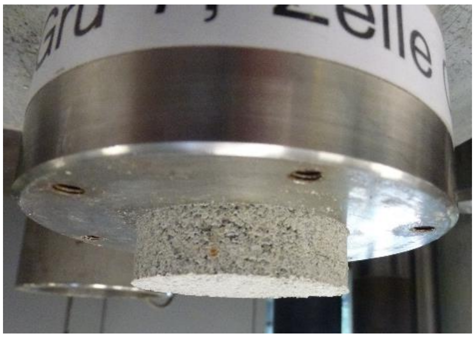

Fig. 3.33 Squeezing the bentonite sample out of the steel ring

As the injection side showed the highest gradient in water content, the thickness of the first discs was kept as low as possible to achieve a good resolution of data points for the distribution. In the progress of cutting discs, the disc thickness was increased. Each disc was weighed after cutting (see Fig. 3.34). Note that approaching the dry end of the sample increased the difficulty of this procedure as discs tended more and more to crumble at cutting.

Fig. 3.34 Bentonite sample after scraping off (left) and weighing (right)

After weighing, the wet bentonite discs were dried at 105 °C for 24 hours after which the weighing was repeated. From the disc’s weights and geometry, water content and dry density as well as the degree of saturation and the porosity of the disc could be determined (for details see subsection 3.3.5.1). These data were allocated to the center of the disc. Repeating this procedure for each individual disc eventually provided a series of data points along the sample axis.

Test series'

Two series' of test were envisioned. Series 1 encompassed tests where the inflow rates varied from 0.01 to 0.05 ml/h over a fixed period of roughly one week. Note that for technical reasons, the actual running time of the tests differs slightly from the approximation that is used in the text for convenience. The correct times are given in the referring tables.

In series 2, the running time was varied from one up to nine weeks at an inflow rate of 0.02 ml/h. Later, it was found that a successful pre-test at 0.05 ml/h running 2 weeks would nicely fit into the test matrix. This allowed for defining two additional mini series' each of which encompassed only two data points, mini series 1 comprising the tests with inflow rates of 0.02 ml/h and 0.05 ml/h for two weeks and mini series 2 comprising the tests with 1 and 2 weeks running time at 0.05 ml/h. Rates and running times are listed in Tab. 3.5 and are also graphically depicted in Fig. 3.35 where series 1 data are connected by red lines and series 2 data by blue lines.

The results from series 1 complemented by mini series 1 give insight into the impact of the flow rate on the water uptake while the results from series 2 together with mini series 2 show the dynamics of water uptake as a complete evolution. The final results of the experiment are reported in short in /NOS 18/. All in all 11 uptake tests provide the basis for this task.

For the model concept in general it is a relevant observation that the test running for 9 weeks at 0.02 ml/h as well as the pre-test running for 2 weeks at 0.05 ml/h ended when the obstruction alarm of the medical pump went off at 0.3 bar and the pump shut down. Unfortunately, these were the only means to relate hydraulic pressures to the tests. However, the alarm means that the bentonite has previously taken up all the water from the pump without posing a serious impediment to the imposed inflow. It is thus believed that this event marks a change in the uptake behaviour from LSWR- to UA-conditions. It can be speculated that afterwards, the pressure at the water-bentonite contact would have gone up further as a consequence of a decreasing permeability of the bentonite sample. Furthermore, the dashed line in Fig. 3.35 indicates where such a change might have been observable for other inflow rates.

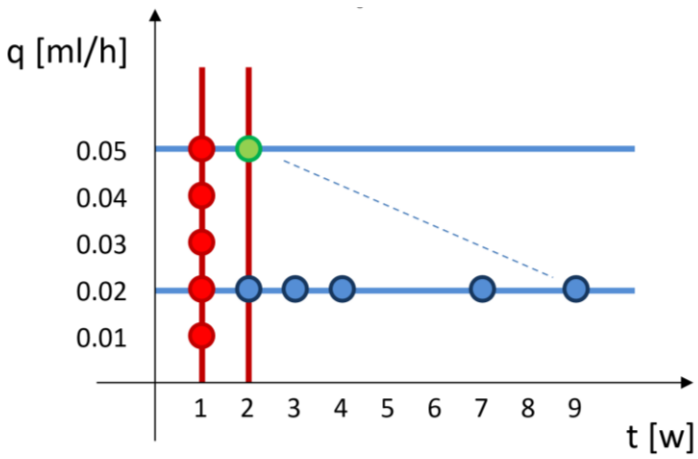

Fig. 3.35 Inflow rates and running times for all tests. See text for details

Tab. 3.5 Inflow rates and running times for all tests

Target test duration [w]	Inflow rate [ml/h]	Actual duration [d]
Series 1: varying inflow rate		
1	0.01	6.39
1*) **)	0.02	5.47
1	0.03	5.59
1	0.04	7.00
1	0.05	6.93
Series 2: varying running times		
2*)	0.02	12.65
3	0.02	18.70
4	0.02	26.12
7	0.02	41.43
9	0.02	63.85
Additional test		
2	0.05	13.0

*) also part of a mini series

**) also part of series 2

3.3.5 Results

3.3.5.1 Calculating the quantities of interest from the measurements

As pointed out in subsection 0 (methodology), the individual discs were weighed before and after drying. The difference provides the amount of hydrated water while the dry mass of the bentonite sample was directly measured. Together, the water content w of a disc can be calculated.

The bulk dry density ρ_d is determined from the ratio of disc dry mass and the disc volume.

Assuming a water[5] density ρ_w of 1000 kg/m³ and a grain density ρ_s of 2780 kg/m³, the degree of saturation S is calculated by

$$S = \frac{w}{w_{max}} \tag{3.1}$$

with the theoretical maximum water content w_{max}

$$w_{max} = \rho_w \left(\frac{1}{\rho_d} - \frac{1}{\rho_s}\right) \tag{3.2}$$

The porosity Φ can be determined by

$$\Phi = 1 - \frac{\rho_d}{\rho_s} \tag{3.3}$$

3.3.5.2 Graphical evaluation

The graphical representation of the results is given twice in this report. For the purpose of comparison and pattern recognition, the results are depicted in Fig. 3.36 to Fig. 3.39 as sets of four plots (one from each series) for each quantity of interest.

Water content

The data points for the water content shown in Fig. 3.36 are connected by step functions in dashed lines that indicate the size of the sample discs for which the data points are representative. In all other plots, the data points are connected directly by dashed lines.

[5] see section 0

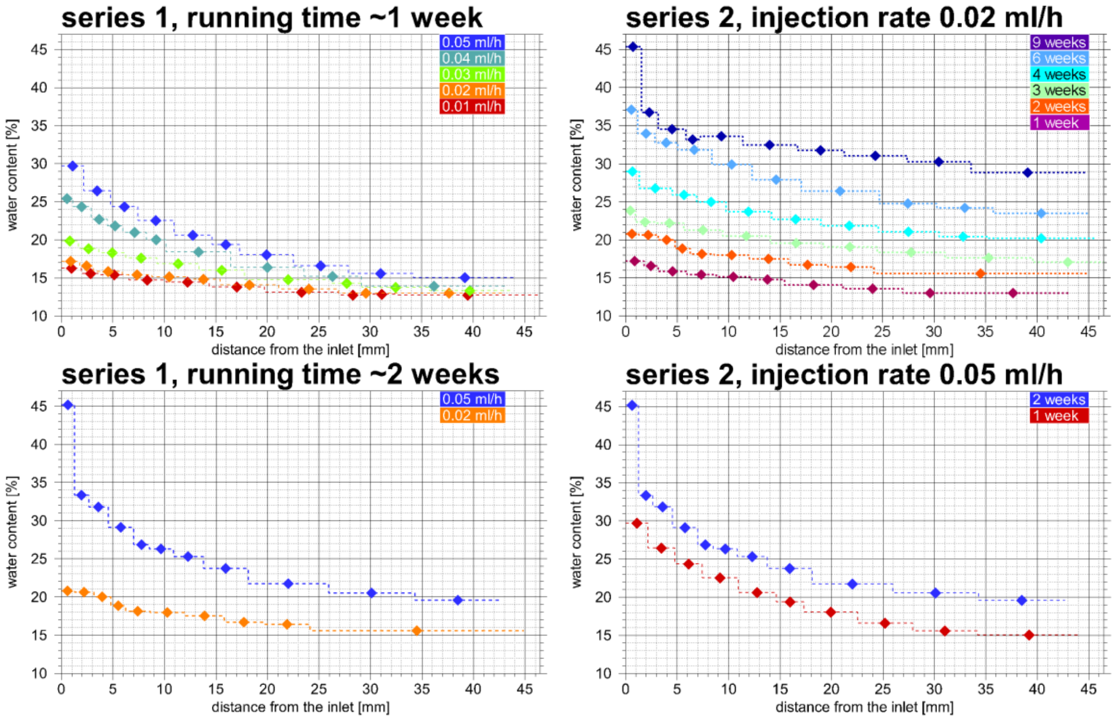

Fig. 3.36 Spatial distributions of the water content in the four series'

Several observations concerning the water content can be made from Fig. 3.36:

- The restricted inflow leads – at least in the beginning (see below) – to diffusion-like spatial profiles of the water content (in general).
- The higher the inflow rate, the faster the water content increase at the bentonite-water contact without losing the diffusion-like character of the curves (series 1).
- After a certain period of time, the water content increases unproportionally fast at the bentonite-water contact, cf. 9 weeks, possibly also 6 weeks[6] running time in series 2 and 2 weeks running time in mini series 2. In the first and in the last case, the theoretical maximum water content based on the mean dry density, namely 41 % and 38 %, respectively, is clearly exceeded.
- Only the inflow of 0.05 ml/h has been sufficient for the water content to reach the closed boundary within a week (series 1).

---

[6] At an early stage of the project, the second to longest running test in series 2 had erroneously been labelled “7 weeks”. In fact, it should have been called “6 weeks”. However, this is purely a matter of labelling. Wherever the running time was relevant as for in numerical simulations, the much more precise value of 42.81 days has been used.

- After reaching the closed boundary (series 1) the gradient of the water content appears to remain horizontal at this boundary (series 2), as expected.

Dry density

The measured distributions of the dry density are not as smooth as those of the water content as the determined dry density depends of the disc geometry (cp. subsection 3.3.5.1). The roughness of the resulting curves therefore reflects errors in the measurement of the height of the discs as well as a possibly inaccurate separation of discs. In both cases, the true volume of the discs would be missed which leads to errors in the dry density. An erroneous height measurement would affect only the related disc and is hard to detect from the results. By contrast, deviations from the ideal separation planes would affect both adjacent discs resulting in an overshooting followed by an undershooting (or vice versa). An example of the latter seems to be visible in the first 3 or 4 data points for the 6 weeks run in series 2. The first and the third point are too low in comparison to the trend while the second point lies way too high. Not as dramatic as that but still clearly visible, the same type of error can be observed in the first data points for 0.03 and 0.04 ml/h inflow in series 1.

In order to facilitate recognition of the overall trends, the dry density curves depicted in Fig. 3.37 are plotted over a broad range of density values, thereby squeezing the curves together.

Horizontal lines are additionally depicted in the four graphs in Fig. 3.37 representing the mean dry densities of the samples. For reasons of clarity and comprehensibility, the lines in the top graphs represent the arithmetic mean for the dry densities of all samples depicted in the referring graph.

Noticeable trends are:

- a systematic slight decrease in the dry density directly at the bentonite-water contact (series' 1 and 2).
- an increase in dry density within a distance of 10 mm (series 2) to 15 mm (series 1) from the bentonite-water contact, and beyond that, a basically constant value.

Note that the constant volume conditions of the tests are indirectly confirmed by the fact that the arithmetic mean of the dry density values after the test coincides roughly with the overall dry density of the sample.

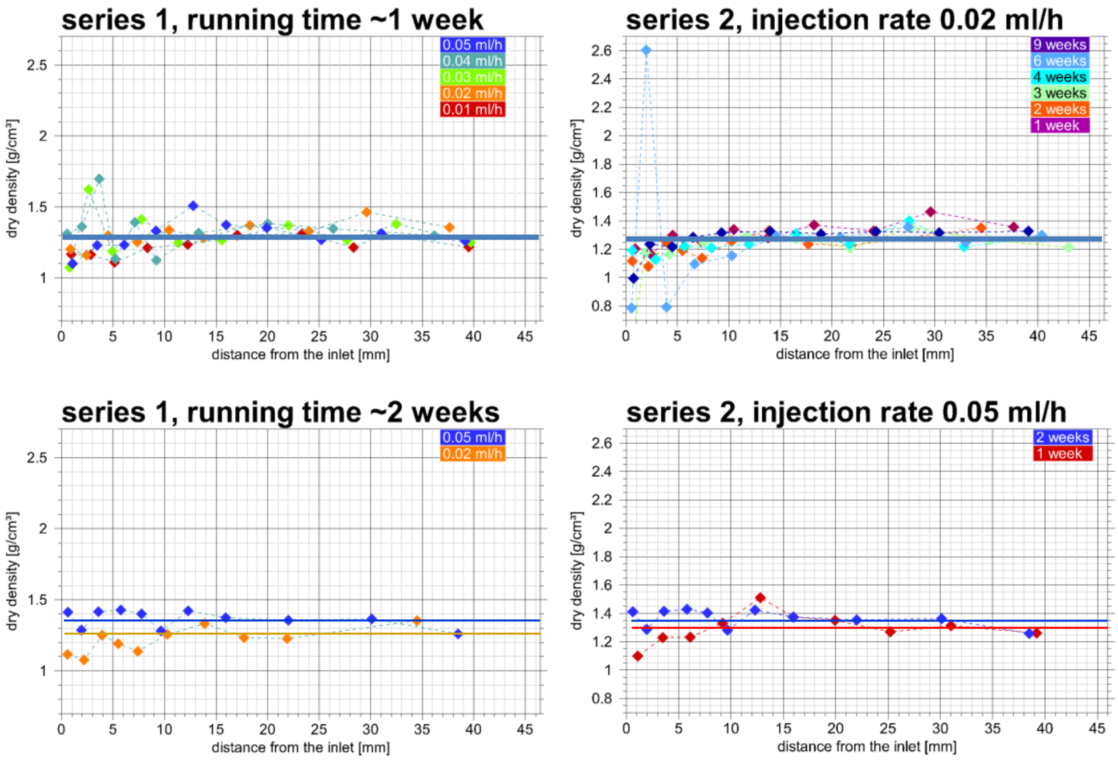

Fig. 3.37 Spatial distributions of the dry density in the four series'; solid lines: see text

Degree of saturation

The degree of saturation depends on the maximum water content which in turn is a function of the dry density. As the dry density is affected by uncertainties in the measurements (see above) the same applies to the degree of saturation. The conclusion that trends rather than well determined curves can be observed thus applies also to the degree of saturation. In principle it be said that

- The degree of saturation rises in series 1 with the inflow rate. As with the water content, the increase reaches about halfway deep into the samples.
- Close to the bentonite-water contact, the data for 0.05 ml/h seem to be lower than those for 0.04 ml/h. A reason is yet to be found.
- The degree of saturation in mini series 1 for 0.05 ml/h closest to the inflow boundary of the bentonite is almost as high as 130 %. Taking the measurement errors into

account as discussed above as well as the trend from the third to the fifth data point it might actually be close to 100 %.

– The saturation distributions at 0.02 ml/h in series 2 show an increase with time. At that, they appear to be basically constant thereby making the dynamics of saturation evolution quite different to those in series 1.

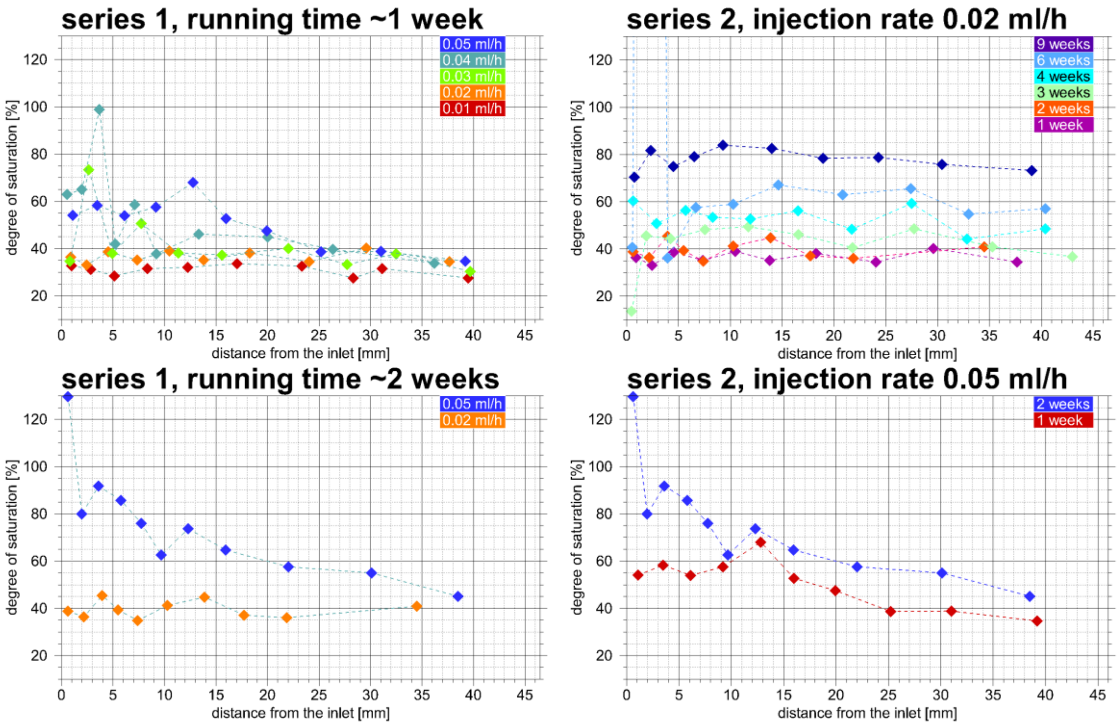

Fig. 3.38 Spatial distributions of the degree of saturation in the four series'

Porosity

Analogously to the degree of saturation, the porosity is derived from the dry density. The porosity curves are therefore also influenced by the same measurement errors. What can nevertheless be observed is that

– the porosities calculated from data of series 1 fall basically into a quite narrow band. What little variability between the individual curves remains in the data seems to be ascribable to the limited accuracy of the data derived.

– While the curves in series 1 between 20 and 40 mm distance from the inflow boundary are more or less constant at 50 to 55 %, the porosity seems to increase slightly to 60 % towards the inflow boundary.

– In principle the same observation can be made in all other series'.

– this increase appears to be linear in series 1 but possibly exponential in series 2.

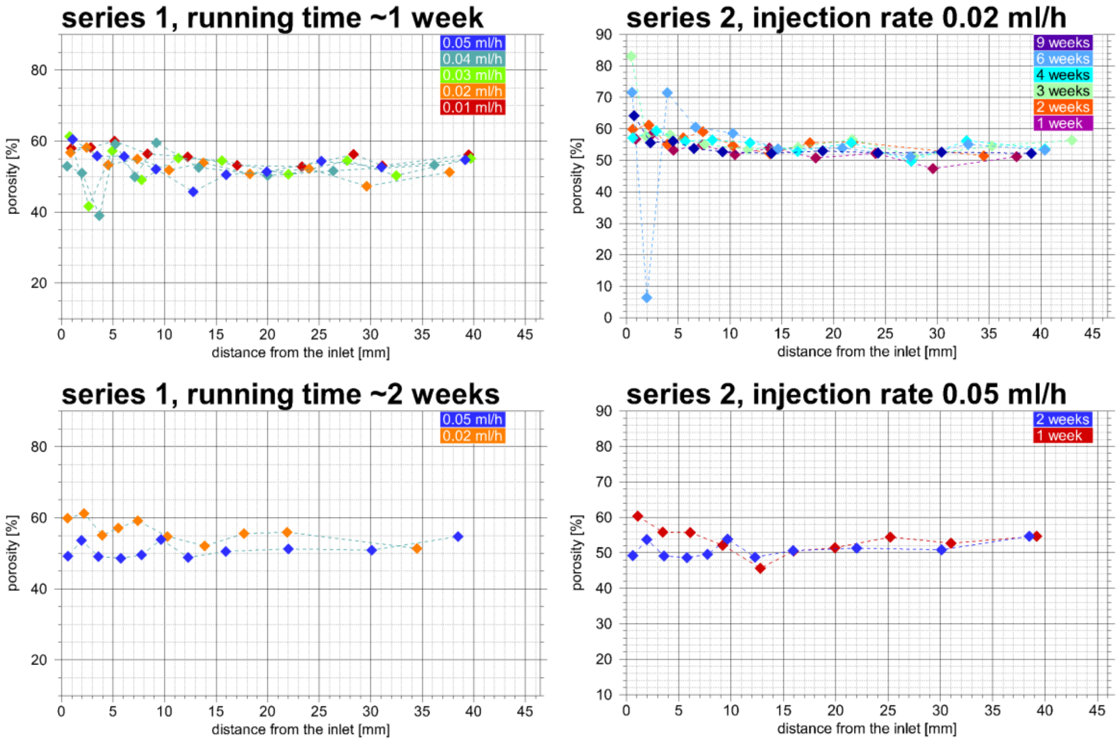

Fig. 3.39 Spatial distributions of the porosity in the four series'

Remark about the unproportionally fast increase

As shown in Fig. 3.36 in section 3.3.5.2, the water content increases unproportionally fast at the bentonite-water contact, particularly in the case of 9 weeks running time at an inflow rate of 0.02 ml/h (series 2) and in the case of 2 weeks running time at 0.05 ml/h (mini series' 1 and 2). The 9 weeks test shows a lowered dry density close to the contact compared to the initial value (section 3.3.5.2, Fig. 3.37) and a consistently increased porosity (section 3.3.5.2, Fig. 3.39) at a more or less constant degree of saturation (section 3.3.5.2, Fig. 3.38).

By contrast, the two weeks test in the mini series' may or may not be characterized by a lowered dry density which is reflected in the related porosity distribution. This in turn leads to a degree of saturation strongly exceeding 100 % which is obviously unphysical. However, it is not entirely improbable that the uncertainties in the results for the 2 weeks test have led to these seemingly contradictive data. Therefore, it should be kept in mind that the data on the water content are by far the most reliable ones among the four presented quantities. Comparison of the modelling results with measured data would thus be most safely based on the water content data.

3.3.6 Tasks

3.3.6.1 Introductory remarks

Task 14 a is divided into three subtasks:

- Task 14 a 1: Reproduction of all measurements with one and the same parameter set.
- Task 14 a 2: Reproduction of the fast increase of the water content at the water-bentonite interface.
- Task 14 a 3: Calculation of reasonable hydraulic pressures in the rock.

Subtasks 1 and 2 are exclusively aiming at an explanation of the laboratory results. Subtask 3, by contrast, is rather focused on the response of the numerical models to the hydraulic conditions at a real deposition hole. Consequently, subtasks 1 and 2 address the bentonite buffer only while subtask 3 needs to include the rock as well.

At a superficial glance, the dimensionality of the three problems appears therefore also to be different. However, the laboratory results can be simplified to just one dimension along the cylinder axis of the test cells. The model results are then basically profiles starting at the wetted end of the sample and ending at the closed end of the test cell. In case of the subtask 3, an 1-D axial symmetry would already be sufficient. Two- or three-dimensional model domains may also be used but note that only profiles in the radial direction will eventually be compared among the different models.

In the previous section it has been discussed that the water content is the one quantity that has been most reliably determined. All other measures are either subject to additional measurement errors as the dry density or are derived from the latter. The comparison of the modelling results will therefore be largely focus on the profiles of the water content in the bentonite and the hydraulic pressure in the rock.

The modelling results – successful or not – should be accompanied by an explanation/speculation illuminating the obtained outcome. Please keep in mind that the tasks are designed to provide insight into processes. A benchmark exercise concerning the computational effort is expressively not intended at this point.

3.3.6.2 Task 14 a 1: Reproduction of all measurements

Subtask 1 is intended as a warm-up exercise in order to make modellers familiar with Task 14 a in general. The model may be set up along the lines of the previous subsection. Aim is to tackle the problem of reproducing in principle the laboratory results for series 1 and series 2 including the related mini series'. Important, though, is to start right away with the idea that all bentonite samples have been prepared to resemble each other in each aspect as much as possible. This must be reflected in the models by using one and the same parameter set for all models. Only changes in the prescribed inflow rates and simulated running times are admissible. Also slight differences in the axial length of the samples[7] were unavoidable and are thus to be accounted for.

3.3.6.3 Task 14 a 2: Reproduction of the fast increase

This subtask focusses on the fast increase of the water content at the water-bentonite interface that develops in case of the longer testing times and at comparatively high inflow rates. While emphasis in subtask 1 is more on the general evolution of the water content profiles, subtask 2 concentrates on the reproduction of this singular feature by the numerical models.

3.3.6.4 Task 14 a 3: Calculation of hydraulic pressure in the rock

Motivation and scope

It is assumed here as in Task 8 that the bentonite buffer is air-dry when installed in a deposition hole. On the one hand, the related suction that begins to pull at the groundwater from the rock when getting in contact with the bentonite is rather high in that case. On the other hand, the permeability of the host rock for a nuclear waste repository has to be quite low to be suitable. High suction of the bentonite is thereby confronted with high flow resistance of the rock. As a result, a numerical model might be calculating considerable initial high negative pressures in the groundwater. It should thus be checked if the predicted negative pressures are physically reasonable.

---

[7] provided in the accompanying excel-file "Task14a-test.characteristics"; see section **Fehler! Verweisquelle konnte nicht gefunden werden.**.

While this effect had not been in the focus of Task 8, some results presented in this framework appear to confirm the theoretical consideration (cp. Fig. 3.26). Subtask 14 a 3 thus aims at having a closer look at simulated initial evolution of the hydraulic pressure in the rock in the vicinity of the buffer-rock interface. The models used/developed in sub-tasks 1 and/or 2 are to be applied for that purpose to check on the simulated groundwater water pressures under conditions that are expected for a real repository in crystalline rock. Note that admissible negative hydraulic pressures in groundwater may be rather low (see Appendix 3.3.7).

Model concept

The envisaged model concept as well as a description of the concrete model set-up are given in detail in Appendix 3.3.8.

Task specifications

As the highest negative hydraulic pressures are expected to occur close to the bentonite-rock interface, the hydraulic pressure should be observed over time at distances of 0, 1, 3, 10, 20 and 50 cm into the rock. The simulation time should be chosen in such a way that the observed hydraulic pressure at each location had time enough to decrease to at least 1/10 of its maximum value. If a model does not produce realistic hydraulic pressures in the rock, the reasons should be discussed, and possible improvements be suggested.

3.3.7 Appendix: Admissible negative hydraulic pressures

In the context of groundwater flow in a rigid porous medium, negative hydraulic pressure means a tensile load on the water. The highest bearable tensile load equals the tensile strength of water which is defined as the tensile stress at the onset of cavitation. While the theoretical strength of pure water lies in the range of 130 to 140 MPa (e.g. /ZHE 91/), experimental values even for purified and degassed water can rather be found in the range of 30 MPa (e.g. /HER 06/). However, these high values refer to the pure substance of water containing no gas bubbles or particles.

Considering water from the everyday environment allows typically only for tensile stresses below 0.1 MPa as “The tensile strength of ordinary water such as tap water or sea water … is governed by cavitation nuclei in the water, not by the tensile strength of the water itself, …” /MØR 15/. The case of groundwater in fractured rock should also fall into this category. For the purpose at hand, the admissible negative hydraulic pressures of groundwater in the rock is thus defined to be 0.1 MPa.

Note that this is consistent with the observation that the transport of water in trees from the roots to the treetop driven by evaporation at the treetop requires a biological filter system located in the roots. It is provided by the monocellular root layer called endodermis that purifies the uptaken groundwater and thereby increases the tensile strength of the natural groundwater. This enables the water to be drawn up against gravity to heights of something more than 100 m /GER 11/ equivalent to a maximum negative pressure of 1 MPa.

Note further that these considerations refer to water in a pore space that is quite large in comparison to the available space for water in compacted bentonite meaning that they are not applicable to water in clays.

3.3.8 Appendix: Model concept and set-up for subtask 3

3.3.8.1 Starting point

Of interest for subtask 3 are the highest absolute values of the negative hydraulic pressures in the groundwater that are calculated by the numerical models. These are expected to occur at the bentonite-rock contact where the rock shows the highest flow resistance. This relates clearly to the rock matrix rather than to fractures. Target of the investigations is therefore the rock matrix.

However, according to /DER 03/, fractures exist on all scales. Consequently, the hydraulic conductivity of the bedrock – defined as the combined system of fractures and matrix by the description for Task 8 /VID 17/ – should thus depend in turn on the scale of interest. This notion is underpinned by an extensive literature review with respect to the Äspö region /SCH 20/. The study addresses measurements of the hydraulic conductivity K and relates the measured data with the characteristic size l of the related tests. By doing this, a strong relation between test size and the resulting hydraulic conductivity has been confirmed. Tab. 3.6 summarizes the outcome. The data are visualized in Fig. 3.40 that also contains a trend curve according to

$$K = 10^{-14} * [(1000 * l)^{1.06} \, (log_{10}(l) + 3) + 1] \qquad (3.4)$$

Tab. 3.6 Relation of test-scale to measured hydraulic conductivity in the Äspö region; from /SCH 20/

Test-scale	Hydraulic conductivity [m s^{-1}]
300 m	4,7E-08
125 m	9,0E-08
100 m	6,0E-09
10 – 30 m	1,5E-09
0.5 – 10 m	7,1E-11
0.02-0.20 m	1,9E-12
0.005 m	4,7E-14

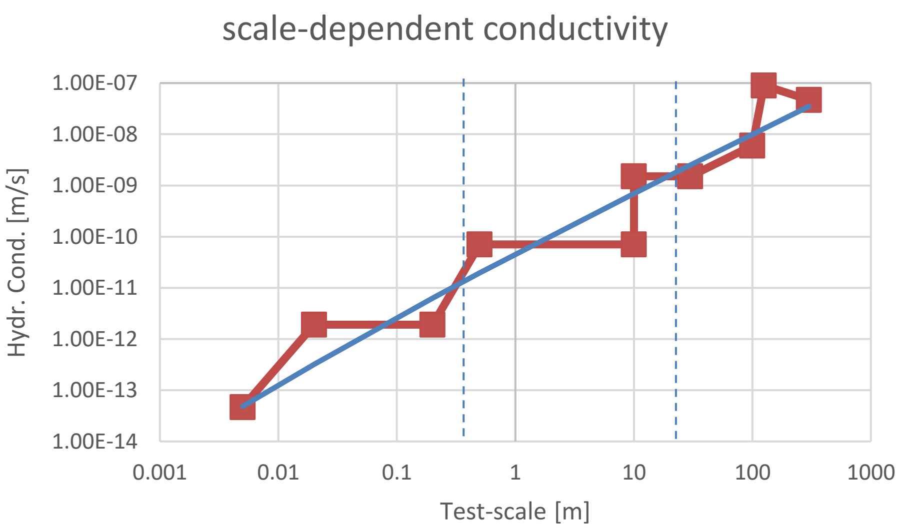

Fig. 3.40 Scale-dependent hydraulic conductivity according to Tab. 3.6; data in red, trend curve in blue

The trend curve (3.4) implies that the effective hydraulic conductivity relates to the scale of interest. This scale of interest thus needs to be defined for subtask 3.

3.3.8.2 Model concepts and scales of interest

According to early planning of the Swedish nuclear waste repository, installation of waste canisters will commence only when all deposition holes are drilled along a deposition tunnel. The expected time for which a deposition hole may stay open could last up to 5 years /HAN 09/. As it stands, this has still to be reckoned with /ERI 23/. During these up to 5 years, the rock is subject to ventilation and therefor to evaporation. The notion thus stands to reason that the rock dries out during this period to a certain extent.

A first attempt to define a scale of interest was therefore based on the maximum drying depth that could be reached in 5 years time. An approximation procedure is described in section 3.3.9 leading to a maximum drying depth of 44 mm in 5 years. A different approach has been used in /ÅKE 24/ where the steady-state position of the drying front was calculated to be in the range of 10 mm. Picking up the ideas from /ÅKE 24/, using a linear model instead of the axial-symmetric approach and including in one or two cases parameters that appeared to be better suited to the case resulted in a steady-state position of the drying front at 52 mm. In summary it can be expected that the rock will not be dried out by evaporation to a significant extent.

3.3.8.3 Model concept

As the inner, dried-out zone is rather small, a low conductivity according to Tab. 3.6 should be expected here. Around the inner zone, there is an outer zone where the rock should show a significantly higher conductivity depending on the model size. Following Task 8a, the size of the outer zone reaches 25 m from the hole axis into the rock.

With these data in mind, the suggested model concept encompasses a comparatively narrow and hydraulically rather tight zone around the deposition borehole wherein drying occurs. The inner zone is surrounded by a much larger outer zone of significantly higher water conduction. This concept had basically been followed in Task 8 by the modelling teams of VTT, ClayTech and GRS /FIN 19/. Interestingly enough, the concept is in line with the hydraulic skin effect that has empirically been observed over decades by many parties and at different circumstances /KRÖ 18b/.

3.3.8.4 Model geometry

In order to answer the question about possibly high negative hydraulic pressures, it is not necessary to have a full 3D-model of the deposition hole. As only the matrix is of interest, a domain cutting perpendicularly through the middle of the canister axis should suffice. In principle, this can be even further simplified to an axi-symmetrical 1D-model whose geometry is depicted in Fig. 3.41. The metrics are based on Task 8e – Prototype Repository /VID 17/. The canister is drawn only for reference and should not be considered in the model. The points “A” and “B” in Fig. 3.41 thus mark the envisioned model boundaries.

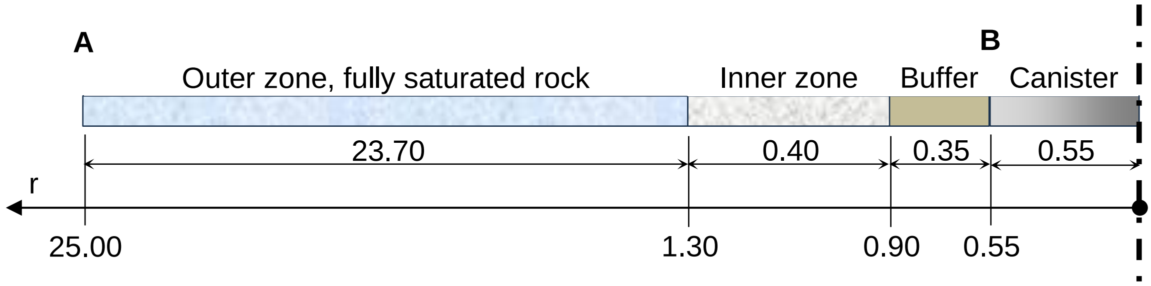

Fig. 3.41 Sketch of the model domain

3.3.8.5 Initial and boundary conditions

With respect to the bentonite, an initial equilibrium with a relative humidity of 50 % is assumed for this task. The outer zone in the rock is initially fully saturated. The inner zone can be envisaged to be either completely dried due to ventilation or to be basically still fully saturated. Quick and simple is the option to start with a fully saturated zone. Otherwise, a fully dried inner zone and subsequent unsaturated flow towards the buffer should be accounted for.

As for Task 8a /VID 17/, a hydraulic pressure of 2 MPa is assigned to the domain boundary at a distance of 25 m from the canister axis, i.e. at boundary A in Fig. 3.41. Note that this is a more or less arbitrary value as the undisturbed hydrostatic pressure at the Prototype Repository amounts to about 4.5 MPa. Boundary B is a no-flow boundary.

3.3.8.6 Materials

Bentonite

For the buffer, pre-compacted air-dry MX-80 bentonite with a dry density of 1500 kg/m³ is assumed to be deployed. Possible gaps between rock and buffer are to be ignored for the model. The initial water content is assumed to be in equilibrium with a relative humidity of 50 %.

Rock

Based on the data in Tab. 3.6, a hydraulic conductivity of $5 \cdot 10^{-12}$ m/s for the 40 cm thick inner zone is estimated to be characteristic around the deposition borehole. Note that the Task 8 description provides a value of $5 \cdot 10^{-12}$ m/s for the one-meter range /VID 17/. For the selected size of the outer zone, Tab. 3.6 suggests a hydraulic conductivity of $1.2 \cdot 10^{-9}$ m/s.

The storativity of the rock matrix is often not accounted for due to its low value. Presumably, this refers to small samples containing microfractures only. However, the storativity of larger volumes of rock including more significant fractures may not be negligible. Referring data are discussed in /VID 17/. Based on the extensive hydraulic testing at the Prototype repository a lot of data about specific storage were compiled by Rhén and Forsmark /RHÉ 01/ that delimits a value to a range between 10^{-7} and 10^{-6} 1/m. A related value may be used if storativity is accounted for in the model.

The description of Task 8 prescribes a porosity of 0.3 vol-% for the rock matrix /VID 17/. A value of 0.5 % was later found for samples from the BRIE site /FRA 17/ and is therefore adopted for subtask 3.

Constitutive equations (CEs) for two-phase flow generally consist of the capillary-pressure saturation relation (CPS) and the relative-permeability saturation relation (RPS). For granitic rock, three sets of CEs had been suggested for Task 8 /VID 17/, one set for the rock at the Grimsel test site (GTS) /FIN 95/, one set for the granite at Äspö /BÖR 99/ and one for the granite of the Canadian shield /THO 03/. Task 8 had also triggered the laboratory work described in this report. Looking for means to estimate breakthrough times in granite samples, an empirical formulation for the CEs for the Canadian shield /GUO 06/ and a fit to first data from the BRIE-site at Äspö based on /ÅKE 14/ were included in a referring compilation /KRÖ 17/. A later fit to the BRIE-data revealed considerably different CEs /FRA 17/, though. All CEs except the empirical approach from /GUO 06/ are based on the van Genuchten approach /VGN 80/ that reads for the CPS

$$p_c = p_{c\,0}\left[(S)^{-\frac{1}{m}} - 1\right]^{\frac{1}{n}} \qquad (3.5)$$

p_c - capillary pressure [Pa]

$p_{c\,0}$ - scaling parameter, related to the air entry pressure [Pa]

S - degree of saturation [-]

n - fitting parameter [-]

where

$$n = -\frac{1}{m-1} \tag{3.6}$$

m fitting parameter [-]

and for the RPS

$$k_r = \sqrt{S}\left[1-\left(1-S^{\frac{1}{m}}\right)^m\right]^2 \tag{3.7}$$

k_r - relative permeability for water [-]

As has been the intention of van Genuchten, the RPS can be calculated if the parameters of the CPS are known. However, alternatively and without explanation an empirical approach for the RPS, the so-called power law is also sometimes used:

$$k_r = S^\delta \tag{3.8}$$

δ - fitting exponent [-]

As discussed in /KRÖ 17/, there is a formal similarity between the exponential formulation for the relative permeability (3.8) and the referring approach by Brooks and Corey /COR 54/. This similarity relates the parameter δ to the pore size distribution giving it the meaning of a degree of non-uniformity of pore sizes. It appears that there is a lower limit $\delta = 3$ that describes an ideal uniform pore size distribution. Note that Brooks and Corey had much earlier already suggested an exponent of 4 based on the observation of a large number of consolidated porous rocks.

The referring parameters for all CEs mentioned above are compiled in Tab. 3.5. All original CPS' and RPS' are graphically arranged in Fig. 3.42 and Fig. 3.43, respectively. For the sake of simplicity, residual water and air saturation are assumed to be 0 which makes the distinction between saturation and effective saturation that can be found in some formulations dispensable.

While a general trend in the CPS and the RPS is recognizable, quite a bandwidth is nevertheless spanned by the different approaches. It appears that the relative permeability derived from /FRA 17/ should result in the highest resistance to flow as it provides significant permeability only above 80 % saturation. For the present task, the CEs from /FRA 17/ are therefore adopted. Moreover, they represent quite recent data from the HRL Äspö and at that also from the BRIE site which should be familiar to those who have participated in Task 8.

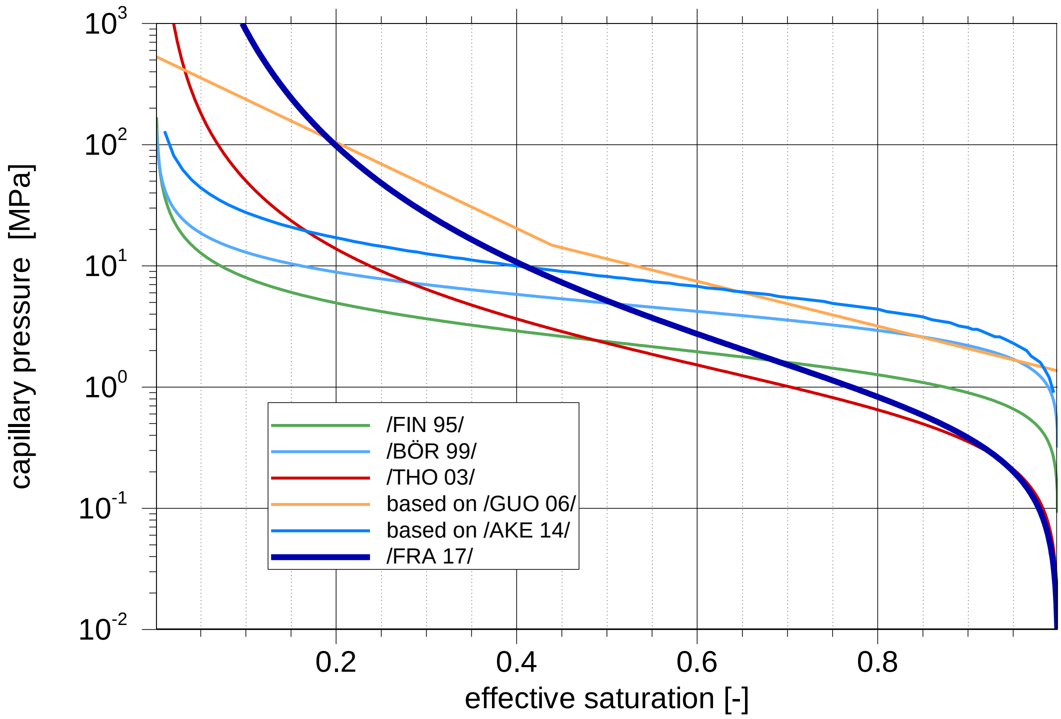

Fig. 3.42 Compilation of CPS for granite from the literature

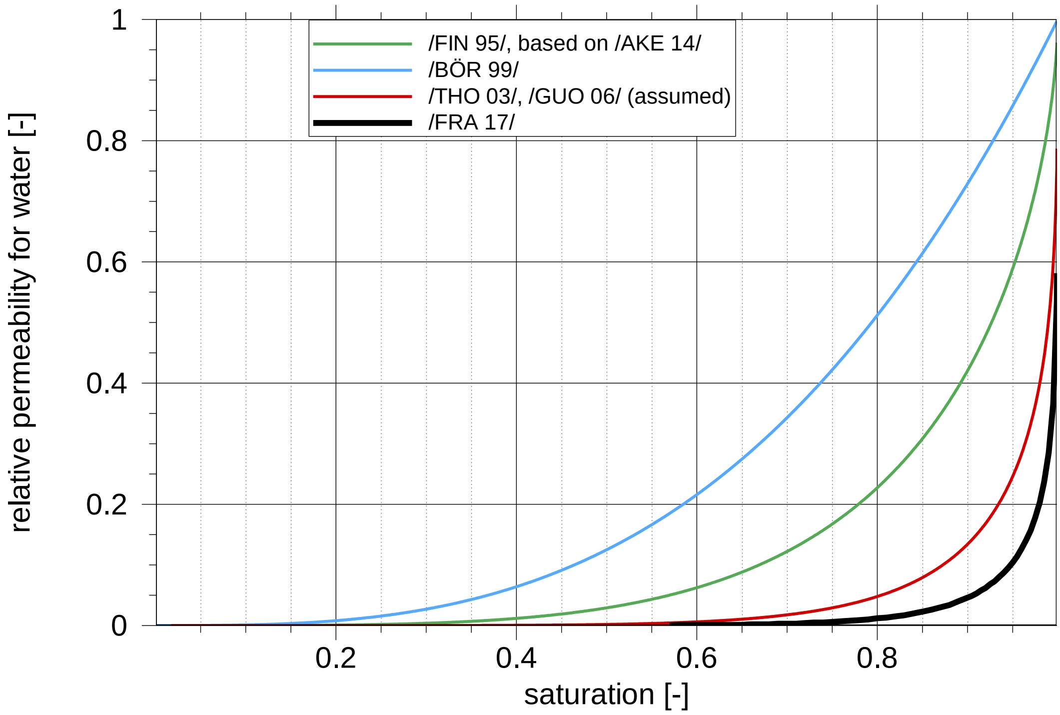

Fig. 3.43 Compilation of RPS for granite from the literature

Tab. 3.7 Parameters for the different suggested CEs

Origin	$p_{c\,0}$ [MPa]	m [-]	δ [-]	Source
GTS	1.74	0.6	(n.a.)	/FIN 95/
HRL Äspö	4.0	0.66	3	/BÖR 99/
Canadian shield	0.7	0.35	(n.a.)	/THO 03/
Canadian shield	(n.a.)	0.35 (for RPS)	(n.a.)	/GUO 06/
HRL Äspö	6.0	0.6	(n.a.)	based on /ÅKE 14/
HRL Äspö	0.6	0.24	(n.a.)	/FRA 17/

Note that the granites from Sweden, Switzerland and Canada are in principle similar in terms of the pore space topology but show different porosities and permeabilities. According to /LEV 41/, the related shape of the retention curves is similar in this case. A known retention curve for one rock can be scaled for another but similar rock by the porosities and permeabilities using Leverett's J-function. This method has been used to adapt the retention data from Switzerland and Canada to the conditions at Äspö. Details of the exercise can be found in /KRÖ 17/. The resulting curves show generally higher capillary pressures than the original ones. The increase lies roughly in the order of 40 %. What this means for the RPS has not been investigated, though.

3.3.9 Appendix: Estimating maximum drying depth for subtask 3

Evaporation of the groundwater at the water-air interface in the pore space of the rock and subsequent vapour diffusion will result in a drying process. The maximum depth to which the rock may dry out can be estimated based on the following assumptions:

- Groundwater flow through the matrix can be neglected.
- Movement of the water-air interface[8] into the rock is slow in comparison to the diffusive vapour flux. Diffusive vapour flux can therefore be well approximated by quasi steady-state conditions i.e. by a constant gradient of the vapour partial density.
- The transition from water to air in the direction perpendicular to the surface of the deposition hole is sharp.
- Relative humidity at the front is always 1.

This set of assumption leads to a recursive algorithm for the calculation of the position of the waterfront. The steady-state diffusive vapour flux J_D depends invers proportionally on the distance d of the front to the wall of the deposition hole which also represents the drying depth. Evaporation of water at the front causes the front to advance into rock with the progress velocity v. This progress depends on the evaporation rate. Assuming temporarily quasi steady-state conditions the evaporation rate should equal the diffusive flux of vapour. The progress velocity v is thus also invers proportional to the drying-depth d. Calculating the drying depth as a function of time thus leads to the following recursive dependencies

$$
\begin{aligned}
d(t) &= d\big(v(t)\big) \\
v(t) &= v\big(J_D(t)\big) \\
J_D(t) &= J_D(d(t))
\end{aligned}
\tag{3.9}
$$

For the purpose at hand, the drying depth is therefore calculated by a series of finite time steps Δt where diffusive flux and front progress are approximated using the distance d of the previous time step for calculating the actual progress Δd:

[8] called “waterfront” in the following

$$J_{D\,i} = D\,\tau \left(\frac{\partial \rho_v}{\partial x}\right)_i = D\,\tau\,(1 - r_{h\,0})\,\rho_{v\,sat}\,\frac{1}{d_i} \tag{3.10}$$

$J_{D\,i}$ - diffusive vapour flux in the i-th time step [kg/(m² s)]

D - coefficient of diffusion of vapour in air [m²/s]

τ - tortuosity [-]

ρ_v - vapour partial density [kg/m³]

$\rho_{v\,sat}$ - saturation vapour density [kg/m³]

$r_{h\,0}$ - relative humidity at the wall of the deposition hole [-]

d_i - distance between the waterfront and the deposition hole wall in the i-th time step [m]

i - step counter

$$\Delta m_i = J_{D\,i}\,A\,\Delta t_i \tag{3.11}$$

Δm_i - mass of water lost at the front in the i-th time step [kg]

A - cross-sectional area [m²]

Δt_i - i-th time step [s]

$$v_i = \frac{J_{D\,i}}{\rho_w} \tag{3.12}$$

v_i - front velocity in the i-th time step [m/s]

ρ_w - density of water [kg/m³]

$$\Delta d_i = v_i\,\Delta t_i \tag{3.13}$$

Δd_i - front progress in the i-th time step [m/s]

Based on the input data for the set of equations (3.10) to (3.13) – compiled in Tab. 3.8 – the evolution dynamics in terms of the drying depth over time and the front velocity over time have been calculated as depicted in Fig. 3.44 and Fig. 3.45, respectively. According to Fig. 3.44, the drying depth of the matrix after 5 years can be estimated to be less than 40 cm. Note that this value is clearly a rough approximation only. But for the purpose at hand, it is adopted, nevertheless. As expected, the front velocity decreases quadratically with time.

Tab. 3.8 Data for the set of equations (3.10) to (3.13)

Quantity	Value	Dimension
coefficient of diffusion of vapour in air at 10 °C	2.3 10^{-5}	[m²/s]
tortuosity	0.1	[-]
saturation vapour density at 10 °C	0.00941	[kg/m³]
relative humidity $r_{h\,0}$	0.8	[-]
density of water	1000	[kg/m³]

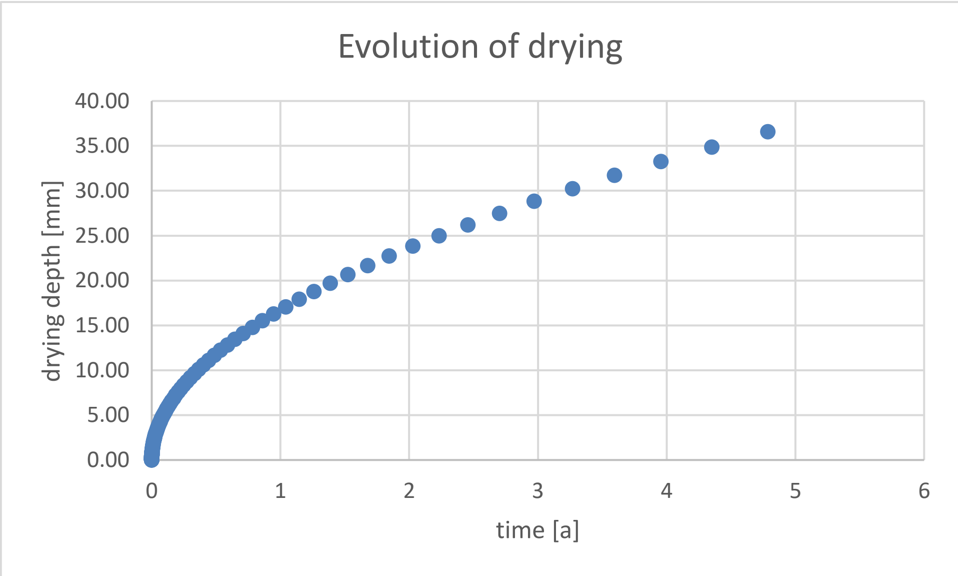

Fig. 3.44 Drying depth over time

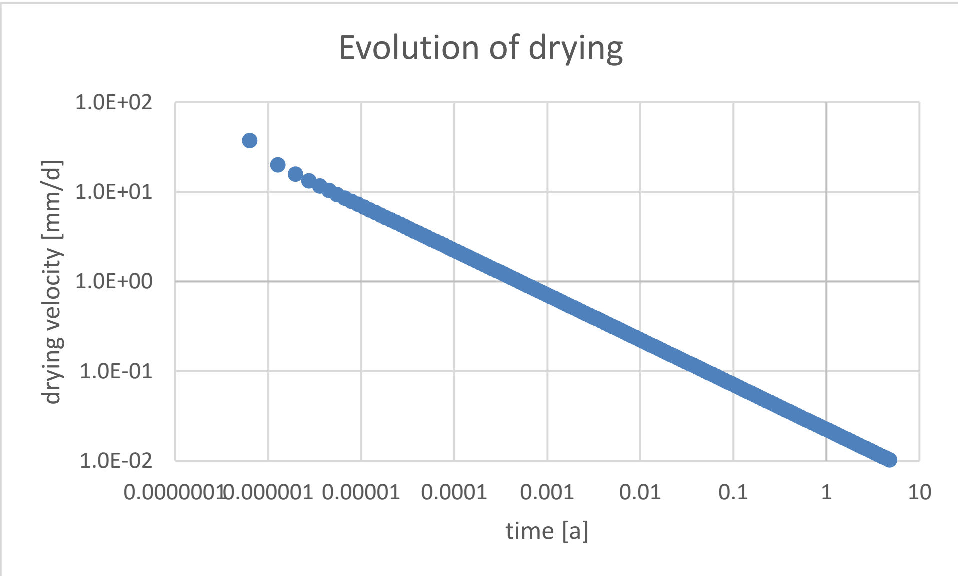

Fig. 3.45 Drying velocity over time

3.4 Groundwater flow in fractured rock, DTU

3.4.1 Introduction

Since mudstone and crystalline rock are considered besides salt formations as host media for a nuclear waste repository in Germany, fractures and fracture systems have become of great interest in long term safety analysis. Regarding flow and transport simulations in the near and far field of the repository, the fractured porous medium must be described with reference to the flow properties. This requires extensive knowledge of the fracture system.

Traditionally, either implicit stochastic modelling or Discrete Fracture Network (DFN) models are used to describe the governing features of fracture networks. Both methods suffer from limited data availability and thus uncertainty because fractures cannot be imaged directly in the subsurface e.g. /WEL 20/.

At Danmarks Tekniske Universitet (DTU) an innovative method has been developed to simulate the growth of natural fracture networks based on the geological history and fundamental geomechanical principles /WEL 19/. Only rather general information about the geological units of a formation in terms of the geometry and mechanical properties are necessary to apply the method, and the result is a geologically realistic fracture network.

The aim of this work was to develop a model with the groundwater flow and transport code d^{3}f++ /SCH 20/ to assess the potential of this approach for groundwater modelling with a focus on repository safety analysis.

3.4.2 Description of the approach

DTU's approach is based on the principle that fracture models are built by simulating the nucleation and growth of the fractures. For this, geomechanical principles and geological knowledge are employed and result in more realistic fractures models compared to purely stochastic DFNs. An extensive description of the approach is provided in /WEL 20/. The approach is designed for brittle layers sandwiched between more ductile layers and considers two types of fractures: small circular microfractures that are entirely contained within the fractured layer, and rectangular layer-bound macrofractures. In the model, microfractures turn to macrofractures when their radius reaches half the bed thickness. As fracture propagation continues, the fractures start to interact. These interactions impede fraction propagation to such an extent that the system eventually reaches an equilibrium stage at the end of a deformation episode.

This approach has been realized in form of the Discrete Fracture Model Generator (DFM Generator, /WEL 23/). From the DFNs generated by DTU for the geological target layers, Oda permeability tensors /ODA 86/ can be derived to transform a DFN in an equivalent porous medium (EPM) by using the respective function implemented in the code Petrel /PET 22/. The resulting tensor fields for the permeability are then ready as input for d^{3}f++ simulations of flow in the target layers.

3.4.3 Hydrogeological model

The Drenthe Aa valley in the north-eastern Netherlands was chosen by DTU as suitable region for demonstrating the potential of the newly developed fracture generation method. Three-dimensional seismic data and other information necessary for their approach is provided free of charge by the Geological Survey of the Netherlands TNO. The model area of 7.3 km times 7.4 km lies a few kilometres northeast of the city Assen in the Dutch province Drenthe (cp. Fig. 3.46). It includes the Anloo diapir in the middle that reaches up to a depth of about 750 m. The work performed by DTU on the Drenthe area providing the input for the model presented here is described in /WEL 22/, p. 179 ff.

Fig. 3.46 Geographical position of the model area

DTU derived geological layers from seismic data /WEL 20/ and provided it for the construction of the hydrogeological model. Unfortunately, the model area was defined by DTU before the collaboration had started so that it was too late to include specific requirements for a hydrogeological model (in particular: boundaries that are defined by watersheds) in the selection process. Therefore, the subsequent cube-like model must be considered as a generic model based on the Drenthe geology and not as a “true” hydrogeological model.

A geometry consisting of about 76,400 prism elements was constructed based on the layer interfaces provided by DTU (see Fig. 3.47). Eleven layers were considered excluding the Zechstein salt of the diapir as its permeability is so low that no significant flow can be expected. The layers correspond mainly to geological groups, but some formations were also subdivided. This applies for instance to the Breda Formation which is a regional aquitard, and the target formation investigated by DTU where the Texel Formation and the Lower Holland Marl Member are differentiated. From a hydrogeological point of view a distinction of further aquifers and aquitards like the Rupel Clay Member and the Brussel Sand Member (both belong to the unit “Middle and Lower North Sea”) would have been desirable but the necessary information was not available. This adds to the generic character of the model.

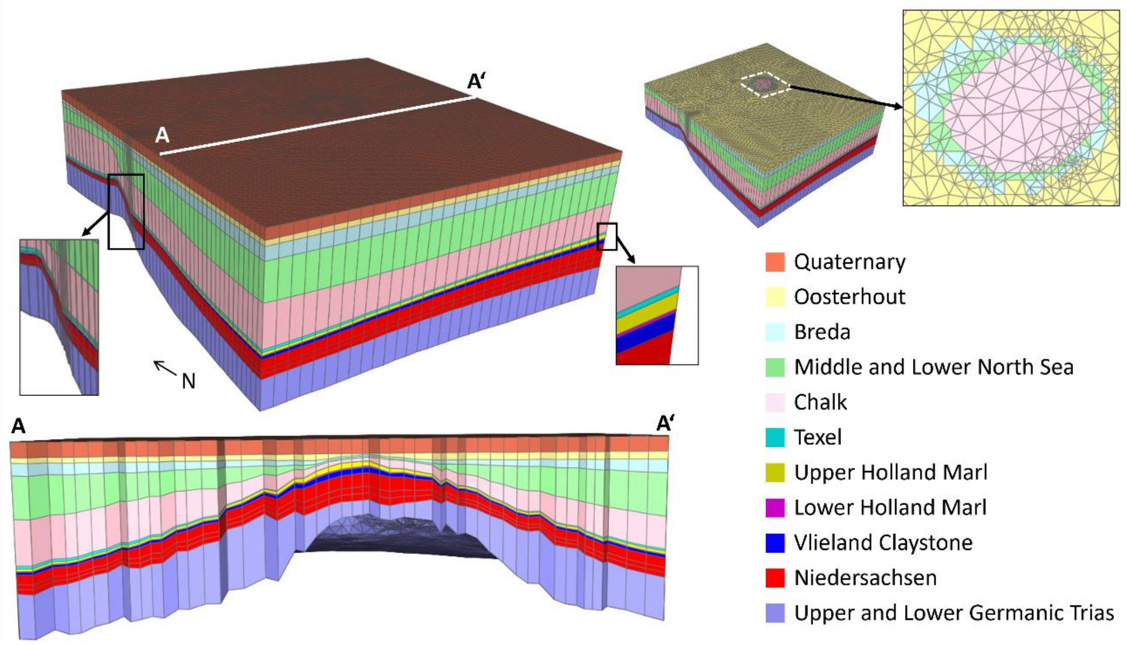

Fig. 3.47 Model geometry used for groundwater flow simulations

The geometry reflects the assumption of /SMI 18/ that the Breda Formation as regional aquitard is eroded above the Anloo diapir. The available layer information was interpreted in such a way that the quaternary sediments overlie the older sediments forming an unconformity. Consequently, the layers Breda Formation, Middle and Lower North Sea Group and Chalk Group have direct contact to the Quaternary deposits (see Fig. 3.47).

Information about permeability and porosity of the modelled layers was provided by Florian Smit of the University of Copenhagen (via personal communication with DTU, see Tab. 3.9). DTU chose probably fractured layers based on a borehole log as target layers (i. e. brittle layers sandwiched between more ductile layers). Often, the fractures are not detected in the drill cores by conventional core analyses and thus fractured layers are missed (Michael Welch, personal communication).

For the target layers Texel Formation and Lower Holland Marl Member, anisotropic and inhomogeneous fracture permeability fields in terms of an EPM (Oda permeabilities) were provided by DTU and were added to the matrix permeability of the Chalk Group and the Rijnland Group, respectively. The resulting permeability fields i. e. the components of the permeability tensors in x-, y-, and z-direction are exemplarily shown in Fig. 3.48.

The maximum permeability values in the Texel Formation occur above the crest of the diapir as well as at its southern (Kxx and Kzz) and its eastern flank (Kyy and Kzz). However, the total permeability (up to $1.6 \cdot 10^{-11}$ m^2) is still dominated by the matrix permeability ($9.62 \cdot 10^{-12}$ m^2) as the fracture permeability calculated with the Oda approach adds only slightly to it.

Different to that, the highest permeabilities in all components of the Lower Holland Marl Member occur north of the diapir where higher fracture intensity and anisotropy showed in DTU's simulations /WEL 20/. Very low values are found south of the most permeable areas. They can be recognized as dark green line from the western boundary to the middle of the model area and they mark the position of a fault (see Fig. 3.48). The highest values ($8.5 \cdot 10^{-12}$ m^2) of the total permeability are increased by two orders of magnitude compared to the base value ($4.8 \cdot 10^{-14}$ m^2).

Tab. 3.9 Permeability and Porosity values applied to the Drenthe models

Layer	Geological group	Horizontal and vertical permeability [m²]	Porosity [-]
Quaternary	Upper North Sea Group	$h = 2.31 \cdot 10^{-11}$ $v = 2.31 \cdot 10^{-12}$	0.4
Oosterhout formation	Upper North Sea Group	$h = 3.47 \cdot 10^{-12}$ $v = 3.47 \cdot 10^{-13}$	0.2
Breda formation	Upper North Sea Group	$h = 3.47 \cdot 10^{-14}$ $v = 3.47 \cdot 10^{-15}$	0.2
Middle and Lower North Sea Group	Middle and Lower North Sea Group	$h = 3.85 \cdot 10^{-12}$ $v = 1.92 \cdot 10^{-13}$	0.315
Chalk Group	Chalk Group	$h = 9.62 \cdot 10^{-12}$ $v = 9.62 \cdot 10^{-12}$	0.255
Texel Formation	Chalk Group	$h = 9.62 \cdot 10^{-12}$ $v = 9.62 \cdot 10^{-12}$ + fracture permeability (Model B only)	0.255
Upper Holland Marl Member	Rijnland Group	$h = 4.81 \cdot 10^{-13}$ $v = 4.81 \cdot 10^{-14}$	0.2
Lower Holland Marl Member	Rijnland Group	$h = 4.81 \cdot 10^{-13}$ $v = 4.81 \cdot 10^{-14}$ + fracture permeability (Model B only)	0.2
Vlieland Claystone Formation	Rijnland Group	$h = 4.81 \cdot 10^{-13}$ $v = 4.81 \cdot 10^{-14}$	0.2
Niedersachsen Group	Niedersachsen Group	$h = 5.0 \cdot 10^{-13}$ $v = 5.0 \cdot 10^{-14}$	0.18
Upper and Lower Germanic Trias Group	Upper and Lower Germanic Trias Group	$h = 7.7 \cdot 10^{-13}$ $v = 7.7 \cdot 10^{-14}$	0.1425

The great benefit of these processed permeability fields is that they reflect the local geology. High permeability values above the diapir's crest as well as low values in the fault are highly plausible. As the DFM Generator accounts for geological and geomechanical information, the resulting permeability fields show realistic patterns that have a direct impact on the groundwater flow in the simulations. No stochastic DFN model would result in comparable permeability fields.

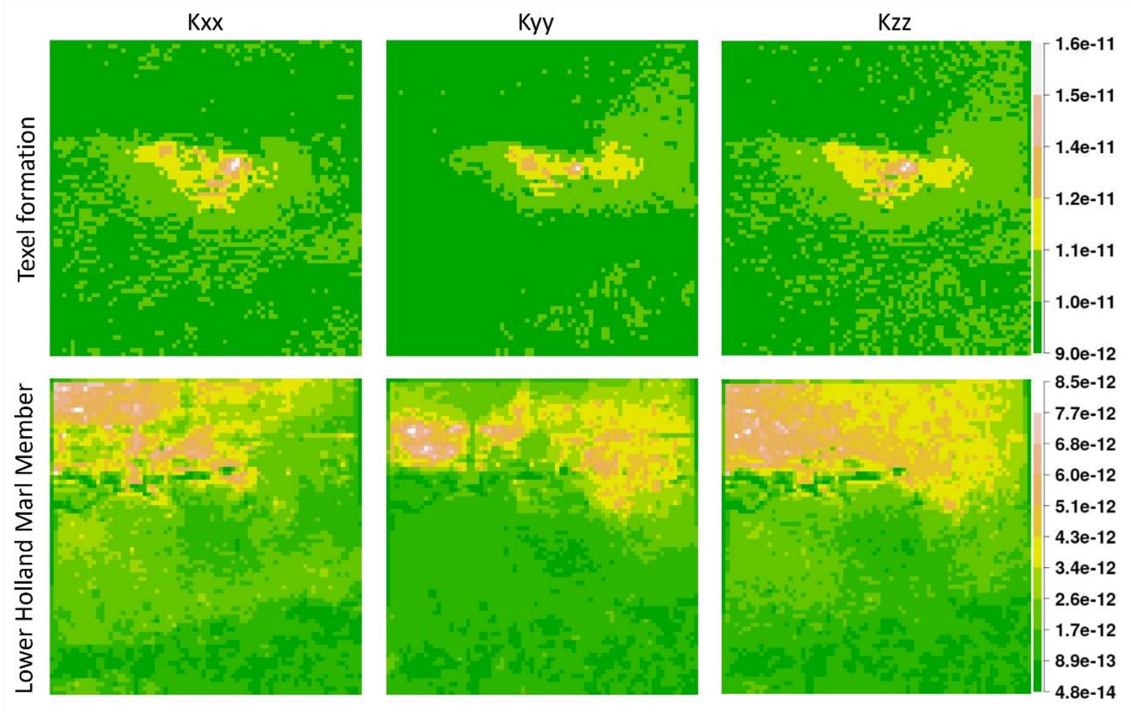

Fig. 3.48 Components of the Oda permeability for the Texel formation (top) and the Lower Holland Marl Member (bottom)

The lateral and upper boundary conditions for the pressure were derived from groundwater monitoring data provided free of charge by the Dutch Geological Service TNO on www.dinoloket.nl. A groundwater surface was interpolated from all available water level measurements in the model region that were performed simultaneous, i.e. on the same day.

At the lateral model boundaries, the hydrostatic pressure gradient for pure water was used. To use a linear pressure gradient is to some extent inconsistent as the permeability of the different layers has an influence on the flow and therewith on the pressure distribution. A simulation of the system is still possible, though. However, this does not apply to the same system if differences in fluid density by salt or temperature are to be considered. In this case, it is much harder (if possible at all) to find an appropriate pressure boundary condition. Therefore, salt and temperature were neglected in the present model. This, however, should not interfere with the hydraulic qualification of DTU's approach.

Equilibrium flow simulations were performed for two alternative models: the permeabilities listed in Tab. 3.9 were applied without (Model A) or with the contribution of the fractures (Model B), i. e. without or with adding the Oda permeability values to the listed permeability values.

3.4.4 Simulation results

Simulations resulted in three-dimensional flow fields for Model A and B, respectively. The flow velocities vary between $1.0 \cdot 10^{-11}$ m/s and $1.8 \cdot 10^{-6}$ m/s for both models (cp. Fig. 3.49). The highest velocities occur in the Quaternary sediments, the lowest in the Breda Formation which is the main aquitard in the model and separates the upper and lower permeable layers from each other except for a circular area above the crest of the diapir. The difference between the two models concerns only the permeabilities of the Texel Formation and Lower Holland Marl Member. However, only the latter can be distinguished in Fig. 3.49 as a thin band of slightly elevated velocity in Model B.

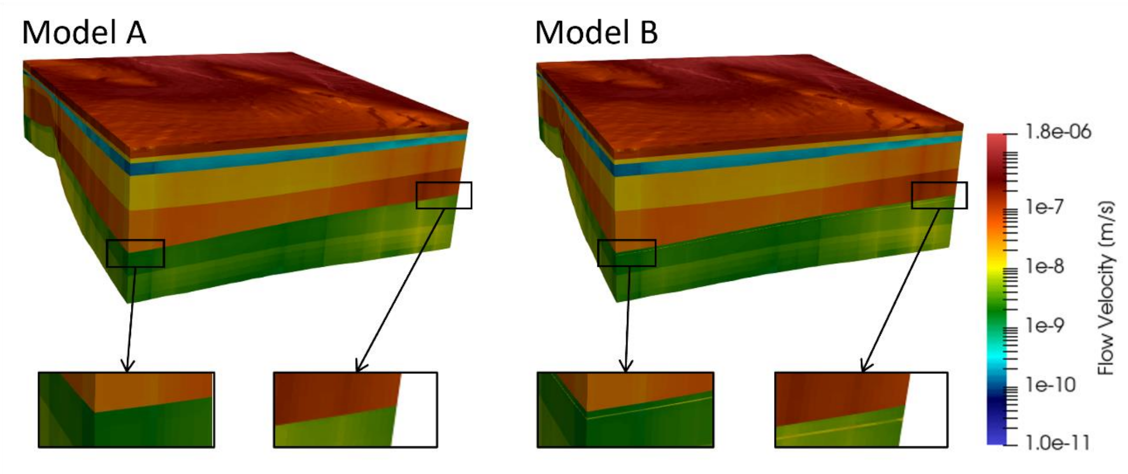

Fig. 3.49 Flow velocities obtained for Model A (constant permeabilities, left) and Model B (Oda permeabilities, right)

A comparison of the flow velocities and directions from Model A and Model B in the Texel Formation reveals no obvious differences (Fig. 3.50). There are very small deviations above the crest of the diapir where the Oda permeabilities are highest (cf. Fig. 3.48) but the contrast to the base permeability is so small that they can only be seen when the velocity fields are superimposed.

Groundwater enters the model domain across the southern and across the central part of the northern boundary (Fig. 3.50). The general flow direction is from the south to the north, diverging south of the diapir's crest and leaving the model across the western, eastern, and the edges of the northern boundary. Above the crest, there is a contact zone between the quaternary and the chalk group sediments which have both relatively high permeabilities. In this zone water converges in the quaternary layer, sinks downwards, and diverges in the chalk group again. As the permeability in the Texel formation is the same (Model A) or slightly higher (Model B) than in the Chalk Group, the water converges above the diapir's crest in this layer, too. The water entering from the north diverges north of the diapir's crest and leaves the model to the north again. The flow runs mainly parallel to the layer surfaces as the permeability of the layer below is one to two orders of magnitude smaller.

Local spots of very low flow velocities are situated south and north to the diapir´s crest. They mark the points where groundwater runs together from opposing directions (i. e. from the north and the south).

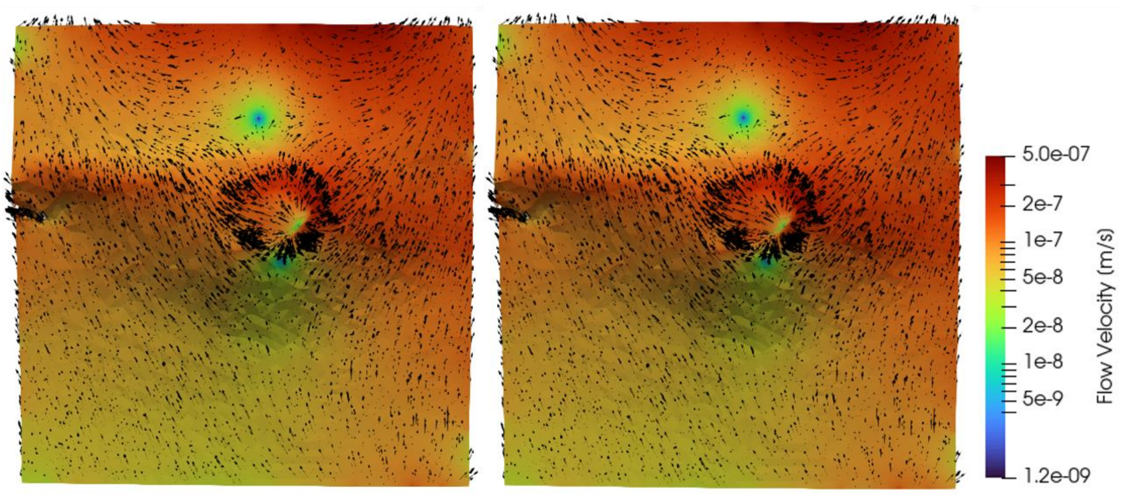

Fig. 3.50 Flow velocities and flow field for the Texel formation for Model A (left) and B (right)

The general flow pattern in the Lower Holland Marl Member is in both models similar to the flow pattern in the Texel formation when it comes to the overall directions (Fig. 3.51). In Model A, the groundwater leaves the layer downwards in the area south of and right above the diapir, and in the central part north of the diapir (Fig. 3.51, left). In the other areas, the flow crosses the layer upwards. There is a spot of very low flow velocity north of the diapir´s crest but otherwise the flow velocity does not vary much over the model area.

In Model B, the flow pattern differs to the flow pattern in Model A as described above (Fig. 3.51, right). South of the diapir the groundwater flows rather along the layer than across it. In this area the flow velocity is slightly raised compared to Model A and it varies spatially between $2 \cdot 10^{-8}$ and $2 \cdot 10^{-9}$ m/s. The differences above and north of the diapir are much more pronounced. The flow velocity is raised by up to one order of magnitude, but the spot of low flow velocity is less prominent. Other spots of relatively low flow velocity can be distinguished on an east-west line from the western boundary to the diapir's crest. The flow runs mainly parallel to the layer interfaces in the northern part of the model.

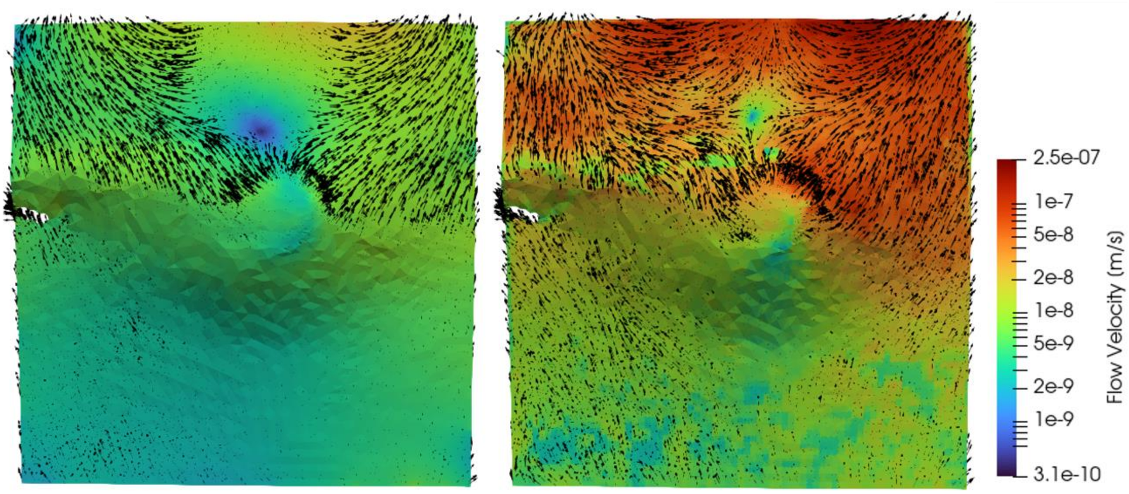

Fig. 3.51 Flow velocities and flow field for the Lower Holland Marl Member for Model A (left) and B (right)

Another difference that cannot be seen in Fig. 3.51 is that in Model A the flow above the diapir always points from south to the north, in some areas with a tendency to the east or the west. In Model B, however, the flow in the central area above the diapir diverges in all directions, like the flow pattern in the Texel Formation (cp. Fig. 3.50), i. e. the Lower Holland Marl Member draws water from the upper layers in this area.

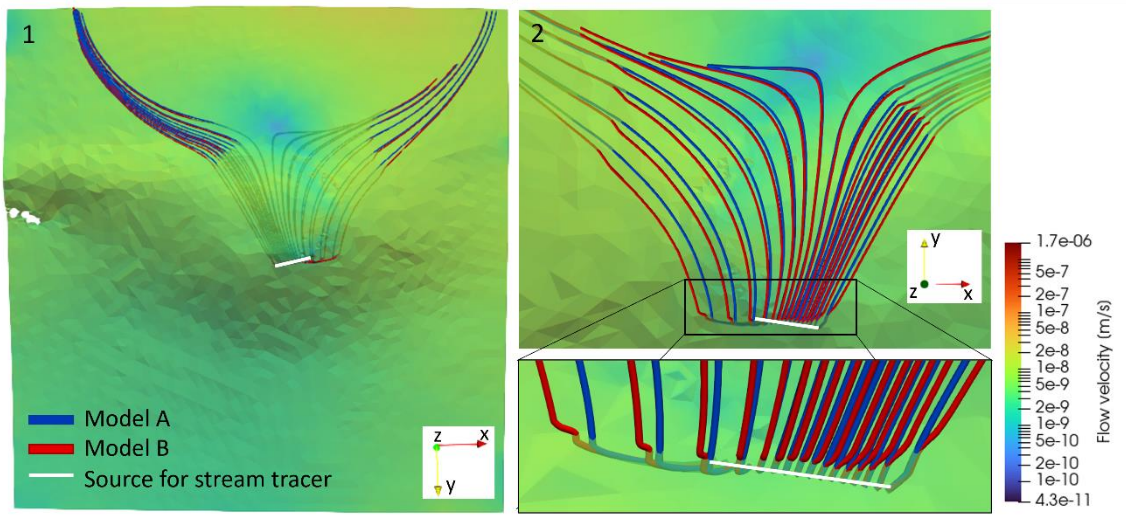

Fig. 3.52 Stream tracers plotted for Model A and B with the flow velocities in the Upper Holland Marl Member. View from above (left) and below (right)

The effect of the changes in the velocity field can be observed in Fig. 3.52. For this figure a line source for 15 stream tracers was inserted in a depth of 330 m and their migration from there on was plotted for both models. The resulting streamlines differ significantly from each other. The difference already begins for the eastern stream tracers in the Upper Holland Marl Member and gets even stronger when the tracers enter the Lower Holland Marl Member. Compared to Model A, the stream tracers are accelerated within the Lower Holland Marl Member and pushed outwards by the water that comes from the upper layers in the center of the diapir (as described above).

3.4.5 Discussion

It could be shown that the Oda permeability fields determined with the help of DTU´s DFM generator (Model B) result in noticeable differences to the homogeneous permeability model (Model A) for the Lower Holland Marl Member. The layer draws water from its surroundings and across the border which changes the flow patterns significantly. The influence on the flow field is rather local, though, as the layer is very thin compared to the whole model (a few meters compared to 800 to 3,000 m model height).

As the model is of relatively small extent, the flow is strongly influenced by the boundary conditions. The hydraulic pressure was fixed on the lateral and top boundary and that limited the variability within the model. This may have prohibited a larger effect of the inhomogeneous permeability fields in Model B on the flow field.

As discussed above, the actual model is not ideal to evaluate DTU's approach. It appears to have a high potential, though, as the permeability fields obtained from the DFM generator result in a plausible flow field. Moreover, the approach indicates possibly fractured layers that could be missed by conventional drill core analyses. As fractured layers show higher permeabilities than unfractured layers, the assumption of fracture systems implies a higher degree of conservativity with respect to flow and transport simulations. This has a great impact on long-term safety analyses.

It is therefore recommended to keep track of DTU's work on the approach. Particularly the intended extension of the approach to crystalline rock would be highly valuable for the site selection process in Germany. Presently, the characterization of fracture fields requires a certain amount of exploratory in-situ work like bore core drilling or tunnel excavation that are expensive and cause damage in the region of interest. Furthermore, even if very accurate, only local information can be received.

The new method suggested by DTU, by contrast, can obviously not be as accurate as direct exploration. But it provides general information about fracture systems on a much larger scale using only available geological knowledge, all this on a more or less theoretical basis. The method thus allows for a first quick and inexpensive check on suitability of potential sites for deep geological storage. A comparison of different sites should thus be facilitated considerably. The potential for local unfractured volumes could be assessed as well as the expected hydraulic conditions around a projected repository.

3.5 Talik evolution[9]

3.5.1 Motivation

In Germany, the safety of a nuclear waste repository legally needs to be investigated for a period of one million years. During the past million years the whole geographic area of present-day Germany has repeatedly experienced permafrost conditions. This will therefore presumably also happen within the time frame that is relevant for the safety

[9] This chapter is largely taken from /KRÖ 24/ which is in essence a summary of the work for the present project. However, the text is updated and supplemented, where applicable, particularly in the subsections 3.5.6, 3.5.7, and 3.5.8 introducing new thoughts about the significance of the results and reflecting the latest considerations about possible further investigations concerning talik evolution.

assessment. An integral part of such a safety assessment is the transport of radionuclides with the groundwater in case of a canister failure. This assessment requires knowledge of groundwater flow systems. These, however, undergo fundamental alterations in the event of permafrost formation as the freezing of near surface layers may shield the biosphere from possibly contaminated water in deeper aquifers.

However, taliks connecting surface waters with deeper aquifers are known to exist in permafrost regions and can potentially lead to a concentrated flux of contaminated groundwater to the surface. Unfortunately, the circumstances of their formation and their stability – highly important for the safety assessment – are largely unknown. Insight can be gained through numerical modelling which is why a mathematical model for groundwater flow under permafrost conditions including equations of state and constitutive equations has been stringently derived /KRÖ 22/. This mathematical model is shortly revisited as a basis for a first thermo-hydraulically coupled numerical model that addresses the conditions of groundwater during the latest cold age. The results are intended to create trust in the modelling framework as a starting point for further investigations in the future.

3.5.2 Introduction

The safety of the biosphere against undesirable release of radionuclides from a deep geological repository (DGR) is principally at risk where groundwater can corrode the metallic waste canisters. For a performance assessment of a DGR, it is therefore imperative to know the groundwater flow system over the projected lifetime of the repository. According to the current legislation in Germany, this will be over a period of a million years /BUN 17/.

Over the past million years, several ice ages have occurred and have brought permafrost conditions all over present-day Germany. As depicted in Fig. 3.53, this has resulted at the last Glacial Maximum (LGM) in continuous permafrost over the majority of the area. Only a small fraction remained to be discontinuous and where ice sheets had moved in, the continuous permafrost had been a precursory phase. It can therefore be expected that any conceivable DGR in Germany will sooner or later also be subject to these conditions during the coming million years. This is significant because permafrost will have a considerable impact on groundwater flow as ground freezing tends to separate deeper aquifers hydraulically from the surface.

However, it is also known that even under permafrost conditions there are local volumes of unfrozen ground, called taliks. According to /VEV 05/, a talik can be defined as “A layer or body of unfrozen ground occurring in a permafrost area due to a local anomaly in thermal, hydrological, hydrogeological, or hydrochemical conditions.”

Large taliks have been documented to hydraulically connecting the surface with deeper unfrozen aquifers (e.g. /BUR 20/, cf. right sketch in Fig. 3.54). /VEV 05/ recommends the expression “open talik” for this phenomenon but also other terms can be found in the literature. Note that from this point on the expression “talik” is used synonymously to “open talik”.

Fig. 3.53 Permafrost conditions during the latest ice age (after /VAN 93/, /REN 03/)

Open taliks are known to exist below large surface water bodies such as lakes and rivers /DEL 98/, /KEL 98/, /SKB 06/. Flow of contaminated waters from a possible leakage in a waste repository could be directed towards such taliks and thus lead to a strongly localized outflow into surface waters e.g. /JOH 16/ (Fig. 3.54). Providing means of radionuclide transport to the biosphere through the permafrost and thereby concentrating the flow from the DGR towards the outlet at the surface makes taliks a key feature in the assessment of a possible exposure of the biosphere to harmful radioactive substances. The mechanisms leading to talik formation must therefore be understood to an adequate level of detail in order to allow for meaningful predictions of groundwater flow and possible subsequent contaminant transport under permafrost conditions.

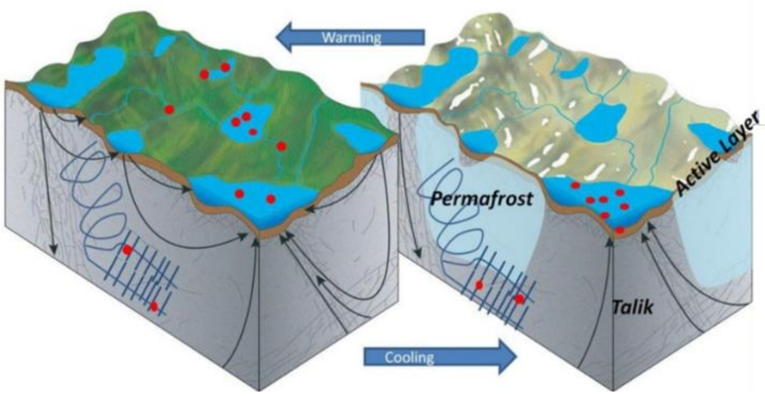

Fig. 3.54 Impact of permafrost on radionuclide migration paths (from /JOH 16/

Taliks cannot be observed directly but require laborious field work to document e.g. /HAR 11/. Furthermore, they provide only a snapshot of a long-lasting evolution which makes it hard to identify the relevant circumstances of its occurrence. Numerical modelling is therefore a welcome tool that can be used to understand talik formation without relying on sparse and challenging field data collections. A surprisingly large variety of mathematical formulations can be found in the literature that describe groundwater flow under freezing conditions including ice formation. Some of them have been compiled and discussed in /KRÖ 22/ (2022) where some formal inconsistencies have been found between assumptions/simplifications during derivation of the balance equations and the ultimately used formulation. Also, no commonly agreed upon set of equations of state[10] (EOS) could be identified as many of the EOS are neither realistic nor appropriate. It was thus concluded that a sound set of formulations should be derived anew to ensure that all relevant processes are properly addressed. Consequently, balance equations, constitutive equations (CE) and EOS were rigorously developed or chosen with care in /KRÖ 22/.

The reported work represents the final preparatory step in providing a trustworthy numerical model for groundwater flow under permafrost conditions. This includes formulations for realistic initial and boundary conditions as well as a definition of a model domain including the related hydrogeologic parameters. As granitic rock is presently considered to be a potential host rock for a nuclear waste repository in Germany, the setting at Two

[10] The expression „equation of state“ is not used here as in the framework of thermodynamics but in a broader sense referring to all material properties that can be measured independently of a specific problem.

Boat Lake in Greenland e.g. /JOH 15/ where a talik has actually been found e.g. /HAR 11/, is used here as a template. Confidence in the modelling framework is built by having a first model run covering the latest climate cooling period leading to the last glacial maximum. Results are checked for being sensible and consistent. At this stage of development, this first model forms a starting point for future investigations.

3.5.3 Methodology

3.5.3.1 Problem definition

Climatic framework

Talik formation may occur either during a change from warmer to colder climates by leaving out an unfrozen "hole" in an otherwise freezing ground, or during a change from cooler to warmer climates by thawing a hole in initially frozen ground. Presently, talik formation is quite intensively investigated in the framework of a warming cryosphere and is most commonly discussed in the context of thawing e.g. /PAR 18/. In cold regions, thawing leads to a variety of serious problems where the permafrost had falsely been assumed to constitute a solid and watertight base for infrastructure such as roads, railways, housing and waste dumps e.g. /SCA 24/, /CRO 24/.

As Germany is currently ice-free, warming climate appears to be not as relevant in the context of geological storage as the question, where will open taliks remain in an otherwise increasingly freezing ground? It is expected that the freezing dynamics are different from the thawing dynamics since the initial temperature for freezing and thawing scenarios and thus all state variables are different. This difference in dynamics may be enhanced by groundwater flow because heat transport by convection depends on the highly non-linear Soil Freezing Characteristic Curve (SFCC) which in turn entails further non-linearities from the relative permeability. The focus is therefore on a freezing scenario in the following.

Domain

It is assumed that cooling and freezing of water is less complex in lakes than in rivers as rivers show considerably more turbulent water flow than lakes. To keep things as simple as possible, the model presented in this work includes a lake in the domain. This lake is located on top of a granitic formation to have some relation to talik investigations on

Greenland e.g. /JOH 15/. Porosity and permeability, however, are chosen to coincide with the conditions at the Grimsel Test Site in Switzerland e.g. /GEN 02/ (Gens et al. 2002) which is also located in crystalline rock.

Axial symmetry is assumed for the hypothetical lake as in /MAC 62/ (Mackey 1962) to reduce the computational cost. The lake has a maximum depth of 25 m at the center and a radial extent of 50 m.

Physical framework

Groundwater flow is bounded by lateral no-flow boundaries in the domain. The system is initially hydrostatic. The thermal temperature boundary at the surface is allowed to evolve in time, while a heat flux according to the geothermal gradient is assigned to the base of the profile. The initial thermal conditions depend on the preceding climate which would be a warm period in this case. Within the domain, the temperature distribution is assumed to be in equilibrium with the initial boundary conditions. Modelling begins at the onset of a cold climate.

The lake is approximated in the model as a porous medium with very high values for permeability and porosity, namely 10^{-11} m² and 99 %, respectively, to avoid modelling free water.

3.5.3.2 Shaping a model

Mathematical framework

The formulations derived in /KRÖ 22/ include the balance equations, the CE as well as their parameters and the EOS considered. They are shortly described in this subsection, being based on the following list of assumptions

- Three phases considered: water, ice, and rock
- No movement of ice or rock
- Constant porosity
- Generalized Darcy flow including
  - Soil Freezing Characteristic Curve (SFCC)
  - Relative permeability dependent on the SFCC
- Local thermal equilibrium
- Fourier’s law

– Isotropic thermal conductivity
– All EOS depend on temperature; EOS for water also on pressure
– No boiling

and including the subsequently listed processes

– Advective water flow
– Sinks/sources for water (not used here)
– Sinks/sources of mass of water and ice due to phase changes; concurrent volumetric changes
– Heat convection and conduction
– Hydromechanical heat dispersion (not used here)
– Sinks/sources for heat (not used here)
– Release/consumption of latent heat

Two balance equations are considered. The first one is the mass balance equation for water describing mass conservation of water and ice. Note that the indices w, i, and m stand for water, ice and matrix.

$$-\nabla\cdot\left(\rho_w\frac{k_{rw}}{\eta_w}\boldsymbol{k}\cdot(\boldsymbol{\nabla}p_w-\rho_w\boldsymbol{g})\right)=\rho_w\,q_w-\left[\Phi(\rho_w-\rho_i)\frac{\partial S_w}{\partial T}+S_w\Phi\frac{\partial\rho_w}{\partial T}\right]\frac{\partial T}{\partial t} \qquad (3.14)$$

ρ - density
η - viscosity
k - permeability
k_r - relative permeability
p - pressure
g - gravitational acceleration
q - volumetric source
Φ - porosity
S - saturation
T - temperature
t - time

The second one is the energy balance for heat describing the conservation of heat energy in the three-phase system water, ice, and rock mass.

$$\begin{aligned}&\left(\begin{array}{c}S_w\,\Phi\rho_w\left[T\frac{\partial c_{s\,w}}{\partial T}+c_{s\,w}\right]+S_i\,\Phi\rho_i\left[T\frac{\partial c_{s\,i}}{\partial T}+c_{s\,i}\right]\\ +(1-\Phi)\rho_m\left[T\frac{\partial c_{s\,m}}{\partial T}+c_{s\,m}\right]-\;L\rho_i\Phi\frac{\partial S_i}{\partial T}\end{array}\right)\frac{\partial T}{\partial t}\\ &+(\boldsymbol{v_a}_{\,w}S_w\rho_w\Phi)\cdot\boldsymbol{\nabla}(c_{s\,w}\,T)-\nabla\\ &\qquad\cdot\left[(S_w\Phi\,\boldsymbol{\lambda_w}+S_i\Phi\,\boldsymbol{\lambda_i}+(1-\Phi)\,\boldsymbol{\lambda_m}+S_w\Phi c_{s\,w}\,\rho_w\boldsymbol{D_w})\cdot\boldsymbol{\nabla}T\right]\\ &\qquad=r_{hQ}+c_{s\,w}\;\rho_w\,q_w\big(T_w-\grave{T}\big)+S_w\Phi\rho_wT\frac{\partial c_{sw}}{\partial p}\frac{\partial p}{\partial t}\end{aligned}\tag{3.15}$$

c_s - specific heat

L - latent heat

v_a - interstitial velocity

λ - thermal conductivity

D - hydrodynamic dispersion

r_{hQ} - source term for directly applied heat

$\grave{T}$ - temperature of inflowing water

Balance equations (3.14) and (3.15) form a system of two non-linearly coupled partial differential equations that describe the thermo-hydraulically coupled groundwater flow under permafrost conditions.

Of all the mathematical formulations that are required to complete the balance equations, the constitutive equations introduce by far the highest uncertainties in the mathematical framework as they provide a parameterized description of micro-scale properties of the porous medium of interest. Furthermore, they are difficult to measure so that often enough the gut feeling of the modeller decides about the relation and the accompanying parameters to be used.

The SFCC and the relative permeability for the present model, for example, are chosen from a comparison of eight related approaches compiled in /KRÖ 22/. This compilation suggests the following choice: the unfrozen water fraction in the pore space S_w is represented by a point symmetric transition curve over the temperature interval -2 °C < T < 0 °C that leaves a residual water fraction of 3 % for T < -2 °C. Dependent on the SFCC is the relative permeability of the water k_{rw} that is taken here to be a cubic function of S_w but leaves a residual value of 10^{-6} for $S_w^3(T) < 10^{-6}$. Both functions are depicted in Fig. 3.55. It should be stressed here again that this choice is not made out of knowledge about the CE in question but out of a feeling of probability.

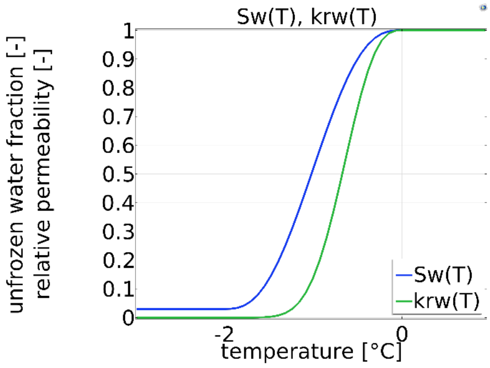

Fig. 3.55 SFCC Sw(T) and relative permeability krw(T).

The complete set of CEs implemented in balance equations (3.14) and (3.15) together with their dependence on other quantities is compiled in Tab. 3.10 (for more details see /KRÖ 22/ and /KRÖ 23/). Note that the gravitational acceleration g is a constant parameter that is needed to allow for density driven flow.

With the equations of state, there is an issue with semantics. In the strict sense of thermodynamics, only density and specific heat are EOS while viscosity and thermal conductivity would be mere parameters. For the purpose at hand, this distinction appears to be impractical. In the context of this work, the expression "EOS" will be used in a broader sense including all material properties that can be described without reference to a specific problem. Following this ad hoc definition, the EOS required for balance and conctitutive equations are compiled in Tab. 3.11.

Tab. 3.10 CEs as implemented in balance equations (3.14) and (3.15)

Constitutive equation	Expression
Flow law	$\boldsymbol{v}_{\boldsymbol{a}\,w} = \boldsymbol{v}_{\boldsymbol{a}\,w}\big(\boldsymbol{v}_{\boldsymbol{f}\,w}\big(k_{rw}(S_w(T))\big), S_w(T), \Phi, g, \rho_w, \eta_w, p_w\big)$
Porosity	$\Phi = const.$
SFCC	$S_w = S_w(T)$
Relative permeability	$k_{rw} = k_{rw}(S_w(T))$
Conductive heat flux	$\boldsymbol{J}_{\boldsymbol{cond}\,\boldsymbol{j}} = \boldsymbol{J}_{\boldsymbol{cond}\,\boldsymbol{j}}(S_j(T), \Phi, \lambda_j, T)$, j = w, i, m
Dispersive heat flux	$\boldsymbol{J}_{\boldsymbol{disp}\,\boldsymbol{w}} = \boldsymbol{J}_{\boldsymbol{disp}\,\boldsymbol{w}}(S_w(T), \Phi, \boldsymbol{D}_{\boldsymbol{w}}(\boldsymbol{v}_{\boldsymbol{a}\,w}, \alpha_l, \alpha_t), c_{s\,w}, \rho_w, T)$

Tab. 3.11 EOS as used in balance equations and CEs

Equation of state	Expression		
	water	ice	rock
density	$\rho_w = \rho_w(p_w, T)$	$\rho_i = const.$	$\rho_m = const.$
viscosity	$\eta_w = \eta_w(p_w, T)$	(n.a.)	(n.a.)
thermal conductivity	$\lambda_w = \lambda_w(p_w, T)$	$\lambda_i = \lambda_i(T)$	$\lambda_m = \lambda_m(T)$
specific heat	$c_{sw} = c_{sw}(p_w, T)$	$c_{si} = c_{si}(T)$	$c_{sm} = c_{sm}(T)$

Simplified equations of state valid in the temperature range between -20°C and +20°C and hydraulic pressures up to 10 MPa had also been developed by Kröhn /KRÖ 22/. Tentative modelling of a changing surface temperature showed, though, that the induced temperature signal went considerably lower than a depth of 1000 m and thereby beyond the initially considered limit of 10 MPa. Thus, a new set of EOS expected to be valid up to +60 °C and down to a depth of about 2 km have been derived /KRÖ 23/ and applied here. Evaluation of the modelling results included a check against transgressing the ranges of validity for the EOS (cp. section 3.5.4.2). Exemplarily, the EOS for water are depicted in Fig. 3.56. All these mathematical formulations are realized in the framework of the Code COMSOL Multiphysics.

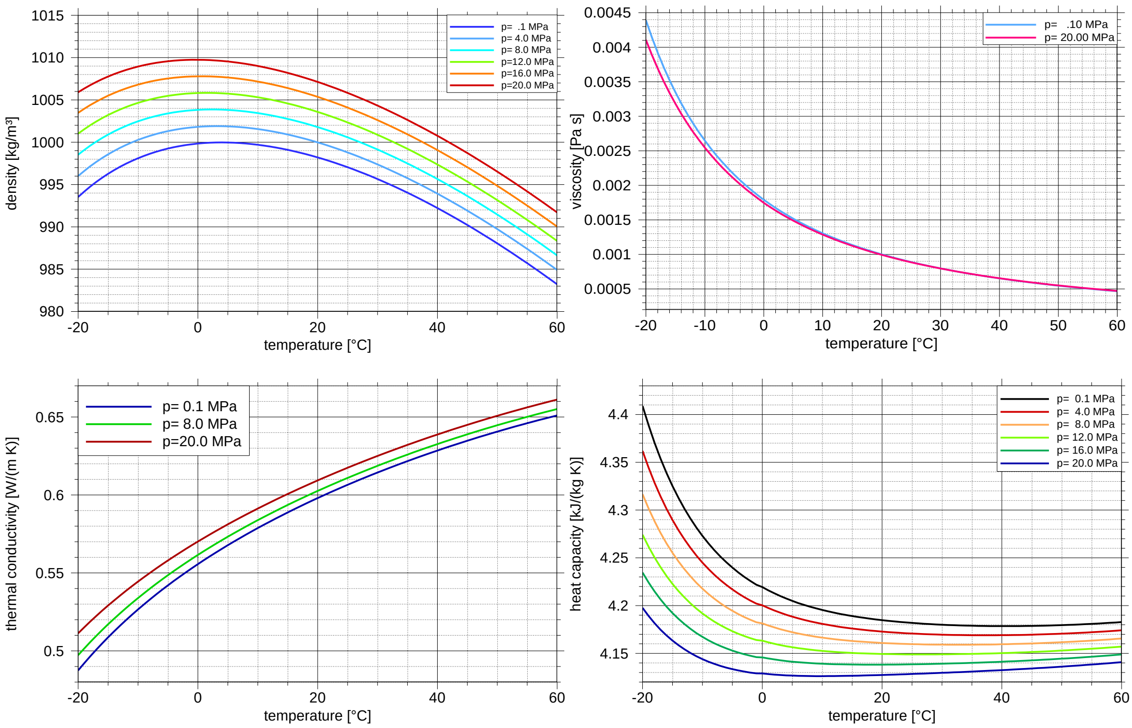

Fig. 3.56 Dependence of the EOS for water on temperature and pressure; upper left: density, upper right: viscosity, lower left: thermal conductivity, lower right: specific heat capacity

Thermal setup

Generally, the temperature distribution in the subsurface is influenced by the temperature at the top, by the geothermal heat flux and by the thermal properties of the subsurface. Basically, two mechanisms determine the geothermal heat flux, namely radiogenic and primordial heat, e.g. /DYE 12/. The former relates to radioactive decay of naturally occurring radioactive elements and the latter to residual heat from planetary accretion. This leads to a complex evolution over geological times. However, over the past million years, the change in heat flux from inner earth amounts only to 0.18 % /LOY 07/ allowing from a rational point of view for the simplification of a constant flux over the period of interest.

According to a recent data survey, heat flux over the area of present-day Germany ranges between 20 and 192 mW/m² /FUC 22b/. For the present model, the average of 78 mW/m² /FUC 22a/ is adopted for the bottom boundary of the model.

A time-dependent temperature boundary condition is applied at the surface. Climate change as a driver for the evolution of permafrost and thereby of taliks is considered over ten thousand to a hundred thousand years. Data on surface temperature evolution determined from ice cores from Antarctica /JOU 07/ are of great interest when reconstructing climate data. These data are given as differences to a reference value, that dates back to pre-industrial conditions. The data from the last cooling climate are taken as an approximation for the cooling dynamics over present-day Germany which in turn may be a template for future climate changes. Only a reference temperature for pre-industrial Germany thus remains to be determined to construct absolute temperatures for the model top.

Systematic climate measurements in Germany go back to the year 1881 e.g. /DWD 21/. At this time, industrial revolution was underway /ERI 23/. Twelve reconstructions of the temperature evolution of earth's northern hemisphere using "multiple climate proxy records" for the past 1300 years /SOL 07/ indicate that the temperature was not affected by industrialization until about 1900 (see Fig. 3.57). The wanted reference temperature can thus be established on the basis of the first 20 years of temperature recorded by the DWD. According to data of the Climate Data Center of the DWD /DWD 23/, this value amounts to about +7.6 °C. Note that these measurements refer to a surface air temperature (SAT) at 2 m height above ground.

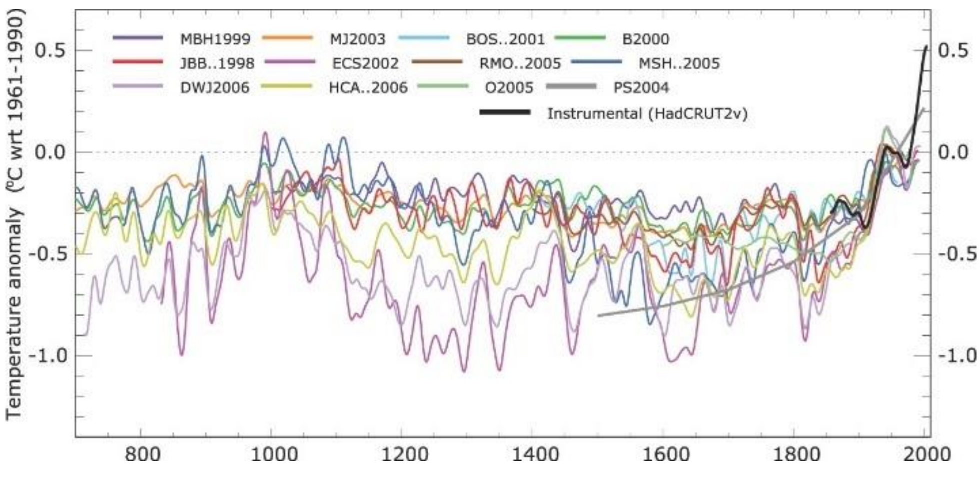

Fig. 3.57 Reconstructions of the temperature anomaly of earth's northern hemisphere; from /SOL 07/

Daily and seasonal variations of the air temperature may reach down up to about 12 m into the ground e.g. /DWD 12/. However, these few topmost meters can be seen as a temporary storage volume for heat energy that is filled during a warm period and drained again during a cold period. Any net effect of the heat flow fluctuations on the temperature field is attenuated over space and time. It is therefore assumed that temperature variations between the SAT and the ground temperature at about 12 m depth can be neglected leaving annual average temperatures to be considered in this work. In other words, the SAT can directly be applied as the thermal surface boundary condition for the model. The temperature evolution for the past 250,000 years is adopted accordingly and shown in Fig. 3.58.

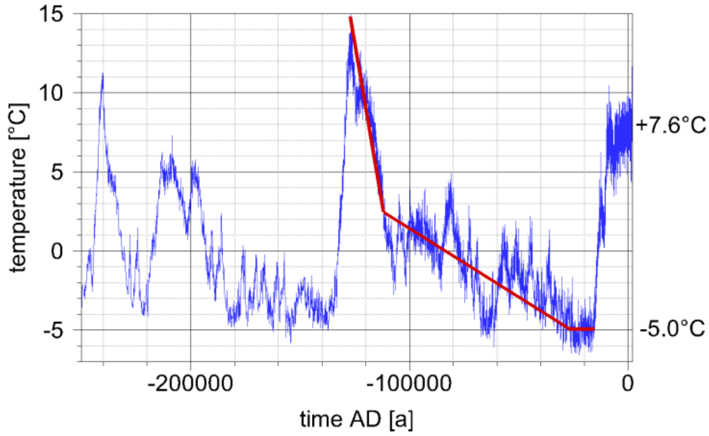

Fig. 3.58 Adopted history of SAT over Germany; adopted data in blue, simplified curve in red

The cooling/cold period of choice has been selected to be the interval between 127,000 and 15,500 years BC. For modelling purposes, the temperature evolution is smoothened to a polygon as indicated by the red line in Fig. 3.58. It is also shifted in time for convenience according to Tab. 3.12.

Tab. 3.12 Simplified temperature evolution

Real time [a BC]	Model time [a]	Temperature [°C]
127,000	0	14.80
111,600	15,400	2.45
26,600	100,400	-5.00
15,500	111,500	-5.00

The initial temperature field is calculated according to a geothermal gradient of 0.0232 °C/m where the initial temperature of 14.8 °C is assigned to the top of the model. Model calculations proved this to be consistent with the heat flux of 78 mW/m² over the bottom boundary.

It has to be noted that the effect of cyclic surface temperature variations discussed above with respect to daily and seasonal changes, applies in principle also to climate-caused fluctuations. Amplitude and frequency of these changes control the depth to which the thermal impact can be observed. The bottom of the model should thus extend beyond the zero amplitude. This is further discussed in section 3.5.4.2.

3.5.4 Modelling

3.5.4.1 Initial and boundary conditions

The set of hydraulic and thermal initial and boundary conditions as depicted in Fig. 3.59 is subsequently discussed.

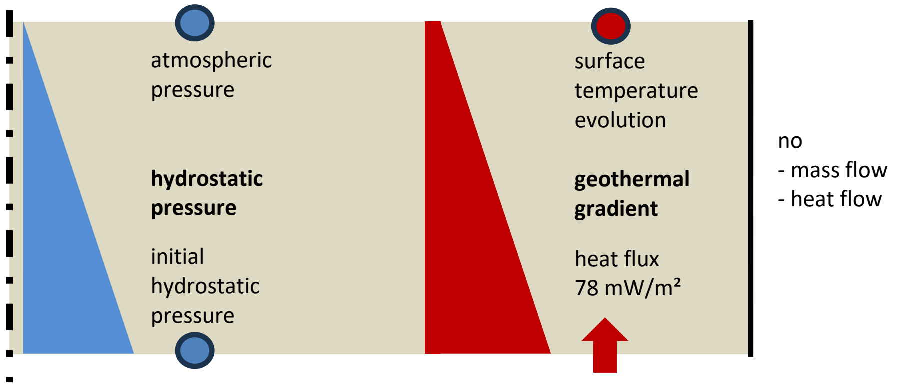

Fig. 3.59 Hydraulic and thermal initial and boundary conditions

As an initial condition, no groundwater flow is assumed in the model which implies a hydrostatic pressure distribution over the domain. The initial pressure distribution is generated using a hydraulic head of 0 m at the top of the model.

The lateral boundary of the axial symmetric domain is a no-flow boundary. It is expected that any influence of the lake on the freezing process can be neglected if this boundary is located sufficiently far from the lake. In this case the flow at the lateral boundary is strictly vertical and no mass exchange occurs across this boundary. The resulting model width is determined in section 3.5.4.2.

The pressure at the bottom boundary is fixed to the initial hydrostatic value of 19.54 MPa assuming a mean water density of 996 kg/m³. This introduces an error over time when phase change of water to ice occurs. The displacement of water due to volumetric expansion during ice formation results in lateral water migration across open model boundaries, thereby changing the weight of the water column and thus the hydraulic pressure at the bottom. Under these circumstances, a lateral no-flow boundary forces excess water out of the model through the top boundary where, in reality, the ice should impede water flow. The error from a fixed pressure at the bottom can only be limited maximizing the depth for the model domain. This is determined in section 3.5.4.2.

The lateral thermal boundary is assumed to be sufficiently far from the model axis that no temperature signal caused by the lake reaches the lateral boundary. In other words, the heat flux along this boundary is assumed to be strictly vertical so that no heat exchange across the boundary occurs.

3.5.4.2 Preparatory modelling

To prepare the final model, some preparatory modelling work was required. This included a) determining an appropriate model width and depth and b) checking for the compliance of model temperatures and admissible temperature ranges for the EOS.

Tentative model runs indicate that lateral boundary should be arranged at a radial distance of 1000 m from the model axis to ensure a sound approximation of no flow and no heat flux across this boundary.

As discussed in subsection 3.5.4.1, the hydraulics require a maximized model depth. In order to ensure validity of the new EOS with respect to temperature and pressure, this depth is set to 2000 m. However, modelling by way of trial indicates that a temperature signal from the top reaches a depth of 2000 m in less than 10,000 years in this model. This is very little compared to the more than 111,500 years assessed in this study.

While further extensions of the formulations for the EOS for water would be rather hard to derive, the EOS for the rock are well-known up to a temperature of 200 °C cf. /KRÖ 10/. It is thus assumed here that exclusion of water in the pore space below a depth of 2000 m constitutes a reasonable approximation for heat transport at great depths. Different domains are consequently considered for hydraulic and for thermal processes. The domain for the hydraulic simulations remains as discussed above but the thermal model is extended downwards by an additional piece of solid rock material with zero porosity. Calculations with this enlarged model indicate that the temperature signal from the top does not reach a depth of 6000 m within 110,000 years. The undisturbed temperature at that depth is 157 °C attesting validity of the thermal EOS for the rock in this model.

3.5.4.3 The full-featured model

Based on the problem definition in section 3.5.3.1, the model shape described in section 3.5.3.2, and the remaining specifications from the previous subsection 3.5.4.2, a single model run has been performed to inspire confidence in the mathematical model and to assess the possible thermo-hydraulic conditions in the subsurface. The related parameters are compiled in Tab. 3.13.

Tab. 3.13 Model parameters

Parameter	Value		Dimension
	rock	lake	
Permeability	10^{-18}	10^{-11}	m²
Porosity	0.01	0.99	-

3.5.5 Results

Simulation times of interest

Three points in time in this simulation appear to be of particular interest: (1) an early time to represent effects at the beginning of cooling, chosen to be 1000 years, (2) 60,000 years which is some time after the onset of freezing, and (3) the end of the cooling climate at 111,500 years. Results with respect to these times are presented in the following subsections.

1000 years: Effect of cooling

After 1000 years model time, the surface temperature has decreased from 14.8 to 14.0 °C. This relatively small difference increases the vertical temperature gradient to the extent that the heat flux over the granitic surface increases by a factor of about 2.5. The water in the lake, however, has a much lower thermal conductivity and thus shields the bottom of the lake from cooling. Heat flux from below is diverted around the lake as visualized left in Fig. 3.60 where heat flux is plotted as a vector field, as the related distribution of absolute velocity values highlighted in colour, and as a couple of pathlines.

The resulting temperature field, given as isolines and a coloured scalar field, right plot in Fig. 3.60, shows the resulting temperature anomaly of a few tenths °C around the lake.

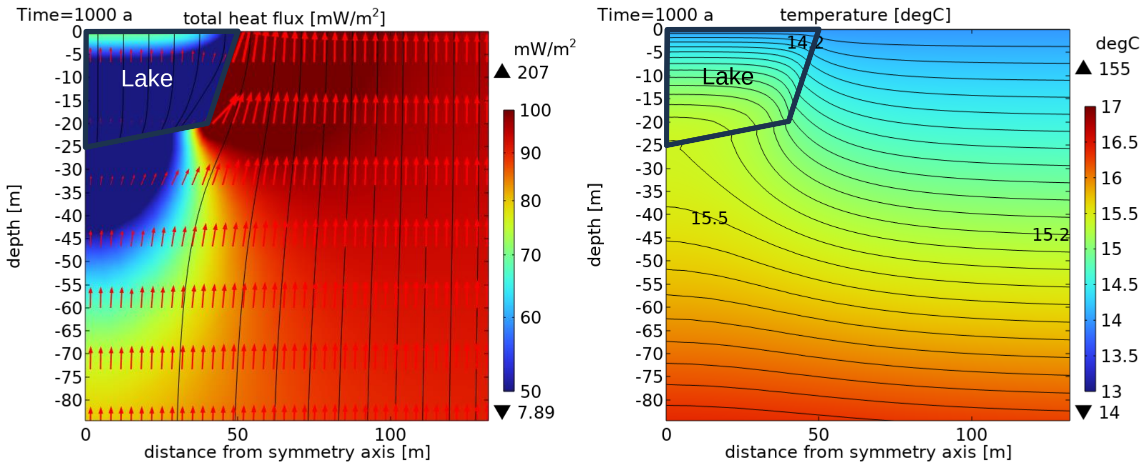

Fig. 3.60 Total heat flux (left) and temperature (right) in the vicinity of the lake at 1000 years modelled time

60,000 years: Effect of freezing

In the model, the surface temperature falls below 0 °C after about 43,400 years as depicted in Fig. 3.61. After 60,000 years simulation time, ice can be found down to about 20 m depth. Since the model accounts for the volumetric increase of water due to freezing but does not allow for ice on the lake to heave, the remaining water in the lake gets squeezed out into the rock as illustrated in the left plot in Fig. 3.62 showing the scalar saturation field and qualitatively the velocity vectors for the water flow.

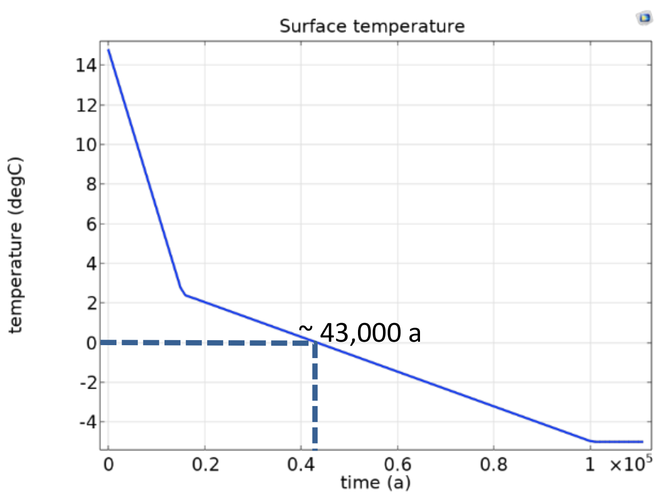

Fig. 3.61 Temperature evolution at the top of the model

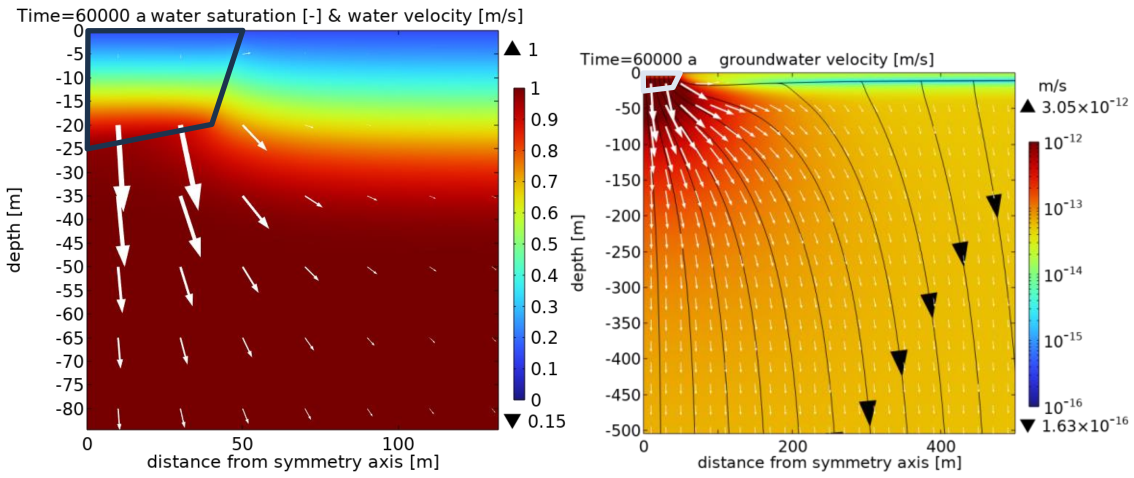

Fig. 3.62 Liquid water saturation and water velocity (left) and water flow (right) in the vicinity of the lake at 60,000 years modelled time

The absolute flow velocity depicted for a large part of the model depicted in Fig. 3.62 is quite small, less than 10^{-12} m². It is consistent, though, with the slow downward progress of the ice front because forming of ice results in volumetric expansion and leads to a downwards directed displacement of water.

111,500 years: End of cold age

The end of the cold age considered here is reached after 111,500 a. The model calculates a thickness of the frozen ground of about 150 m (see Fig. 3.63, left). The freezing front becomes horizontal as the effect of the lake is no longer felt.

As the thermal conductivity for ice is lower than for the rock (but higher than for water), the frozen lake still forms an impediment for heat flow even if not as effective as the water at the beginning of the simulated cold age. The temperature anomaly around the lake at the end of the simulation (see Fig. 3.63, right) is therefor probably a permanent feature.

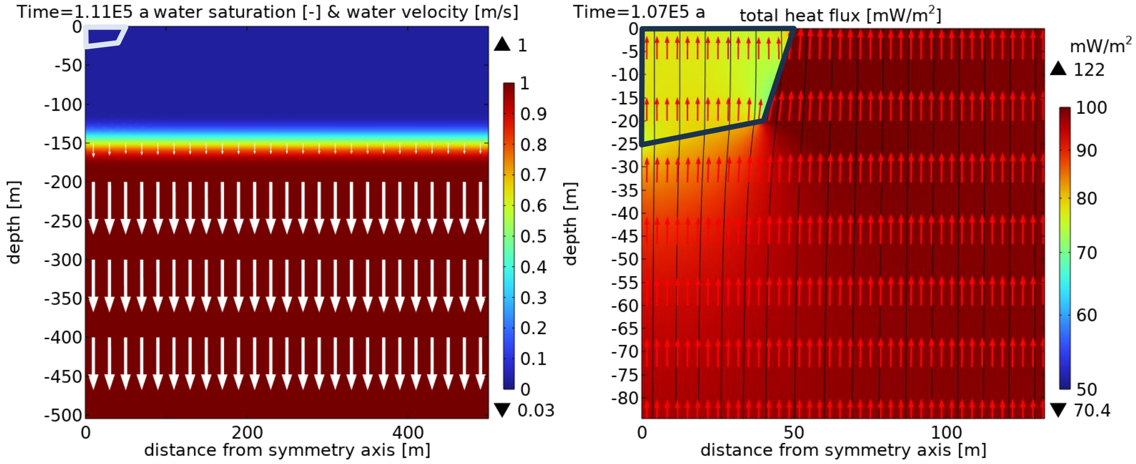

Fig. 3.63 Water saturation and water velocity (left) and total heat flux (right) after 111,500 years

Evolution of water density

The interplay of increasing temperature and hydraulic pressure with depth results in a peculiar evolution of the vertical water density distribution. While the density at the top varies only by about 1 kg/m³, it differs by 5 kg/m³ at 2000 m depth. Furthermore, the maximum water density of 999.1 kg/m³ is initially located at a depth of about 100 m but increases to 1002.3 kg/m³ and moves down to 700 m depth after 111,500 years model time (see Fig. 3.64).

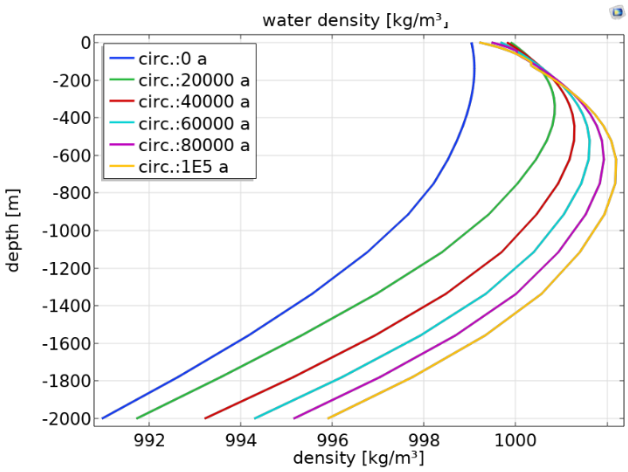

Fig. 3.64 Evolution of the water density with depth

3.5.6 Discussion

In the model, groundwater flow is basically driven by the freezing of water as the less dense ice displaces the unfrozen water in the pore space due to expansion during phase change. The resulting flow velocity is consistent with the progress of the ice front and thus very low, lying in the range of µm/a. The calculated groundwater flow can therefore not provide any significant convective heat transport. This leaves heat conduction as the only heat transport mechanism in the model.

The thermal conductivity of water – and later also that of ice – is much lower than that of granite which makes the granite a heat conductor in comparison to rather insulating properties of water and ice. However, this difference is by far not sufficient to shield the underground from heat loss to the extent that taliks can develop. A permanent signature of these properties can be identified in the temperature fields, though.

In fact, the evolution of convection cells in the underground as a possible mechanism for (additional) upward heat transport had been anticipated when setting up the conceptual model (see Fig. 3.65). Simulation of density-dependent groundwater flow has thus been provided for in the model equations by considering gravity in the flow law.

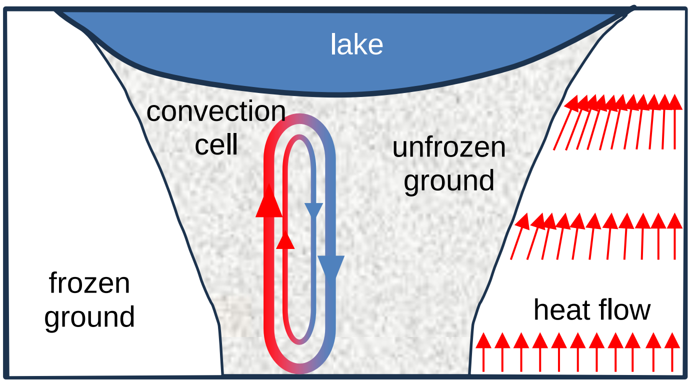

Fig. 3.65 Mechanisms of heat transport: convection cells and deflection of heat flow

However, a prerequisite for the initiation of convection cells is a certain instability which can be quantified with the help of the dimensionless Rayleigh number Ra

$$Ra = \frac{\rho \beta \Delta T k l g}{\eta \alpha} \tag{3.16}$$

Ra - Rayleigh number [-]

ρ - mass density of the fluid [kg/m³]

β - thermal expansion coefficient [1/K]

ΔT - temperature difference across distance l [K]

k - permeability [m²]

l - size of domain [m]

g - gravitational acceleration [m/s²]

η - dynamic viscosity [Pa s]

α - thermal diffusivity [m²/s]

where the thermal diffusivity α is defined as

$$\alpha = \frac{\lambda}{\rho c_s} \tag{3.17}$$

λ - thermal conductivity [J/(m s K)]

c_s - specific heat capacity [J/(kg K)]

The Rayleigh number represents basically the “ratio of driving to damping forces” /WEN 19/ or, more specifically, the ratio of convective flux to diffusive flux thereby making it in principle similar to the Peclet number /SQU 05/. However, the Rayleigh number applies where the transported quantity itself changes the fluid density while the Peclet number describes essentially the same conditions but for a perfectly neutral tracer. Evolution of a convection cell requires the Rayleigh number to exceed the critical value Ra_c (e.g. /HOR 45/, /LAP 48/)

$$Ra_c = 4\pi^2 \tag{3.18}$$

Ra_c - critical Rayleigh number [-]

Based on data from the model as compiled in Tab. 3.14, typical Rayleigh numbers for the lake and for the underground are determined as 0.75 and 0.00012. Under these circumstances, development of convection cells cannot be expected.

Tab. 3.14 Model parameters for calculation of the Rayleigh number

Parameter	Value		Dimension
	rock	**lake**	
density	1000		kg/m³
thermal expansion coefficient	$69 \cdot 10^{-6}$		1/K
temperature difference	23	0.58	K
permeability	10^{-18}	10^{-11}	m²
size of domain	1000	25	m
gravitational acceleration	9.81		m/s²
dynamic viscosity	0.001		Pa s
thermal diffusivity	7.6		m²/s

Squeezing water from the lake due to the volumetric expansion during freezing is the result of having a geometrically fixed top boundary that forces the newly formed ice downwards. This is of course unrealistic as the ice would be floating on top of the lake water – at least for quite some time – and thus exerting less pressure on the lake water. In a more realistic treatment of the lake, the effect of squeezing water out under the lake ice would therefore be much less pronounced. As a result, the progress of the ice front with time would be even less disturbed by the lake and the ice front would be even less deviating from a horizontal course. However, it would also put up less resistance against a hypothetical rising of warmer water from under the lake.

3.5.7 Conclusions and outlook

The first attempt of reproducing talik formation during a change to a cooler climate has failed. Instead, the water in the lake at the top of the model completely freezes. An important question (that should have been asked right away) thus concerns the expected condition of lakes and rivers at a glacial maximum. If they stay unfrozen even then, a talik may be persistent over the whole climatic cool period as initially presumed.

However, if large surface waters completely freeze during an ice age, it is easily conceivable that open taliks become closed taliks. In that case it can be speculated that the open taliks that are presently observed have simply opened up again during the presently warming climate. Taliks could then be transient features in the permafrost that occur only during cooling and during warming climates but not at permanently freezing conditions. Interestingly, this would highly increase the relevance of the vast field of talik investigations in the context of climate warming for the safety analyses of radioactive waste repositories.

While the primary goal concerning talik development has been missed, modelling has led to reasonable results. There is a temperature anomaly in the vicinity of the lake because the lake is shielding the ground below to a certain extent from heat loss due to its comparatively low thermal conductivity. This feature is visible over the whole simulated time and should still be visible when equilibrium of heat flow according to the thermal boundary conditions is reached. Also, consistency of phase change and water flow due to the related volumetric change of the water indicates the validity of the implementation.

Since the simulation did not show even a short-lived temporary talik, it appears that the present model is too simple. The model may geometrically be too simple and/or one or more processes are missing. Heat transport based on conduction alone is apparently not sufficient and convection cells cannot evolve in the present model. The geothermal gradient alone thus appears to be insufficient to cause convection cells.

What has been fully neglected in the present study, though, is the impact of the temperature oscillations on the freezing dynamics as only mean values over very long periods of time have been considered. Such oscillations occur on quite different time scales: daily, seasonal and climatic. But climatic temperature variations are apparently too slow to affect the ground(water) differently than in the present model. Daily variations, by contrast, are probably too fast to have a measurable influence on freezing in a lake.

At the scale of seasonal variations, however, periods with and without ice on the lake could be resolved. This is significant as the thermal regime in the lake water is radically different during these specific periods. While the water in summer is more or less completely mixed, it becomes stratified during the winter season e.g. /BUR 05/. It can be speculated that this phenomenon prevents a lake from completely freezing over for a much longer time than in the present model. This would then sustain the insulating properties of the lake water and keep up the increased temperature below the lake. The resulting difference to the otherwise freezing ground might be sufficient to form a talik.

An additional effect that becomes noticeable at seasonal differences is that of changing albedo particularly on top of the lake. In summer during the phase of complete water mixing in the lake, the surface is comparatively dark and rather absorbs heat from the sun thereby adding to the downward heat transport. In winter, by contrast, the sun beams are reflected by the ice on top of the lake to a significantly higher degree than in summer.

A recent suggestion from the experts of the CatchNet group was to look into bacterial activities at a lake bottom that might be heat producing.

Finally, the top of the lake shouldn't be fixed in the model when the water starts to freeze as this results in unrealistic pressure build-up in the water.

3.5.8 Recommendations

A realistic numerical framework for groundwater flow under permafrost conditions has been presented. While the main goal to track talik forming numerically has been missed, the otherwise reasonable modelling results encourage further systematic investigations. They should relate on the one hand to physical processes that need to be included in the model, and on the other hand to the model setting.

In the first category falls investigating possible mechanisms that could heat up the lake bottom and particularly looking into the freezing dynamics of lakes. The second category comprises parameter variations e.g. heat flux from the inner earth or permeability and porosity of the rock as well as introducing new features in the model such as a (possibly non-horizontal) groundwater table, heterogeneities in the rock or a deep aquifer. For all these reasons, pursuing the present work is strongly recommended.

3.6 Freezing in fractures

3.6.1 Introduction

The study of freezing processes in granitic fractures is essential for understanding sub-surface flow dynamics during ice age events. These processes can lead to significant changes in the permeability of the host rock, which is of particular importance for the safety assessment of nuclear waste repositories in crystalline rock formations. Given the long-term nature of such assessments, German law requires safety evaluations that consider a time span of at least one million years. During this period, multiple ice ages are likely to occur, and the freezing of fractures could have a profound impact on the behavior of groundwater flow and, consequently, on the safety of the repository.

To better understand these processes, a series of laboratory experiments has been conducted using 3D printed fracture replicas. These replicas provide a unique opportunity to simulate and observe freezing behavior in a controlled environment. The transparent nature of the fracture replicas allows for direct, real-time observation of the freezing processes within the fractures, facilitating a more detailed analysis of the mechanisms involved. By replicating the underground conditions during potential ice age events, these experiments aim to contribute valuable insights into the behavior of groundwater flow in fractures of crystalline rock under freezing conditions, which is essential to supplement the reliability and accuracy of safety evaluations for nuclear waste storage for permafrost conditions.

3.6.2 Components

Climate chamber (from stock)

The climate chamber, shown in Fig. 3.66, is a critical component of the test setup, as it ensures quite precise temperature control. The temperature is controlled within a range of -42°C to 180°C with spatial accuracy of up to ± 2 K and a temporal deviation of up to ±0,5 K. The chamber provides sufficient space for the entire test setup and is also equipped with specially insulated cable bushings to allow sensor cables and tubing to pass through the chamber walls.

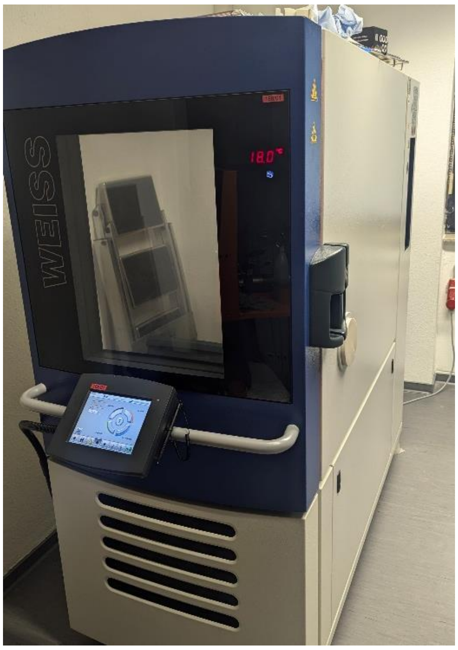

Fig. 3.66 Climate chamber in the GRS laboratory

Syringe pump (from stock)

The syringe pump was already used for laboratory tests with bentonite in the project WiGru-7 /NOS 18/, /KRÖ 19/. It allows for injection of water at variable rates from 0,01ml/h to up to 100 ml/h. As it was originally designed for medical application, it shuts off at a backpressure of 1,1bar. The pump is depicted in Fig. 3.67 while it is injecting fresh water.

Fig. 3.67 Syringe pump

Industrial camera

An industrial camera, depicted in Fig. 3.68, was used to monitor the state of matter of the injected methylene blue solution. The camera has a resolution of 3264 x 2448 pixels and is equipped with a 5 to 50 mm lens. Due to the sub-zero conditions, a special camera was required, which is rated to function at temperatures as low as -10°C.

Fig. 3.68 Industrial camera

LED-light source

A LED ring light, depicted in Fig. 3.69 was used as the light source, to be mounted directly on the camera lens. The advantage of using a ring light over a conventional light source is the reduction of reflections from the sample surface. Additionally, the light intensity could be adjusted to enhance the contrast of the captured images.

Fig. 3.69 LED ring light

3D printed fracture replica / test cell

A test cell was constructed based on 3D scan data of large fracture samples from the Hard Rock Laboratory Äspö /KRM25/. The cell features a cut-out section of the fracture measuring 7 by 10 cm, a pointwise inflow, and an outflow over the entire fracture opposing the inflow side. Printing the two related fracture surfaces separately proved to be necessary to avoid incorrect merging of the surfaces in areas of small apertures. The assembled and sealed test cell is shown in Fig. 3.70.

Fig. 3.70 3D printed test cell, including realistic fracture surfaces

Tracer solution

To visually detect the freezing of the injected liquid in the fracture replica, a special type of tracer was required that shows a color change corresponding to the change in state of the matter. Liquids with such properties, like low-concentration methylene blue solutions, are commonly used in the field to measure the thickness of permafrost layers /FUK82/. To determine the appropriate methylene blue concentration for the tracer solution, preliminary tests were conducted using syringes filled with the solution that were placed in a climate chamber. A concentration of 0.05% methylene blue was found to be the most suitable, as it showed the desired color change while reducing possible staining by the tracer solution. As shown in Fig. 3.71, the tracer clearly changed color when crystallization occurred.

Fig. 3.71 Syringe filled with partially frozen 0,05% methylene blue solution; dark color: solution in liquid form; light blue: partially frozen; transparent: frozen

Data acquisition system

Additionally, an Ahlborn measurement system, shown in Fig. 3.72 with nine PT100 sensors was installed to monitor the temperature at different points in the climate chamber, in addition to the temperature displayed on the chamber. The sensors were initially calibrated to match the temperature shown on the climate chamber. While accurate temperature measurements are not possible without a calibration against a known reference, the focus was on detecting spatial deviations in the temperature distribution inside the climate chamber.

Fig. 3.72 Data acquisition system

3.6.3 Test setup

Except for the syringe pump and the data acquisition system, all the components were placed inside the climate chamber during the experiment. Initially the test cell was placed horizontally levelled in the chamber, which allowed for an easy observation of the fracture but lead to remaining air bubbles in the fracture after flooding it with the methylene blue solution from one side. A significant reduction of residual air in the fracture replica was achieved by placing the test cell in an upright position. The methylene blue solution was then slowly injected from the bottom, entrapping only very few small air bubbles at random locations. A further disturbance of the experiment at the air-water interface, by the air bubbles, could no longer be detected.

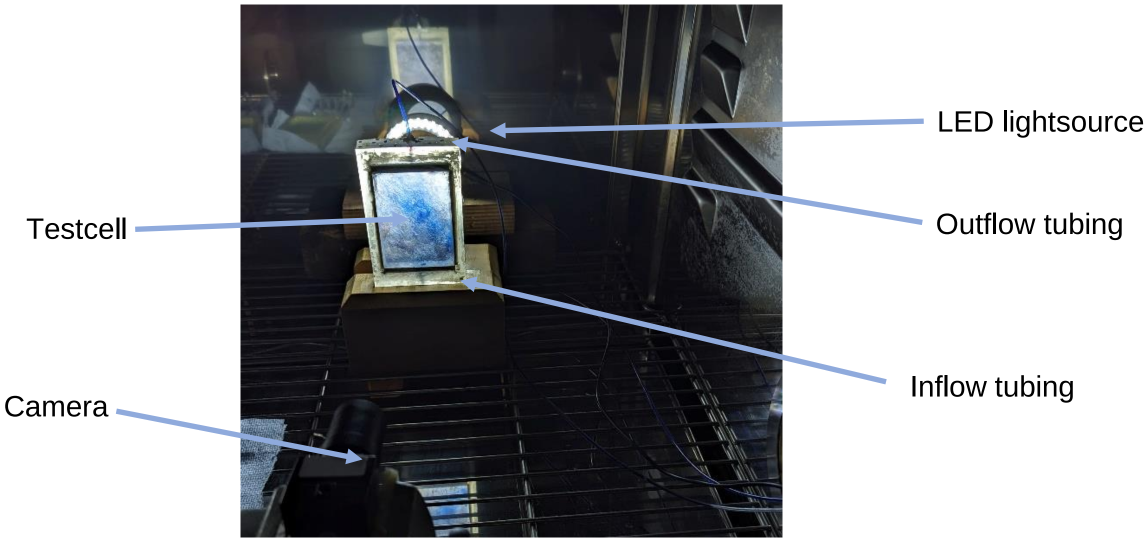

Fig. 3.73 Assembled test setup inside the climate chamber

3.6.4 Test procedure

Initially, the test cell was assembled and sealed using Neukasil, a special type of silicone, along with parcel tape. The setup was then placed into the climate chamber, with the inlet and outlet tubing passing through a cable bushing in the chamber wall. The climate chamber was subsequently cooled down to -8°C for a duration of 3 days, allowing both the fracture replica and the interior of the chamber to equilibrate at the set temperature of -8°C.

Once equilibrium is reached, the LED light was turned on, and image acquisition began at intervals of 5 seconds. The fracture replica was then slowly flooded with the methylene blue solution using a large syringe, while the procedure could only be observed by the images from the camera. When the solution appeared in the outflow tubing, the syringe was transferred to the syringe pump, and continuous injection commenced at a constant flow rate of 5 ml/h. When all flow paths were blocked by the formed ice, the backpressure on the syringe pump increases until the pump shut off at 1.1 bar. As the replicas were almost entirely frozen at this point, the temperature in the climate chamber was increased again to 20°C to observe the thawing processes and to prepare the test cell for its dis-assembly.

Data processing

To analyze the acquired images, threshold segmentation was applied using a custom-written Matlab script. This segmentation step produced a binary array that indicates the state of matter of the tracer solution for regions of 150 by 150 µm, corresponding to a single pixel in the camera image. However, an issue arose due to the increasing discoloration of the test cell, caused by repeated exposure to the tracer solution. This discoloration resulted in false classifications during the segmentation process, highlighting the limited lifespan of a printed fracture replica under the experimental conditions[11]. Although some discoloration of the fracture surfaces was observed after the very first test, a noticeable degradation in image quality and segmentation accuracy occurred after approximately 7 to 10 tests, depending on the duration of exposure. This deterioration underscores the challenge of maintaining consistent experimental conditions over multiple test cycles.

3.6.5 Observations

Supercooling

The initial goal of the experiments was to observe freezing in fractures at sub-zero temperatures. To this end, the first tests were conducted at a temperature of -3°C. While the equipment performed well, no repeatable freezing was observed. To minimize potential interfering factors, simple freezing tests were carried out using small syringes filled with tracer solution, which were then placed in different locations within the climate chamber to ensure that the results were not location dependent. After a few days, some syringes froze as expected, while others still contained liquid tracer solution. Interestingly, it was noted that flicking the syringes caused them to freeze over completely within seconds, even though the syringes were no longer exposed to the cooling in the climate chamber. This behavior is characteristic for supercooled liquids. Supercooling of water can occur at temperatures as low as 231 K /DEB03/ if the water is of very high purity and not subject to mechanical disturbances such as vibrations. Since groundwater typically contains various minerals that act as crystallization nuclei, the occurrence of supercooling in a

[11] This effect highlights the advantage of 3D-printed replicas as these can be reproduced in a well-nigh infinite number.

groundwater aquifer is considered unlikely. Consequently, further tests were conducted at a temperature of -8°C, where supercooling was no longer observed.

Partial freezing

After terminating the tests at -8°C, the test cell was promptly removed from the climate chamber for a visual inspection of the fracture's condition. For that purpose, the two fracture halves were separated immediately.

As the fracture was not completely frozen, a significant portion of the tracer solution remained in a liquid state. Some parts of the fracture were thus completely filled with water while other parts were fully frozen. However, also parts have been observed where ice had formed only on one side of the fracture replica. The thin ice layer was complemented by a thin water layer on the opposite side of the fracture.

An example of a partial freezing pattern is shown in Fig. 3.74, which was captured directly after removing the fracture replica from the climate chamber. In principle, it shows areas in dark blue where the fracture was completely filled with liquid water, areas in white that represent completely frozen water and areas in light blue where partial freezing is assumed. Transmitted light was used to enhance the contrast at the phase boundaries, increasing the visibility of the partially frozen areas. Notably, near the larger volume of liquid tracer on the left-hand side of the image, the two kinds of interface boundaries are visible, the ones that limit a fully liquid-filled fracture and the ones that limit a partially liquid-filled fracture. Since the tracer in the replica began to thaw immediately after the replica was taken out of the climate chamber, some of the partially frozen areas appear already light blue. This indicates that local partial freezing and, consequently, a change in permeability due to ice formation, is achievable using this test setup. After capturing the image depicted in Fig. 3.74, the replica was quickly disassembled to confirm the initial hypothesis of partial freezing.

Given the limitations of the observation and the processing technique, it was not possible to clearly distinguish from the images between partial freezing and the end states, meaning fully liquid and solid, respectively. As a result, partial freezing could only be detected by direct visual inspection after removing the sample from the climate chamber.

Conducting more systematic investigations on the thickness and extent of the ice layer proved to be challenging, though. The thawing process begins almost immediately once the replica is removed from the climate chamber, while prolonged exposure to low temperatures could potentially induce further freezing.

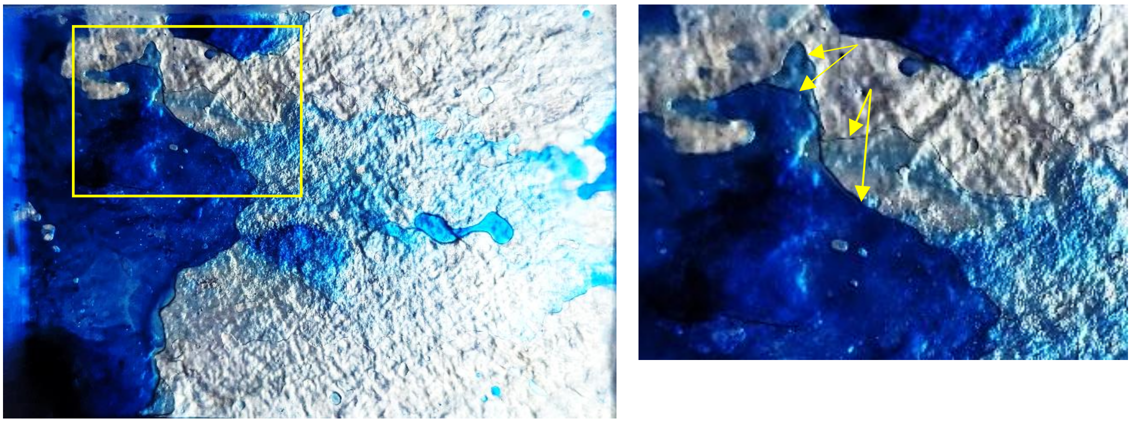

Fig. 3.74 Partially frozen fracture replica right after the test; left: complete sample, right: cut-out region, arrows: phase boundaries

Freezing dynamics

A characteristic ring-like freezing zone can be observed in the vicinity of the sample boundaries as depicted exemplarily for two tests in Fig. 3.75. It is recognizable by its whitish coloration. The evolution of the freezing zone is illustrated in Fig. 3.76, exemplarily showing cut-out sections for the test on the left-hand side in Fig. 3.75. According to Fig. 3.76, the freezing front progresses from the boundaries towards the center of the sample. This has been found to be generally the case in all tests. Initiation of the freezing process varies, however, without a recognizable pattern.

Spikes

During the cooling process, the formation of distinctive spikes in a still water-filled fracture was observed in several tests. As illustrated for the two tests in Fig. 3.75, these spikes appeared at seemingly random locations showing varying intensities. The formation of these spikes appears to indicate a specific type of crystallization process, in which the crystals grow more rapidly in length than in width. The evolution of spike patterns is exemplarily shown in Fig. 3.76 for the test depicted on the left-hand side in Fig. 3.75.

The spike-forming suggests a directional crystallization behavior, where the rate of growth could be influenced by local variations in temperature, the concentration of the tracer, or the microstructure of the fracture replica. Given the delicate nature of these processes and the potential for disrupting the crystallization pattern, further investigations that involved opening or disturbing the sample were not feasible at this point.

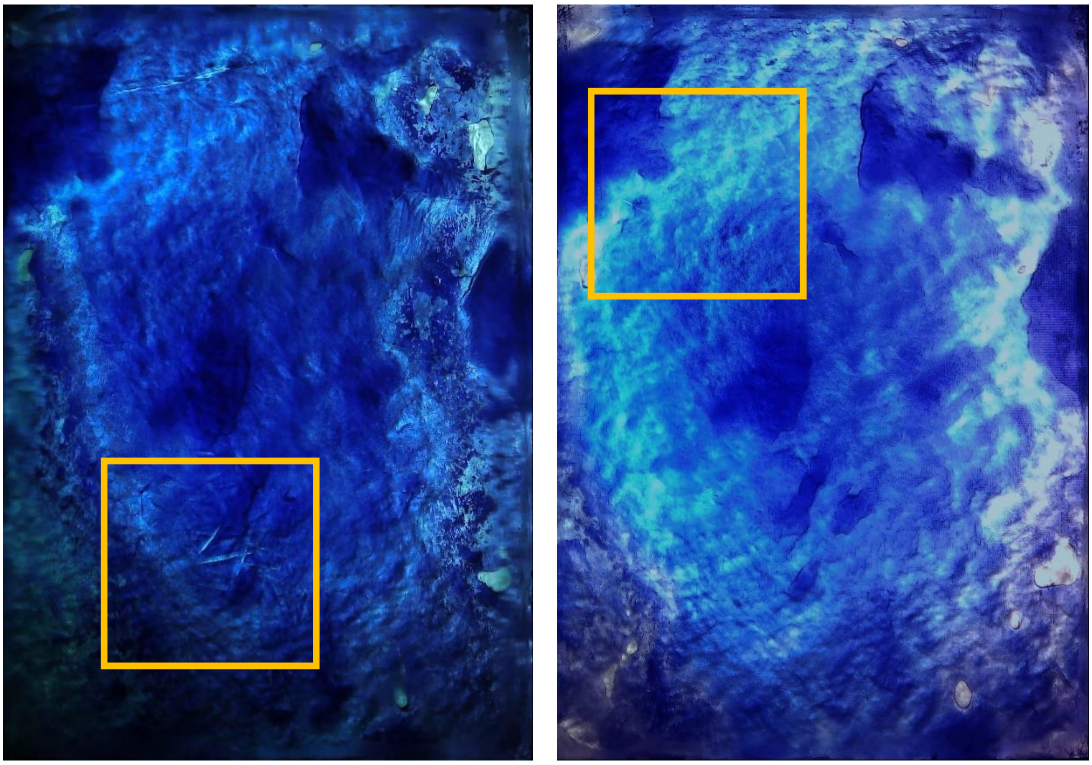

Fig. 3.75 Camera images from two different tests, showing peculiar spikes at different locations; inflow from the bottom, outflow at the top

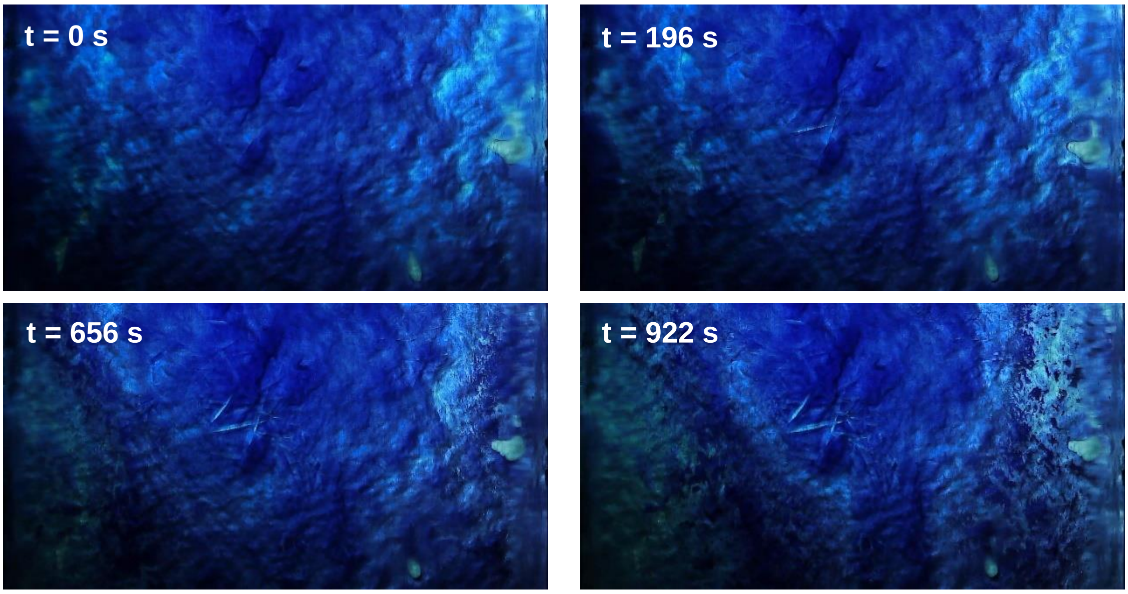

Fig. 3.76 Development of spikes and crystallization from the closed boundaries referring to the test depicted on the left-hand side in Fig. 3.75

3.6.6 Conclusions and outlook

In order to investigate fracture flow dynamics during ice age events, a flow experiment has been set up using highly detailed 3D-scans of related fracture surfaces for producing a realistic transparent 3D-printed fracture replica. The experiment as well as the test procedure were carefully devised to ensure accurate and consistent results.

In the tests, a freezing front was observed that consistently originated at the closed boundaries of the fracture and progressed towards the center of the sample. This may be associated with the slower flow velocities near the boundaries. However, the freezing front initiated at different locations.

At a first glance, it may have come as a surprise that the initiation of freezing as well as the observed spikes were not systematically appearing at one location despite the careful test preparations. However, it may have to do with the phenomenon of partial freezing, meaning the formation of ice only on one of the two fracture surfaces, that is presently also hardly predictable. Partial freezing induces a local reduction of the permeability, which in turn affects the local flow field. As with the sample-sized freezing front mentioned above, a locally reduced flow velocity may potentially create favorable conditions for the crystallization process thereby changing the flow field and thereby possibly allowing also for further freezing. Note that partial freezing as defined here is an effect on the scale of the fracture aperture. As such, it is different from the macroscopic concept of relative permeability that refers to a representative elementary volume (REV) whose size depends on the size and distribution of blocking features in the (fractured) porous medium.

The seemingly random crystallization may also be linked to a specific interaction between the methylene blue tracer and the developing ice structure. The behavior of the tracer, especially its response to freezing and the formation of ice, could contribute to the unusual spike formation. Additionally, it has to be noted that the use of methylene blue solution as an indicator for freezing of water usually refers to very low water velocities. It is not entirely clear if the flow dynamics in the present tests have an impact on the color changing behavior of methylene blue solutions.

An ongoing discoloration of the printed replicas by the tracer solution has been observed when repeatedly using the same replica. This is apparently an effect of the period of time during which the methylene blue solution was in contact with the printed fracture surfaces. Unfortunately, the discoloration makes segmentation and interpretation increasingly difficult and thus limits the usability of an individual printed fracture. However, prints of the same real fracture sample can freshly be reproduced as often as required, thereby highlighting the advantage of using 3D-printed replicas for hydraulic tests.

All in all, the present tests indicate that the used setup is suitable to achieve freezing of the whole sample in parts as well as local partial freezing with related reductions of the hydraulic permeability. However, further work appears to be advisable. The work presented here was contributed to the CatchNet group /SKB19/, which is working on permafrost related topics. After consultation with the experts from the CatchNet the following set of problems remained to be unanswered.

- Develop a test set-up with controlled inflow and outflow pressure to allow for permeability measurements.
- Develop a method to detect the flow field directly.
- Ensure that the methylene blue tracer does not interact with the ice or the printed sample.
- Investigate how flow dynamics and the tracer properties influence the freezing behavior and the resulting patterns in the fracture.
- Conduct more systematic investigations on the thickness and extent of the ice layer.
- Look deeper into the nature of spike-forming.
- Supplement test set-up with a confining metal frame against the expansion of ice.

4 Summary and conclusions

The project has contributed to the deepening of the understanding, the evaluation of new findings from international research work for the national safety case and to further development of the procedure and methodology for long-term safety assessments in accordance with the state of the art. Further activities contributed to the development and – through comparative calculations with other programs – to the verification and qualification of the calculation codes used. Other activities dealt with the topic of preservation of information and knowledge about a final repository and passing it on to future generations. The project thus made an important contribution to various aspects of the safety case for final repositories.

An important task of the project is the participation and concrete work in international committees and working groups to follow new developments in other countries and on the international level and to contributing the development of strategies, methods and tools related to the safety case of deep geological repositories. In this context the participation in the NEA Integration group for the safety case (IGSC), its subgroups, namely the salt club and crystalline club and the NEA Working Party on Information, Data and Knowledge Management (WP-IDKM) played a key role. During the last three years (duration of this project) IGSC has started new tasks, amongst others an update of the project on methods for safety assessment (MeSA) addressing the relationship between requirement management and safety assessment in the context of the safety case. New flowcharts are being developed including interfaces to implementation, safety concept, repository layout and describe the evolution of the safety case over time. The evolution of the safety case is also regarded in the GeneSiS project from IGSC, where experiences from the safety case development from the generic stages to site-specific stages are compiled and made available to countries in early stages. The highlight of the current IGSC work was the planning and preparation of the 4th Safety Case symposium, which was successfully hold in October 2024 in Budapest. A key task of the NEA Salt Club was the analysis of the current state of scenario development for safety case development of deep geological repositories for radioactive waste in salt formations. The work reflects the implementation differences in the regulations that govern the process in the member states of the NEA Salt Club and describes the commonalities and differences between the approaches. Since salt has been an important resource during the history of mankind, human intrusion into the repository in salt requires special attention in scenario development in comparison to other host rocks and has been separately treated in online meetings. Beside others one focus of the Crystalline Club work was the development of a database with publications that improve understanding of chemical conditions in the repository system in crystalline rock, how they are controlled, how they originate, and how they may evolve due to repository perturbations and global temperature cycles. It includes available literature on models that have been developed to simulate and predict chemical conditions as well as literature on canister materials and canister corrosion. The database is hosted online and to date contains 629 references. It is aimed at publishing the database in 2025.

National programmes for radioactive waste management require very large amounts of data and information across multiple and disparate disciplines of science and technology such as nuclear science, waste management, geoscience and engineering. Numerous records and data are being created during the active lifetime of a radioactive waste repository, the pre-operational and operational periods, considered to embrace a period of upward 100 years. Managing very large amounts of data requires considerable resources, reducing the large number of records to an essential set of records can increase the future accessibility and survivability of vital repository records. NEA established in 2019 the Working Party on Information, Data and Knowledge Management (WP-IDKM) to examine the management of information, data and knowledge for/in radioactive waste disposal programmes. A particular topic dealt with in one of WP-IDKM's expert groups EGAR is to further develop the Set of Essential Records (SER) concept. The SER concept and lessons learned from its application to national cases are being published by NEA and highlights are presented in this report here.

The Joint Sensitivity Analysis Group (JOSA) has been working for seven years. The focus of JOSA is on the use of sensitivity analysis in case studies involving geologic disposal of spent nuclear fuel with the overall aim of providing guidelines for performing such analyses in the context of safety assessments or safety cases for geological repositories. The goal of the sensitivity analysis exercise is to gain a better understanding of the strengths and weaknesses of various SA methods, identify cost vs. performance trade-offs of the methods, and highlight best practices and lessons learned. Several countries participated and demonstrated various SA methods on a series of case studies. The second phase of JOSA described here addressed more sophisticated methods and more complex model cases. The focus was laid on the investigation of metamodel methods, higher sensitivity orders (parameter interactions) and newer approaches. A question of interest was where different methods agree or disagree about the sensitivity of parameters and parameter combinations. The investigated systems exhibit particularities like strong nonlinearity, bimodality, bifurcation and stochastic influences. At the end of phase 2, the JOSA team formulated a detailed recommendations for executing sensitivity studies. The work of GRS concentrated on investigating the LILW model and the crystalline reference case with metamodeling methods in order to analyse parameter interactions, which is not (or not satisfyingly) possible with standard methods. It was found that meta-modelling methods are appropriate for that purpose, but the results depend to a high degree on metamodel settings like polynomial orders. There are many issues still to be resolved in sensitivity analyses which support nuclear waste repository analyses. Some of the topics proposed for the next phase are nested sampling, nonparameterized (e.g. spatial) uncertainty, influence of sample types, screening methods, bifurcation effects, active subspaces, and use of input or output transformations.

DECOVALEX 2023 Task F2 was initiated to bring together modelling teams from different organisations who use different frameworks and tools for simulating the contaminant transport from a mined repository in rock salt, and to compare their results in a benchmark exercise. For this purpose, two simple benchmark tests were identified for which analytical solutions are available. Moreover, a reference case representing a simple repository structure with emplacement drifts for SNF and boreholes for vitrified HLW was defined. Participating teams made a wide range of model assumptions from compartmentalized networks to full 3D models of the salt formation. No single contributed model includes full-fidelity representation of all the features, events, and processes (FEPs) detailed in the task specification, but almost all features and processes are represented in at least one model. Deterministic calculations were performed, and several variants of the reference case were considered. Considerable differences between the models were found regarding liquid saturation and flow and are most pronounced at early time, before 1000 years. These differences are believed to be driven largely by the difference in creep-closure modelling between the teams and the resultant rate of reduction of porosity, which in turn depend on the assumptions in the compaction models. They reflect the importance of implementing a high-fidelity salt compaction mechanism in the salt conceptual model to study performance of the repository. Results show that tracer transport out of the waste drifts and through the seal is largely diffusive in all models. Though the differences in diffusive transport are generally smaller than the fluid flow differences, this indicates that diffusion is a key physical mechanism that impacts long-term transport of radionuclides in the repository. Diffusivity is closely linked to the salt creep-closure mechanism via porosity reduction and the coupling between porosity and effective diffusivity.

Moreover, diffusion in the models will be impacted by numerical dispersion. Although there are no striking contradictions or incompatibilities and the differences can be widely understood, the task showed that different modelling concepts for repositories in salt can lead to quite different results. Further research is necessary to investigate the importance of model features and to improve their understanding for long-term PA. The work will be continued in DECOVALEX- 2027.

Bentonite re-saturation as a specific safety case topic has been addressed by active participation in the Task Force on Engineered Barrier Systems (TF EBS) over the last two decades. In spring 2023 an uptake experiment with limited water supply performed in the framework of the project WiGru-7 was suggested and accepted as a new task for the TF EBS and GRS was appointed to be the principal investigator (PI) of this task. The assignment as a PI includes writing a task description, clarifying open questions that may arise from the participants while working on the task, collecting and comparing the results and, finally, writing a summary report. The task description has been completed a few months before the end of the present project and some preliminary simulation results have been presented at the latest TF workshop. In this report a detailed task description is presented. This includes the description of all technical aspects and details of the experiment, performed at GRS, investigating water uptake by compacted MX-80 bentonite under conditions of limited water supply as expected under low flow rock conditions and resulting spatial distributions of dry density, degree of water saturation and porosities. Finally, the tasks to be performed by the benchmark participants are outlined. Results of the benchmark will be presented in the report of the follow-up project FLANKE.

At Danmarks Tekniske Universitet (DTU) an innovative method has been developed to simulate the growth of natural fracture networks based on the geological history and fundamental geomechanical principles. Only rather general information about the geological units of a formation in terms of the geometry and mechanical properties are necessary to apply the method, and the result is a geologically realistic fracture network. The aim of this work was to develop a model with the groundwater flow and transport code d^3f++ to assess the potential of this approach for groundwater modelling with a focus on repository safety analysis. The Drenthe Aa valley in the north-eastern Netherlands was chosen as suitable region for demonstrating the potential of the newly developed fracture generation method. The results suggests that the method has a high potential as the permeability fields obtained from the DFM generator result in a plausible flow field. Moreover, the approach indicates possibly fractured layers that could be missed by conventional drill core analyses. As fractured layers show higher permeabilities than unfractured layers, the assumption of fracture systems implies a higher degree of conservativity with respect to flow and transport simulations. The new method can obviously not be as accurate as direct exploration. But it provides general information about fracture systems on a much larger scale using only available geological knowledge, all this on a more or less theoretical basis. The method thus allows for a first quick and inexpensive check on suitability of potential sites for deep geological storage. A comparison of different sites should thus be facilitated considerably. The potential for local unfractured volumes could be assessed as well as the expected hydraulic conditions around a projected repository.

Over the past million years, several ice ages have occurred and have brought permafrost conditions all over present-day Germany. Permafrost will have a considerable impact on groundwater flow as ground freezing tends to separate deeper aquifers hydraulically from the surface. However, taliks connecting surface waters with deeper aquifers are known to exist in permafrost regions and can potentially lead to a concentrated flux of contaminated groundwater to the surface. Insight into the circumstances of their formation and their stability, which are largely unknown, can be gained through numerical modelling. Therefore, a realistic numerical framework for groundwater flow under permafrost conditions has been applied and the results are illustrated and discussed. The main goal to track talik forming numerically has been missed, though, and the potential reasons are discussed. However, the otherwise reasonable modelling results encourage further systematic investigations. These should relate on the one hand to physical processes that need to be included in the model, and on the other hand to the model setting. Further work should be directed towards possible mechanisms that could heat up the lake bottom which requires probably looking into the freezing dynamics of lakes in general. Moreover, parameter variations should be performed, e.g. heat flux from the inner earth or permeability and porosity of the rock as well as introducing new features in the model such as a (possibly non-horizontal) groundwater table, heterogeneities in the rock or a deep aquifer. All in all, there remain many open issues so that systematically pursuing the present work is strongly recommended.

As future ice ages are expected to affect the whole area of Germany, all potential sites for nuclear waste repository should experience either permafrost conditions or coverage by ice shields. Groundwater in fractures of crystalline rock, a possible host rock for such a repository, will freeze under these conditions. For a first insight into the freezing characteristics of water in fractures, a flow experiment has been set up with a realistic transparent 3D-printed fracture replica based on highly detailed 3D-scans. The experiment as well as the test procedure were carefully devised to ensure accurate and consistent results. It turned out that some observations were indeed repeatable, but some were not. Also, some unexpected phenomena like the appearance of frozen spikes or a partial freezing, meaning the formation of ice only on one of the two fracture surfaces, were observed. In any case, the testing set-up proved to be suitable for experiments concerning freezing in fractures. Even problems arising from a discoloring of the printed fracture surfaces by the methylene blue tracer could be circumvented by printing new replicas and by this, exploiting the advantage of using 3D-printed fracture replicas for the tests. Further work on the topic of freezing in fractures appears therefore to be advisable. Questions should be addressed that were raised in the course of the experiments like the nature, extension and evolution of the partial frozen areas or the exact conditions for initiation of the freezing. In parallel, the experimental set-up should be advanced to allow for measurements of the hydraulic permeability of freezing fractures. Ultimate goal would then be to determine the effective permeability as a function of temperature.

References

/ADA 22/ Adams, B., Bohnhoff, W., Dalbey, K., Ebeida, M., Eddy, J., Eldred, M., Winokur, J. (2022). Dakota, A Multilevel Parallel Object-Oriented Framework for Design Optimization, Parameter Estimation, Uncertainty Quantification, and Sensitivity Analysis: Version 6.16 User's Manual. Albuquerque, New Mexico: Sandia National Laboratories, SAND2022-6171.

/ÅKE 14/ Åkesson, M., Fransson, Å: Buffer Rock Interaction Experiment (BRIE). Presentation at the joint meeting of the Task Forces on EBS and on Groundwater Flow and Transport of Solutes, Berkeley, 2014.

/ÅKE 24/ Åkesson, M.: Task 14 a 3 - 1st analysis. Presentation at the 37th Workshop of the Task Force on EBS, Hannover, 2024.

/BAR 25/ Bartol, J., Becker, D.A., Benbow, S., Bond, A., Frank, T., LaForce, T., Nicholas, J., Jayne, R., Stauffer, P.H:, Stein, E., Stone, J., Wolf, J.: Designing a repository in domal salt: what is important? Submitted to Geomechanics for Energy and the Environment, to be published.

/BAT 06/ Batu, V. 2006. Applied Flow and Solute Transport Modelling in Aquifers. CRC Taylor and Francis.

/BEC 09/ Becker, D.-A., Buhmann, J. Mönig, U. Noseck, A. Rübel, S. Spießl: Endlager Morsleben - Sicherheitsanalyse für das verfüllte und verschlossene Endlager mit dem Programmpaket EMOS. Verfahrensunterlage P278 zum Planfeststellungsverfahren zur Stilllegung des Endlagers für radioaktive Abfälle Morsleben, BfS 2009. https://www.bge.de/fileadmin/user_upload/Morsleben/Wesentliche_Unterlagen/Archiv_Downloads/Planfeststellungsverfahren/20091023_lfdnr106-278-00-v01-p278.publicationFile.pdf.

/BÖR 84/ Börgesson L.: Water flow and swelling pressure in non-saturated bentonite based clay barriers. In: Clay Barriers for Isolation of Toxic Chemical Wastes, International Symposium, May 28–30, Stockholm, 1984.

/BÖR 99/ Börgesson, L., Hernelind, J.: Coupled thermo-hydro-mechanical calculations of the water saturation phase of a KBS-3 deposition hole – Influence of hydraulic rock properties on the water saturation phase. Technical Report TR-99-4, Svensk Kärnbränslehantering AB (SKB), Stockholm, 1999.

/BRA 24/ B. Braun: Manual for Perfusor Compact S. https://www.manualslib.de/manual/268269/B-Braun-Perfusor-Compact-S.html?page=11#manual, as of January 2024.

/BUR 05/ Burn, C.R.: Lake-bottom Thermal Regimes, Western Arctic Coast, Canada. Permafrost and Periglac. Process. 16: 355–367, 2005.

/BUR 20/ Burn, C.R.: Permafrost Landscape Features, *In* Encyclopedia of the World's Biome, Vol. 2, pp. 303-320. doi https://doi.org/10.1016/B978-0-12-409548-9.12423-6, 2020.

/CAP 22/ Capouet, M., Noseck, U., Smith, P.: Proceedings of the International High-Level Radioactive Waste Management Conference. Phoenix, AZ, November 13-17, 2022, pp. 574-584.

/CRO 24/ Cronmiller, D., DeLaplante, G., Nagano, P.: Widespread permafrost landslides caused by intense late-season rainfall in the Klondike, Yukon, a region at a climogeomorphic tipping point. in: Beddoe, R. and Karunaratne, K (eds.): Proceedings of the 12th International Conference On Permafrost (ICOP), vol. 2, Extended Abstracts. Whitehorse, Yukon, Canada, 2024.

/DEB03/ Debenedetti, P. G., Stanley, H. E.: Supercooled and glassy water, Physics Today Volume 56, Issue 6, 01.06.2003.

/DEL 98/ Delisle, G.: Numerical simulation of permafrost growth and decay, Journal of Quarternary Science 13 (**4**), 325-333, 1998.

/BUN 17/ Deutscher Bundestag: Gesetz zur Suche und Auswahl eines Standortes für ein Endlager für hochradioaktive Abfälle (Standortauswahlgesetz - StandAG), decision of the Deutscher Bundestag, 2017.

/DER 03/ Dershowitz, W., Winberg, A., Hermanson, J., Byegård, J., Tullborg, E.-L., Andersson, P., Mazurek, M.: Äspö Task Force on modelling of groundwater flow and transport solutes; Task 6c - A semi-sythetic model of block scale conductive structures at the Äspö HRL. International Progress Report IPR-03-13, Swedish Nuclear Fuel and Waste Management Company (SKB), 2003.

/DWD 12/ Deutscher Wetterdienst (DWD): Klimastatusbericht Deutschland, Jahr 2011, Deutscher Wetterdienst, Selbstverlag, 2012.

/DWD 21/ Deutscher Wetterdienst (DWD): Klimastatusbericht Deutschland, Jahr 2020, Deutscher Wetterdienst, Selbstverlag, 2021.

/DWD 23/ Deutscher Wetterdienst (DWD) as of 2023. CDC – Climate Data Center, annual air temperature over Germany, 2023. https://opendata.dwd.de/climate_environment/CDC/regional_averages_DE/annual/air_temperature_mean/regional_averages_tm_year.txt.

/DYE 12/ Dye, S.T.: Geoneutrinos and the radioactive power of the Earth, Reviews of Geophysics, Volume **50**, Issue 3, 2012. https://doi.org/10.1029/2012RG000400.

/ERI 23/ Eriksson, P. (SKB): personal communication, 2023.

/FEK 25/ Fekete, J., Berckmans, A., Eliáš, M., Noseck, U. (2025): “Set of Essential Records (SER) - A mechanism to preserve essential information about a repository to future generations”. In: Proceedings of IGSC Safety Case Symposium 2024: Moving towards the construction of a safe DGR – Getting real. 8-11 October 2024, Budapest, Hungary NEA/RWM/R(2024)8, Paris 2025.

/FIN 95/ Finsterle, S. and Pruess, K.: Solving the estimation-identification problem in two-phase flow modeling. Water Resources Research, Vol. 31, NO. 4, pp. 913-924, 1995.

/FIN 19/ Finsterle, S.: Overall evaluation of Tasks 8A–D, F, and water-uptake test related to modelling of the interaction between engineered and natural barriers - Task 8 of SKB Task Forces EBS and GWFTS. Technical Report TR-17-07, Svensk Kärnbränslehantering AB (SKB), Solna, 2019.

/FRA 24/ Frank, T., Becker, D.A., Benbow,S., Bond, A., Jayne, R., LaForce, T., Wolf, J.: Value of abstraction in performance assessment – When is a higher level of detail necessary? GeoMech. Engin. Env. 39, 100577 (2024). https://doi.org/10.1016/j.gete.2024.100577

/FRA 17/ Fransson Å, Åkesson M, Andersson L.: Bentonite Rock Interaction Experiment, Characterisation of rock and installation, hydration and dismantling of bentonite parcels. Report SKB R-14-11, Svensk Kärnbränslehantering AB, Solna, 2017.

/FRE 20/ Freeze, G., Sevougian, S.D., Kuhlman, K., Gross, M., Wolf, J., Buhmann, D., Bartol, J., Leigh, C., Mönig, J.: Generic FEPs catalogue and salt knowledge archive (SAND2020-13186, 151 pp.). Sandia National Laboratories, Albuquerque, NM, 2020.

/ERI 23/ ERIH (European Route of Industrial Heritage): Industrial history of European countries, as of 2023. https://www.erih.net/how-it-started/industrial-history-of-european-countries.

/FUC 22a/ Fuchs, S., Förster, A., Norden, B.: Evaluation of the terrestrial heat flow in Germany: A case study for the reassessment of global continental heat-flow data, Earth-Science Reviews 235 (2022) 104231, 2022a. https://doi.org/10.1016/j.earscirev.2022.104231.

/FUC 22b/ Fuchs, S., Norden, B., Förster, A.: The German Heat Flow Database 2022, GFZ Data Services, 2022b. https://doi.org/10.5880/GFZ.4.8.2022.015.

/FUK82/ Fukuda, M.: Heat flow measurements in freezing soil with various front advancing rates, Hokkaido University, Proceedings of the 4th Canadian Permafrost Conference 1982.

/GEN 02/ Gens, A., Guimaraes, L. do N., Garcia-Molina, A., Alonso, E.E.: Factors controlling rock–clay buffer interaction in a radioactive waste repository, Engineering Geology **64,** 297 – 308, 2002.

/GER 11/ Gerber, H.-J.: Zur Physik des Saftaufstiegs in Bäumen. Paper at the ETH Zürich, 2011; in German; link as of 24th November 2023. https://ethz.ch/content/dam/ethz/main/eth-zurich/ArbeitenLehrenundForschen/professuren/ihre-professur/Emeritenstamm/110530_Gerber_Referat.pdf

/GRA 25/ Gray, L., Noseck, U., Brown, J., Peake, Th., Nishikawa, S., Capouet, M., Doudou, S., Kaempfer, Th., Stein, E., Leone, R., LaForce, T., Major, J., Marble, J., Bailey, L.: GeneSiS: Generic to Site-Specific – the evolution of the safety case. In: Proceedings of IGSC Safety Case Symposium 2024: Moving towards the construction of a safe DGR – Getting real. 8-11 October 2024, Budapest, Hungary, NEA/RWM/R(2024)8, Paris 2025.

/GUO 06/ Guo, R. and Dixon, D.: The Isothermal Test: Description and Material Parameters for Use by the Engineered Barriers Systems Taskforce. Technical Mem-orandum, 06819(UF)-03700.3 SKB-T05, Ontario Power Generation, 2006.

/HAN 09/ Hansen, B., Magnusson, J., Söderlund, P.: Underground design Forsmark, Layout D2 – Layout and construction plan. Report R-08-113, Svensk Kärnbränslehantering AB, Stockholm, 2009.

/HAR 11/ Harper, J., Hubbard A., Ruskeeniemi, T., Claesson Liljedahl, L., Lehtinen, A., Booth, A., Brinkerhoff, D., Drake, H., Dow, C., Doyle, S., Engström, J., Fitzpatrick, A., Frape, S., Henkemans, E., Humphrey, N., Johnson, J., Jones, G., Joughin, I., Klint, K.E., Kukkonen, I., Kulessa, B., Landowski, C., Lindbäck, K., Makahnouk, M., Meierbachtol, T., Pere, T., Pedersen, K., Pettersson, R., Pimentel, S., Quincey, D., Tullborg E.-L., van As, D.: The Greenland Analogue Project, Yearly Report 2010, Report R-11-23, Svensk Kärnbränslehantering AB, Stockholm, 2011.

/HER 06/ Herbert, E., Balibar, S., Caupin, F.: Cavitation pressure in water. Phys. Rev. E 74, 041603, 2006. doi:10.1103/PhysRevE.74.041603; cited in /LI 17/, /LIZ 18/, /MØR 18/.

/HIR 99/ Hirsekorn, R.-P., Boese, B., Buhmann, D. (1999): LOPOS: Programm zur Berechnung der Schadstofffreisetzung aus netzwerkartigen Grubengebäuden. GRS-157, Gesellschaft für Anlagen- und Reaktorsicherheit (GRS) mbH, ISBN 3-931995-19-4, Braunschweig

/HOR 45/ Horton, C.W. and Rogers, F.T.: Convection currents in a porous medium. J. Appl. Phys. 16, 367–370, 1945.

/HYM 15/ Hyman, J., Karra, S., Makedonska, N., Gable, C., Painter, S., & Viswanathan, H. (2015). dfnWorks: A discrete fracture network framework for modeling subsurface flow and transport. Computers & Geoscience, 84, 10-19.

/IAEA 06// IAEA: Geological Disposal of Radioactive Waste", IAEA Safety Requirements No. WS-R-4, International Atomic Energy Agency, Vienna (2006).

/IAP 03/ IAPWS (The International Association for the Properties of Water and Steam): Revised Release on the IAPS Formulation 1985 for the Viscosity of Ordinary Water Substance, 2003. Homepage: http://www.iapws.org.

/IAP 08/ IAPWS (The International Association for the Properties of Water and Steam): Revised Release on the IAPWS Formulation 2008 for the Viscosity of Ordinary Water Substance, 2008. Homepage: http://www.iapws.org.

/IAP 11/ IAPWS (The International Association for the Properties of Water and Steam): Revised Release on the IAPWS Formulation 2011 for the Thermal Conductivity of Ordinary Water Substance, 2011. Homepage: http://www.iapws.org.

/IAP 15/ IAPWS (The International Association for the Properties of Water and Steam): Revised Guideline on Thermodynamic Properties of Supercooled Water, 2015. Homepage: http://www.iapws.org.

/JAR 10/ Jarsjö, J. Desouche, C., Frampton, A.: Initiation of Task 8. Presentation from the Workshop of the Task Force on Groundwater Flow and Transport of Solutes, Lund, 2010.

/JOH 16/ Johansson, E.: The influence of climate and permafrost on catchment hydrology. Thesis, Department of Physical Geography, Stockholm University, 2016.

/JOH 15/ Johansson, E., Gustafsson, L.-G., Berglund, S., Lindborg, T., Selroos, J.-O., Claesson Liljedahl, L., Destouni, G.: Data evaluation and numerical modeling of hydrological interactions between active layer, lake and talik in a permafrost catchment, Western Greenland, Journal of Hydrology, **36**. 10.1016/j.jhydrol.2015.05.026, 2015.

/JOU 07/ Jouzel, J., and Masson-Delmotte, V.: EPICA Dome C Ice Core 800KYr deuterium data and temperature estimates. PANGAEA, 2007. https://doi.org/10.1594/PANGAEA.683655.

(Supplement to: Jouzel, J., Masson-Delmotte, V., Cattani, O., Dreyfus, G., Falourd, S., Hoffmann, G., Minster, B., Nouet, J., Barnola, J.-M., Chappellaz, J.A., Fischer, H., Gallet, J.C., Johnsen, S.J., Leuenberger, M.C., Loulergue, L., Luethi, D., Oerter, H., Parrenin, F., Raisbeck, G.M., Raynaud, D., Schilt, A., Schwander, J., Selmo, E., Souchez, R.A., Spahni, R., Stauffer, B., Steffensen, J.P., Stenni, B., Stocker, T.F., Tison, J.-L., Werner, M., and Wolff, E.W. 2007. Orbital and millennial Antarctic climate variability over the past 800,000 years, Science, 317 (5839), 793-797. https://doi.org/10.1126/science.1141038).

/JOY 14/ Joyce, S., Hartley, L., Applegate, D., Hoek, J., & Jackson, P. (2014). Multi-scale groundwater flow modeling aduring temperate climate conditions for the safety assessment of the proposed high level nuclear waste repository site at Forsmark, Sweden. Hydrogeology Journal, 22(6), 1233-1249.

/KEL 98/ Keller, S. 1998: Permafrost in der Weichsel-Kaltzeit und Langzeitprognose der hydrogeologischen Entwicklung der Umgebung von Gorleben / NW Deutschland, Z. Angew. Geol. 48, 111-119, 1998.

/KOL 15/ Kolditz, O., H. Shao, W. Wang, and S. Bauer 2015. Thermo-Hydro-Mechanical-Chemical Processes in Fractured Porous Media: Modelling and Benchmarking Closed-Form Solutions (O. Kolditz, H. Shao, W. Wang, & S. Bauer Eds.). Switzerland: Springer International Publishing.

/KRÖ 04/ Kröhn, K.-P.: Modelling the re-saturation of bentonite in final repositories in crystalline rock. Final report, FKZ 02 E 9430 (BMWA), Gesellschaft für Anlagen- und Reaktorsicherheit (GRS) mbH, GRS-199, Köln, 2004.

/KRÖ 10/ Kröhn, K.-P.: State Variables for Modelling Thermohaline Flow in Rocks. FKZ 02 E 10336 (BMWi), report GRS-268, Gesellschaft für Anlagen- und Reaktorsicherheit (GRS) mbH, Köln, 2010.

/KRÖ 11/ Kröhn, K.-P.: Code VIPER - Theory and Current Status. Status report, FKZ 02 E 10548 (BMWi), Gesellschaft für Anlagen- und Reaktorsicherheit (GRS) mbH, GRS-269, Köln, 2011.

/KRÖ 17/ Kröhn, K.-P.: Hydraulic Interaction of Engineered and Natural Barriers – Task 8b-8d,8f of SKB. Summary report, FKZ 02 E 10336, 02 E 10548, 02 E 10558, 02 E 11102, and 02 E 11213 (BMWi), Gesellschaft für Anlagen- und Reaktorsicherheit (GRS) mbH, GRS-430, Köln, 2017.

/KRÖ 18a/ Kröhn, K.-P.: Re-saturation of compacted bentonite under repository-relevant flow conditions. FKZ 02 E 11102 (BMWi). Geomechanics for Energy and the Environment, Elsevier, 2018. DOI:10.1016/j.gete.2018.09.003

/KRÖ 18b/ Kröhn, K.-P. and Lanyon, B.: Observations of Hydraulic and Transport „Skin Effects“ SKB Task Force Workshop Prague 2016. FKZ 02 E 11476A (BMWi), Gesellschaft für Anlagen- und Reaktorsicherheit (GRS) mbH, GRS-504, Köln, 2018.

/KRÖ 19/ Kröhn, K.-P.: Bentonite Re-saturation – limited Access to Water and high Temperature Gradients. FZK 02E10548 and 02E11102 (BMWi), Report GRS-503, Gesellschaft für Anlagen- und Reaktorsicherheit (GRS) mbH, Braunschweig, 2019.

/KRÖ 22/ Kröhn, K.-P.: Basics for groundwater flow under permafrost conditions in the context of radioactive storage FKZ 02 E 11809A (BMUV), report GRS-707, Gesellschaft für Anlagen- und Reaktor-sicherheit (GRS) gGmbH, Braunschweig, 2022.

/KRÖ 23/ Kröhn, K.-P.: Investigations On Talik Formation During Changes To Cold Climates, COMSOL Conference 2023, Munich, Germany, 2023.

/KRÖ 24/ Kröhn, K.-P.: Groundwater flow under permafrost conditions and talik formation. Proceedings of the 12th International Conference on Permafrost (ICOP), Whitehorse, Kanada, Juni 2024

/KRÖ 25/ Kröhn, M., Stigsson, M., Kröhn, K.-P.: Preparing and fabricating highly detailed fracture replicas by 3D-scanning and -printing for hydraulic lab-tests. FKZ 02 E 11880 (BMUV), Report GRS-798, Gesellschaft für Anlagen- und Reaktorsicherheit (GRS) mbH, Braunschweig, 2025, (in preparation)

/KUH 24/ Kuhlman, K., Bartol, J., Carter, A., Lommerzheim, A., Wolf, J. (2024): Scenario development for safety assessment in deep geologic disposal of high-level radioactive waste and spent nuclear fuel: A review. Risk Analysis 44(8): 1850-1864.

/LAF 23/ LaForce, T. et al.: DECOVALEX-2023 Task F Specification Revision 10, Sandia National Laboratories, SAND-2023-04005R.

/LAF 24a/ LaForce, T. et. Al.: DECOVALEX-2023 Task F2 Final Report. Lawrence Berkeley National Laboratories, LBNL-2001627

/LAF 24b/ LaForce, T., Bartol,J., Becker, D.A., Benbow, S., Bond, A., Dietl, C.R., Frank, T., Kock, I., Magri, F., Nicholas, J., Jayne, R., Pekala, M., Stauffer, P.H., Stein, E., Stone. J., Wolf, J.: Comparing modelling approaches for a generic nuclear waste repository in salt. GeoMech. Energy. Env. 40, 100621 (2024). https://doi.org/10.1016/j.gete.2024.100621

/LAP 48/ Lapwood, E.R.: Convection of a fluid in a porous medium. Proc. Camb. Phil. Soc. 44, 508–521, 1948.

/LES 87/ Leshchinsky, D., and Perry, E.B.: A Design Procedure for Geotextile Reinforced Walls, In Geosynthetics ‘87, IFAI, New Orleans, LA, USA, 1: 95-107, 1987.

/LEV 41/ Leverett, M. C.; Capillary behavior in porous solids; Petroleum Transactions of AIME (1941); 142; 152-169, 1941.

/LIB 17/ Li, B., Gu, Y. and Chen, M.: An experimental study on the cavitation of water with dissolved gases. *Exp Fluids* 58, 164 (2017). https://doi.org/10.1007/s00348-017-2449-0

/LIZ 18/ Li, Z.G., Xiong, S., Chin, L.K., Ando, K., Zhang, J.B., Liu, A.Q.: Water's tensile strength measured using an optofluidic chip. Lab Chip, **15**, 2158-2161, 2015; DOI: 10.1039/C5LC00048C.

/LOY 07/ Loyd, S., Becker, T., Conrad, C., Lithgow-Bertelloni, C., Corsetti, F.: Time variability in Cenozoic reconstructions of mantle heat flow: Plate tectonic cycles and implications for Earth's thermal evolution. Proceedings of the National Academy of Sciences of the United States of America. 104. 14266-71. DOI: 10.1073/pnas.0706667104, 2007.

/MAC 62/ Mackay, J.R.: Pingos of the Pleistocene Mackenzie Delta area. Geographical Bulletin, **18**: 21–63, 1962.

/MAR 16/ Mariner, P., Stein, E., Frederick, J., Sevougian, S., Hammond, G., & Fascitelli, D. (2016). Advances in Geologic Disposal System Modeling and Application to Crystalline Rock. Albuquerque, New Mexico: FCRD-UFD-2016-000440, SAND2016-9610R, Sandia National Laboratories.

/MØR 15/ Mørch, K.A.: Cavitation inception from bubble nuclei. Interface Focus **5**: 20150006, 2015. http://dx.doi.org/10.1098/rsfs.2015.0006.

/MØR 18/ Mørch, K.A.: Cavitation nuclei and tensile strength of water. 10th International Symposium on Cavitation, Baltimore, Maryland, USA, May 14 – 16, 2018.

/NEA 19/ NEA: Preservation of Records, Knowledge and Memory (RK&M) Across Generations: Compiling a Set of Essential Records (SER) for a Radioactive Waste Repository. OECD/NEA, Report Paris, 2019.

/NEA 19b/ NEA: Information, Data and Knowledge Management (IDKM). Roadmap. OECD/NEA Report 2019.

/NEA 20/ NEA: "Two decades of Safety Case Development. An IGSC 20th Anniversary Brochure" OECD/NEA Report No. 7559 (2020).

/NEA 22/ NEA: Proceedings of the IGSC Safety Case Symposium 2018. Current Understanding and Future Direction for the Geological Disposal of Radioactive Waste. 10-11 October 2018, Rotterdam, Netherlands. NEA/RWM/R(2018)7, November 2022.

/NEA 25a/ NEA: Proceedings of the IGSC Safety Case Symposium 2024: Moving towards the construction of a safe DGR – Getting real. 8-11 October 2024, Budapest, Hungary, NEA/RWM/R(2024)8, Paris 2025.

/NEA 25b/ NEA: The Concept of the Set of Essential Records to Preserve Information About a Repository for Future Generations. Experiences from application to real programmes and additions to the concept. OECD/NEA, Report to be published.

/NOS 18/ Noseck, U., Becker, D., Brasser, T., Buhmann, D., Fahrenholz, C., Flügge, J., Kröhn, K.-P., Meleshyn, A., Mönig, J., Moog, H., Rübel, A., Spießl, S., Wolf, J.: Scientific Basis for a Safety Case of Deep Geological Repositories. Final Report, FKZ 02E11102 (BMWi), GRS-501, GRS Braunschweig, 2018.

/NOS 21/ Noseck, u. et al.: Scientific Basis for a Safety Case of Deep Geological Repositories. FKZ 02E11647 (BMWi), GRS-643, Braunschweig 2021.

/NOS 25a/ Noseck, U., Brown, J., Gray, L., Doudou, S., Peake, T., Capouet, M., Nishikawa, S.: From Generic to Site-specific Safety Cases: Development of Topic-specific Guidance. In: *Proceedings of the of the IGSC Safety Case Symposium 2024: Moving towards the construction of a safe DGR – Getting real*. 8-11 October 2024, Budapest, Hungary. NEA/RWM/R(2024)8, 2025.

/NOS 25b/ Noseck,U., Fekete, J., Berckmans, A., Böhmer, J., Maugis, V., Petterson, C., Wellmann. P.: (2024), “Experiences on the preservation of essential information, data and knowledge gathered throughout repository implementation and operation”. In: Proceedings of IGSC Safety Case Symposium 2024: Moving towards the construction of a safe DGR – Getting real. 8-11 October 2024, Budapest, Hungary, NEA/RWM/R(2024)8, 2025.

/ODA 86/ Oda, M.: An equivalent continuum model for coupled stress an fluid flow analysis in jointed rock masses, Ressources Research, John Wiley & Sons Ltd., 22 (13), pp. 1845-1856, 1986.

/PAR 18/ Parazoo, N.C., Koven, C.D., Lawrence, D.M., Romanovsky, V., and Miller, C.E. Detecting the permafrost carbon feedback: talik formation and increased cold-season respiration as precursors to sink-to-source transitions. The Cryosphere, **12**, 123–144, 2018. https://doi.org/10.5194/tc-12-123-2018.

/PET 22/ Petrel 2022.1, SLB, https://www.software.slb.com/products/petrel, 2022.

/PIA 15/ Pianosi, F., & Wagener, T. (2015): A simple and efficient method for global sensitivity analysis based on cumulative distribution functions. Environmental Modeling and Software, 67, 1-11.

/PIA 18/ Pianosi, F., & Wagener, T. (2018): Distribution-based sensitivity analysis from a generic input-output sample. Environmental Modelling & Software, 108, 197-207.

/PLI 10/ Plischke, E.: An effective algorithm for computing global sensitivity indices (EASI). Reliability Engineering and System Safety, 95: 354–360, 2010.

/REI 11/ Reiche, T., Becker, D.-A., Buhmann, D., Lauke, T. (2011): Anpassung des Programmpakets EMOS an moderne Softwareanforderungen: ADEMOS – Phase 1. FKZ 02E10367, GRS-A-3623, Gesellschaft für Anlagen und Reaktorsicherheit (GRS) mbH, Braunschweig.

/REI 16/ Reiche, T. (2016): RepoTREND - Das Programmpaket zur integrierten Langzeitsicherheitsanalyse von Endlagersystemen, Version 4.5 (Stand März 2016). GRS-413.

/RHÉ 01/ Rhén I, Forsmark T.: Äspö Hard Rock Laboratory. Prototype Repository. Hydrogeology. Summary report of investigations before the operation phase. SKB IPR-01-65, Svensk Kärnbränslehantering AB, Stockholm, 2001.

/RÖH 25/ Röhlig, K.J. et al.: IGSC MeSA-2 initiative: Repository implementation and safety assessment – towards a holistic approach. In: *Proceedings of the of the IGSC Safety Case Symposium 2024: Moving towards the construction of a safe DGR – Getting real*. 8-11 October 2024, Budapest, Hungary, NEA/RWM/R(2024)8, Paris 2025.

/RÜB 16/ Rübel, A., Buhmann, D., Kindlein, J. and Lauke, T. (2016): Performance assessment of sealing systems. Conceptual and integrated modelling of plugs and seals (No. GRS-415). Gesellschaft fuer Anlagen-und Reaktorsicherheit (GRS) gGmbH.

/SCA 24/ Schetselaar, A.B. and Burn, C.R.: Increases in highway maintenance costs in a permafrost environment undergoing climate change, Yukon, Canada. in: Beddoe, R. and Karunaratne, K (eds.): Proceedings of the 12th International Conference On Permafrost (ICOP), vol. 1, Conference Papers. Whitehorse, Yukon, Canada, 2024.

/SCH 12/ Schneider, A. (ed.): Enhancement of d^3f und r^3t (E-DuR). Final report, FKZ 02 E 10336 (BMWi), Gesellschaft für Anlagen- und Reaktorsicherheit (GRS) mbH, GRS-292, 2012.

/SCH 20/ Schneider, A., Britz, S., Gehrke, A., Kröhn, K.-P., Lampe, M., Nägel, A., Reiter, S., Wittum, G., Zhao, H.: Groundwater Flow and Transport in Complex Real Systems. Final report, FKZ 02 E 11476A-B (BMWi), Gesellschaft für Anlagen- und Reaktorsicherheit (GRS) mbH, GRS-566, 2020.

/SEV 18/ Sevougian, S., Stein, E., Hammond, G., Mariner, P., Frederick, J., & Basurto, E. (2018). Simulating the Effect of Fracture Connectivity on Repository Performance with GDSA Framework - 18589, SAND2017-12677C. WM2018 Conference. Phoenix, AZ.

/SHA 17/ Shao, Q., Younes, A., Fahns, M., & Mara, T. (2017). Bayesian sparse polynomial chaos expansion for global sensitivity analysis. Computer Methods in Applied Mechanics and Engineering, 318, 474-496.

/SKB 06/ Svensk Kärnbränslehantering AB (SKB): Climate and climate-related issues for the safety assessment SR-Can, Technical report TR-06-23, SKB, Stockholm, 2006.

/SKB 10/ Svensk Kärnbränslehantering AB: Design, construction and initial state of the underground openings. Report TR-10-22, Svensk Kärnbränslehantering (SKB), Stockholm, 2010.

/SKB19/ Svensk Kärnbränslehantering AB: This is CatchNet, https://skb.se/catchnet/this-is-catchnet/, 2019, as of: 23.01.2025.

/SMI 18/ Smit, F., Magri, F., Bregman, E.: Coupling earth surface processes and geological structures to explain environmental features as observed onshore Northern Netherlands. SEG Technical Program Expanded Abstract, 1519-1523, 2018.

/SPI 17/ Spiessl, S.M., Becker, D.-A.: Investigation of Modern Methods of Probabilistic Sensitivity Analysis of Final Repository Performance Assessment Models (MOSEL). FKZ 02E 10941 (BMWi), GRS-412, ISBN 978-3-944161-94-5.

/SPI 24/ Spiessl, S. M., Plischke, E., Becker, D.-A.: Elastic Sensitivity: Higher Order Effects Via Search Curves - A Comparison. 2024 SIAM Conference on Uncertainty Quantification.

/SOL 07/ Solomon, S., Qin, D., Manning, M., Marquis, M., Averyt, K., Tignor, M.M.B., Miller, H.L. jr., Chen, Z. (eds.) 2007. Climate Change, The Physical Science Basis, Contribution of Working Group I to the Fourth Assessment Report of the Intergovernmental Panel on Climate Change, Cambridge University Press, New York, NY, USA, 2007.

/SQU 05/ Squires, T.M. and Quake, S.R.: Microfluidics: Fluid physics at the nanoliter scale. The American Physical Society, reviews of modern physics, volume 77, July, 2005.

/STE 17/ Stein, E., Frederick, J., Hammond, G., Kuhlman, K., Mariner, P., & Sevougian, S. (2017). Modeling Coupled Reactive Flow Processes in Fractured Crystalline Rock. 16th International High-Level Radioactive Waste Management (IHLRWM 2017) Conference, American Nuclear Society. Charlotte, North Carolina.

/SWI 21a/ Swiler, L. P., Becker, D.-A., Brooks, D., Govaerts, J., Koskinen, L., Plischke, E., Röhlig, K.-J., Saveleva, E., Spiessl, S. M., Stein, E., Svitelman, V. (2021). Sensitivity Analysis Comparisons on Geologic Case Studies: An International Collaboration. report no. SAND2021-11053, Sandia National Lab., Albuquerque. doi:10.2172/1822591.

/SWI 21b/ Swiler, L., Basurto, E., Brooks, D., Eckert, A., Leone, R., Mariner, P., . . . Stein, E. (2021). Uncertainty and Sensitivity Analysis Methods and Applications in the GDSA Framework (FY2021). Albuquerque, New Mexico: Sandia National Laboratories, SAND2021-9903R.

/SWI 25/ Swiler, L. P., Becker, D.-A., Brooks, D., Govaerts, J., Koskinen, L., Plischke, E., Röhlig, Samper, J., K.-J., Spiessl, S. M., Stein, E.: Sensitivity Analysis Comparisons on Geologic Case Studies: An International Collaboration (Volume 2). SAND2025-00230.

/THO 03/ Thomas, H. R., Cleall, P. J., Chandler, N., Dixon, D., Mitchell, H. P.: Water infilration into a large-scale in-situ experiment in an underground research la-boratory. *Geotechnique*, 53 (2), 2003.

/VEV 05/ van Everdingen, R.O. (ed.): Multi-language Glossary of Permafrost and Related Ground-ice Terms. International Permafrost Association, Terminology Working Group, 1998 (revised 2005).

/VAN 93/ Vandenberghe, J. and Pissart, A.: Permafrost changes in Europe during the Last Glacial, Permafrost and Periglacial Processes **4**, 121–135, 1993.

/VGN 80/ Van Genuchten, M.T.: A Closed-Form Equation for predicting the hydraulic Conductivity of Unsaturated Soils. - Soil Sci. Soc. Am. J., 44:892-898, 1980.

/VID 17/ Vidstrand, P., Stigsson, M., Åkesson, M., Fransson, Å.: SKB Task Forces EBS and GWFTS. Modelling the interaction between engineered and natural barriers. A compilation of Task 8 descriptions. Report SKB P-16-05, Svensk Kärnbränslehantering AB, Solna, 2017.

/WAS 25/ Wasselin, V., Capouet, M., Voinis, S., Schiffmann, S., De Preter P., Hemery, C.: Application of the graded approach to the long-term management of “in-between”waste : Preliminary outcomes of a seminar of the IGSC “graded approach” group. In: *Proceedings of the of the IGSC Safety Case Symposium 2024: Moving towards the construction of a safe DGR – Getting real*. 8-11 October 2024, Budapest, Hungary, NEA/RWM/R(2024)8, Paris 2025.

/WEL 19/ Welch, M. J., Lüthje, M., Glad, A.C.:Influence of fracture nucleation and propagation rates on fracture geometry: insights from geomechanical modelling. Petroleum Geoscience, Vol. 25, pp. 470–489, 2019.

/WEL 20/ Welch, M. J., Lüthje, M., Oldfield, S. J.: Modelling the Evolution of Natural Fracture Networks – Methods for Simulating the Nucleation, Propagation and Interaction of Layer-Bound Fractures. Springer Cham, p. 230, 2020.

/WEL 23/ Welch, M. J., Lüthje, M., Oldfield, S. J.: Dynamic Fracture Model Generator. Petrel version. Installation and User guide. https://gitlab.gbar.dtu.dk/offshore/dfm-generator/-/blob/main/Documentation/DFM_Generator_Petrel_UserGuide.pdf, Version 20/06/2023

/WEN 19/ Wen, B. and Chini, G.P.: On Moderate-Rayleigh-Number Convection in an Inclined Porous Layer. *Fluids* **2019**, *4*(2), 101; 2019. DOI: https://doi.org/10.3390/fluids4020101

/ZHE 91/ Zheng, Q., Durben, D.J., Wolf, G.H.: Liquids at large negative pressures: Water at the homogeneous cavitation limit. Science 254, 829-832, 1991; cited in /LIZ 18/, /MØR 18/.

List of Figures

List of Tables

**Gesellschaft für Anlagen-
und Reaktorsicherheit
(GRS) gGmbH**

Schwertnergasse 1
50667 Köln
Telefon +49 221 2068-0
Telefax +49 221 2068-888

Boltzmannstraße 14
85748 Garching b. München
Telefon +49 89 32004-0
Telefax +49 89 32004-300

Kurfürstendamm 200
10719 Berlin
Telefon +49 30 88589-0
Telefax +49 30 88589-111

Theodor-Heuss-Straße 4
38122 Braunschweig
Telefon +49 531 8012-0
Telefax +49 531 8012-200

www.grs.de

ISBN 978-3-910548-63-3